

T-Cal: An optimal test for the calibration of predictive models

Donghwan Lee,^{*†} Xinmeng Huang,^{*‡} Hamed Hassani,[§] and Edgar Dobriban[¶]

March 4, 2022

Abstract

The prediction accuracy of machine learning methods is steadily increasing, but the calibration of their uncertainty predictions poses a significant challenge. Numerous works focus on obtaining well-calibrated predictive models, but less is known about reliably assessing model calibration. This limits our ability to know when algorithms for improving calibration have a real effect, and when their improvements are merely artifacts due to random noise in finite datasets. In this work, we consider detecting mis-calibration of predictive models using a finite validation dataset as a hypothesis testing problem. The null hypothesis is that the predictive model is calibrated, while the alternative hypothesis is that the deviation from calibration is sufficiently large.

We find that detecting mis-calibration is only possible when the conditional probabilities of the classes are sufficiently smooth functions of the predictions. When the conditional class probabilities are Hölder continuous, we propose T-Cal, a minimax optimal test for calibration based on a debiased plug-in estimator of the ℓ_2 -Expected Calibration Error (ECE). We further propose Adaptive T-Cal, a version that is adaptive to unknown smoothness. We verify our theoretical findings with a broad range of experiments, including with several popular deep neural net architectures and several standard post-hoc calibration methods. T-Cal is a practical general-purpose tool, which—combined with classical tests for discrete-valued predictors—can be used to test the calibration of virtually any probabilistic classification method. T-Cal is available at <https://github.com/dh7401/T-Cal>.

Contents

1	Introduction	2
1.1	Related works	4
2	Preliminaries	6
2.1	Definitions and setup	6
3	An adaptive debiased calibration test	9
3.1	Debiasing	9
3.2	An adaptive test	11
3.3	Necessity of debiasing	12
4	Experiments	13
4.1	Synthetic data: Power analysis	13
4.2	Results on empirical datasets	15
5	Lower bounds for detecting mis-calibration	17
5.1	Impossibility for general continuous mis-calibration curves	17
5.2	Hölder alternatives	18

^{*}Equal Contribution.

[†]Graduate Group in Applied Mathematics and Computational Science, Univ. of Pennsylvania. dh7401@sas.upenn.edu.

[‡]Graduate Group in Applied Mathematics and Computational Science, Univ. of Pennsylvania. xinmengh@sas.upenn.edu.

[§]Department of Electrical and Systems Engineering, Univ. of Pennsylvania. hassani@seas.upenn.edu.

[¶]Department of Statistics and Data Science, Univ. of Pennsylvania. dobriban@wharton.upenn.edu.

6 Reduction to two-sample goodness-of-fit testing	19
6.1 Comparison with the debiased plug-in test	22
7 Conclusion	23
8 Appendix	23
8.1 Proofs	24
8.1.1 Proof of Theorem 3.1	24
8.1.2 Proof of Theorem 3.2	29
8.1.3 Proof of Proposition 3.4	29
8.1.4 Proof of Proposition 5.1	31
8.1.5 Proof of Theorem 5.2	32
8.1.6 Proof of Lemma 5.3	36
8.1.7 Proof of Theorem 6.1	37
8.1.8 Proof of Corollary 6.2	39
8.2 Background	39
8.2.1 Hölder continuity on the simplex	39
8.2.2 Two-sample goodness-of-fit tests	39
8.2.3 Binning scheme for the simplex	41
8.2.4 Calibration test for discrete predictions	42
8.3 More experiments	42

1 Introduction

The prediction accuracy of contemporary machine learning methods such as deep neural networks is steadily increasing, leading to adoption in more and more safety-critical fields such as medical diagnosis (Esteva et al., 2017), self-driving vehicles (Bojarski et al., 2016), and recidivism forecasting (Berk, 2017). In these applications and beyond, machine learning models are required not only to be accurate, but also to be well-calibrated: giving precise probability estimates for the correctness of their predictions.

To be concrete, consider a classification problem where the goal is to classify features \mathbf{x} (such as images) into one of several classes \mathbf{y} (such as a building, vehicle, etc.). A probabilistic classifier (or, probability predictor) f assigns to each input \mathbf{x} a probability distribution $f(\mathbf{x})$ over the classes. For a given input \mathbf{x} , the entries of $f(\mathbf{x})$ represent the probabilities assigned by the classifier to the event that the outcome belongs to the k -th class for all $k = 1, \dots, K$. This classifier is *calibrated* if for any value \mathbf{z} taken by $f(\mathbf{x})$, and for all classes k , the probability that the outcome belongs to the k -th class, i.e., $[\mathbf{y}]_k = 1$, equals the predicted probability, i.e., the k -th coordinate $[\mathbf{z}]_k$ of \mathbf{z} :

$$P([\mathbf{y}]_k = 1 | f(\mathbf{x}) = \mathbf{z}) = [\mathbf{z}]_k.$$

This form of calibration is an important part of uncertainty quantification, decision science, analytics, and forecasting (see e.g., Hilden et al., 1978; Miller et al., 1991, 1993; Steyerberg et al., 2010; Hand, 1997; Jolliffe and Stephenson, 2012; Van Calster and Vickers, 2015; Harrell, 2015; Tetlock and Gardner, 2016; Shah et al., 2018; Steyerberg et al., 2019, etc). Unfortunately, however, recent works starting from at least Guo et al. (2017) have reported that modern machine learning methods are often poorly calibrated despite their high accuracy; which can lead to harmful consequences (e.g., Van Calster and Vickers, 2015; Steyerberg et al., 2019).

To address this problem, there has been a surge of works aimed at improving calibration of machine learning models. These methods seek to achieve calibration either by modifying the training procedure (Harrell, 2015; Lakshminarayanan et al., 2017; Kumar et al., 2018; Thulasidasan et al., 2019; Zhang et al., 2020; Mukhoti et al., 2020) or by learning a re-calibration function that transforms, in a post-hoc way, the predictions to well-calibrated ones (Cox, 1958; Steyerberg et al., 2010; Platt, 1999; Zadrozny and Elkan, 2001, 2002; Guo et al., 2017; Kumar et al., 2019).

In this regard, a key challenge is to rigorously assess and compare the performance of calibration methods. Without such assessments, we have limited ability to know when algorithms for improving calibration have

a real effect, and when their improvements are merely artifacts due to random noise in finite-size datasets. As it turns out, existing works do not offer a satisfactory solution to this challenge.

In more detail, in this work, we consider the problem of detecting mis-calibration of predictive models using a finite validation dataset. We focus on models whose probability predictions are continuous functions of the features—which is generally true of most modern machine learning methods, including deep neural nets. We develop efficient and provably optimal algorithms to test their calibration.

Detecting mis-calibration has been studied from the perspective of statistical hypothesis testing. The seminal work of Cox (1958) formulated a test of calibration for a collection of binary (yes-no) predictions, and proposed using a score test for a logistic regression model. This has been widely used and further developed, leading to various tests for the so-called calibration slope and calibration intercept, which can validate various qualitative versions of model calibration, see e.g., Hosmer and Lemeshow (1980); Miller et al. (1991); Steyerberg et al. (2019) and references therein. In pioneering work, Miller (1962) suggested a chi-squared test for testing calibration of multiple series of binary predictions. To deal with the challenging problem of setting critical values (i.e., how large of an empirical mis-calibration is statistically significant?) for testing calibration, bootstrap methods have become common, see e.g., Harrell (2015). We refer to Section 1.1 for more details and for a discussion of other related works.

In contrast to the above works that aim to test calibration slopes and intercepts, we aim to develop a *nonparametric hypothesis test* for calibration, which does not assume a specific functional form (such as a logistic regression model), for the deviations to be detected from perfect calibration. A nonparametric approach has the advantage that it can detect subtle forms of mis-calibration even after re-calibration by parametric methods. However, existing approaches for nonparametric testing often rely on ad hoc techniques for binning the probability predictions, which is a limitation because the results can depend on the way that the binning has been performed (Harrell, 2015; Steyerberg et al., 2019). In contrast, our *adaptive tests* automatically select an optimal binning scheme. Finally, as a new development in the area of testing calibration, T-Cal has theoretically guaranteed *minimax optimality properties* for detecting certain reasonable types of smooth mis-calibration. These properties make T-Cal both practically and theoretically appealing.

We consider a given multi-class probabilistic classifier, and are interested to test if it is calibrated. We make the following contributions:

- As a candidate test statistic, we consider the the plug-in estimator of ℓ_2 -expected calibration error (ECE), which is the expectation of the squared distance between the probability predictions and class probabilities given these predictions. This is also known as the mean calibration error (e.g., Harrell, 2015, p. 105). While the plug-in estimator is biased (i.e., its expectation is not zero even under perfect calibration), we show to how to construct a *debiased plug-in estimator* (DPE).

We consider detecting mis-calibration when the deviation between predicted class probabilities and their true values—the “mis-calibration curve”—satisfies a classical smoothness condition known as Hölder continuity. We later show that such a condition is essentially unavoidable. Under this condition, we show that T-Cal can detect mis-calibration if the ECE is sufficiently large and the number of bins is chosen appropriately, depending on the smoothness (Theorem 3.1).

- To make T-Cal practical, we present a version that is adaptive to the unknown smoothness parameter (Theorem 3.2). This makes T-Cal fully tuning-free and practically useful. From a theoretical perspective, adaptivity only requires a minor additional increase in the level of mis-calibration that can be detected; by a $\log n$ factor.
- We support our theoretical results with a broad range of experiments. We provide simulations, which support our theoretical optimality results. We also provide experiments with several popular deep neural net architectures (ResNet-50, VGG-19, DenseNet-121, etc), on benchmark datasets (CIFAR 10 and 100, ImageNet) and several standard post-hoc calibration methods (Platt scaling, histogram binning, isotonic regression, etc).
- To complement these results, we argue that T-Cal is optimal, by providing a number of fundamental lower bounds. We prove that detecting mis-calibration from a finite dataset is only possible when the mis-calibration curve is sufficiently smooth (Proposition 5.1).

- When the mis-calibration curves are Hölder smooth, we show that the calibration error required for reliable detection of mis-calibration has to be appropriately large (Theorem 5.2). This minimax result relies on Ingster’s (or the chi-squared) method. Combined with our previous results, this shows that T-Cal is minimax optimal.
- To further put our problem in context, we show that testing calibration can be reduced to a well-known problem in statistical inference—the two-sample goodness-of-fit problem—by a novel randomization technique. Based on this insight, and building on the results of Arias-Castro et al. (2018); Kim et al. (2022) on goodness-of-fit testing, we present another asymptotically minimax optimal test for mis-calibration that matches the lower bound (Theorem 6.1). While this method is theoretically optimal, it relies on sample splitting; and in experiments it is not as sample-efficient as our previous method.

Our numerical results can be reproduced with code available at <https://github.com/dh7401/T-Cal>. We now summarize some key takeaways:

- **The need for statistical significance to claim calibration.** It is crucial to perform rigorous statistical tests to assess the calibration of machine learning methods. While models with smaller empirical ECE generally tend to be better calibrated, these values can be highly influenced by noise and randomness inherent in finite datasets. Hence it is crucial to develop and use tools to assess statistical significance—such as the hypothesis tests of calibration that we develop—when claiming improved calibration.
- **Potential suboptimality of popular approaches.** The currently prevalent usage of popular metrics, such as the empirical ECE, may be suboptimal. The current standard is to evaluate mis-calibration metrics using a fixed number of bins (such as 15) of the probability scores, for all prediction models (ResNet, VGG, etc), and all datasets. Our results show theoretically that the optimal number of bins increases with the level of oscillations and non-smoothness expected in the probability predictor. Modern machine learning methods are becoming more and more over-parametrized and data-adaptive. This suggests that it is ever more important to use a careful model- and data-adaptive test (and number of bins) when testing calibration.

1.1 Related works

There is a great body of related work on evaluating the calibration of prediction methods, on improving calibration accuracy, and on nonparametric hypothesis testing techniques. We only review the most closely related works.

Broader context. Broadly speaking, the study of calibration is an important part of the study of classification, prediction, analytics, and forecasting (e.g., Hilden et al., 1978; Miller et al., 1991, 1993; Steyerberg et al., 2010; Hand, 1997; Jolliffe and Stephenson, 2012; Van Calster and Vickers, 2015; Harrell, 2015; Tetlock and Gardner, 2016; Shah et al., 2018; Steyerberg et al., 2019, etc).

Calibration. As recounted in Lichtenstein et al. (1977), research on calibration dates back at least to the early 1900s, when meteorologists suggested expressing predictions as probabilities, and comparing them to observed empirical frequencies. Calibration has since been studied in a variety of areas, including meteorology, statistics, medicine, computer science, and social science; and under a variety of names, such as realism or realism of confidence, appropriateness of confidence, validity, external validity, secondary validity, and reliability (Lichtenstein et al., 1977). A general finding in this area is that human forecasters are often overconfident and thus mis-calibrated (e.g., Keren, 1991, etc), as codified for instance in Tversky and Kahneman’s celebrated work on prospect theory (Kahneman and Tversky, 2013).

Beyond our hypothesis testing perspective, approaches to study calibration include Bayesian perspectives (e.g., Dawid, 1982; Kadane and Lichtenstein, 1982, etc.) and online settings (e.g., Foster and Vohra, 1998; Vovk and Shafer, 2005, etc.). See also Section 10.9 of Harrell (2015), Section 15.3 of Steyerberg et al. (2019), and Hastie and Tibshirani (1997); Ivanov et al. (1999); Gareczarek (2002); Buja et al. (2005); Toll et al. (2008); Gebel (2009); Serrano (2012); Van Calster et al. (2019); Huang et al. (2020), among others.

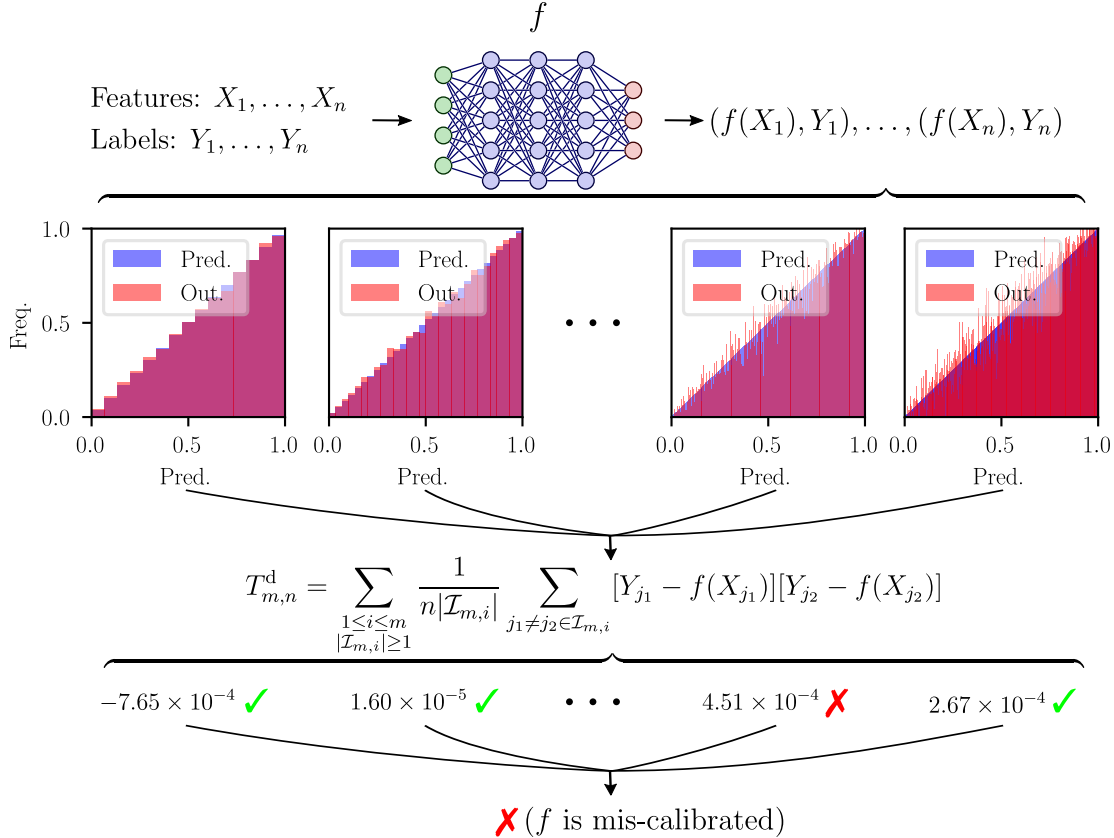


Figure 1: An overview of T-Cal. For a given probability predictor f , we compute $T_{m,n}^d$, the debiased plug-in estimator (DPE), binned over several scales (See (6) for the definition). We then compare each value with the hypothetical distribution of DPE that we would get if the model were perfectly calibrated. The hypothesis of perfect calibration is rejected if at least one of the scales is detected to be mis-calibrated. This multi-scale approach ensures that T-Cal adaptively detects mis-calibration.

Calibration Measures. Proper scoring rules (Good, 1952; De Finetti, 1962; Savage, 1971; Winkler et al., 1996; DeGroot and Fienberg, 1983; Gneiting et al., 2007) such as the Brier score (Brier, 1950) and negative log-likelihood (e.g., Winkler et al., 1996, etc) are objective functions of two probability distributions (a true distribution and a predicted distribution). They are minimized when the predicted distribution equals the true distribution; see also Bickel (2007).

As discussed in Sections 4.5 and 10.9 of Harrell (2015), some of the standard techniques in the area include plotting calibration curves, also known as reliability diagrams (estimated probabilities against predicted ones); which can be bias-corrected using the bootstrap; and re-calibration by fitting statistical models to these curves (e.g., Austin and Steyerberg, 2014, etc). More recently, the notion of ECE, also known as mean absolute calibration error (e.g., Harrell, 2015, p. 105) is popularized in Naeini et al. (2015) and later generalized to multi-class settings in Vaicenavicius et al. (2019). Gupta et al. (2020b) develop a binning-free calibration measure based on the Kolmogorov-Smirnov test.

Calibration in Modern Machine Learning. Guo et al. (2017) draw attention to the mis-calibration of modern neural networks and compare different recalibration methods based on ECE. Many other works (Milios et al., 2018; Kull et al., 2019; Zhang et al., 2020) also evaluate their methods using ECE or its variants. In the following works of Vaicenavicius et al. (2019); Kumar et al. (2019), it has been recognized that ECE evaluated on a fixed binning scheme can underestimate the calibration error. The limitation of fixed binning has been known for the analogous problems of testing probability distributions and densities, see e.g., Mann and Wald (1942), or page 19 of Ingster and Suslina (2012). Kumar et al. (2019) proposes

a debiased ECE, but only for probability predictors with a finite number of outputs. Nixon et al. (2019) empirically study various versions of ECE obtained by adjusting hyperparameters involved in the estimator of ECE (such as norm, binning scheme, and class conditionality), and find that the choice of calibration measure is crucial when comparing different calibration methods. Roelofs et al. (2020) propose a heuristic for choosing an optimal number of bins when computing ECE. Zhang et al. (2020) use kernel density estimation to estimate ECE without relying on a binning scheme. Zhao et al. (2020) show that individual calibration is possible by randomized predictions and propose a training objective to enforce individual calibration. See also Niculescu-Mizil and Caruana (2005); Kull et al. (2017), among others.

There has been interest in a variety of forms of calibration. We study the strongest form, multi-class calibration, which is stronger than other definitions such as marginal calibration and confidence (top) calibration (Vaicenavicius et al., 2019; Widmann et al., 2019).

Nonparametric Hypothesis Testing. Ingster (1987, 2000) considers the problem of testing goodness-of-fit for nonparametric densities and derives a minimax separation rate with respect to L^p metrics. Ingster (1986) derives the minimax testing rate for two-sample testing where densities are separated in an ℓ_2 sense, and shows that the chi-squared test is minimax optimal. Arias-Castro et al. (2018) extend this result to arbitrary dimensions. Kim et al. (2022) prove that a permutation test can also achieve the optimal separation rate. Butucea and Tribouley (2006) study two-sample testing in more general Besov spaces, but for one-dimensional densities; they also prove adaptivity.

Hypothesis testing for calibration. Cox (1958) formulates a test of calibration for a collection of Bernoulli random variables, as a test that their success probabilities are equal to some given values; and proposed using a score test for a logistic regression model. These tests are referred to as testing the calibration slope and intercept, and they are part of a broader hierarchy of calibration (Van Calster et al., 2016). See also Miller et al. (1991); Steyerberg et al. (2019) and references therein. Miller (1962), Section 5, suggests chi-squared test for testing calibration of a collection of sequences of Bernoulli random variables. The Hosmer-Lemeshow test (Hosmer and Lemeshow, 1980) is a goodness-of-fit test for logistic regression models. The test is based on a chi-squared statistic that measures differences between expected and observed numbers of events in subgroups, and thus has, on the surface, a similarity to the types of test statistics we consider.

Seillier-Moiseiwitsch and Dawid (1993) study testing the calibration of sequential probability forecasts. Bröcker and Smith (2007) study the bootstrap-based procedure they call consistency resampling to produce standard error bars in reliability diagrams; without focusing on its optimality. Vaicenavicius et al. (2019) use consistency resampling to test a hypothesis of perfect calibration; again without studying of its optimality. Widmann et al. (2019) propose kernel-based mis-calibration measures together with their estimators, and argue that the estimators can be viewed as calibration test statistics. Tamás and Csáji (2021) suggest distribution-free hypothesis tests for the null $H_0 : \mathbb{E}[Y | X] = X$ based on conditional kernel mean embedding.

Note on terminology. The term calibration sometimes has a differing meaning in a variety of areas of human activity, including measurement technology, engineering, economics, and even statistics etc., see e.g., Franklin (1999); Dawkins et al. (2001); Kodovský and Fridrich (2009); Osborne (1991). These generally mean adjusting a measurement to agree with a desired standard, within a specified accuracy. However, in our work we focus only on the notion of probabilistic calibration described so far.

2 Preliminaries

2.1 Definitions and setup

For $K \geq 2$, consider a K -class classification problem where $X \in \mathcal{X}$ is the input feature vector (for instance, an image) and $Y \in \mathcal{Y} := \{\mathbf{y} = (y_1, \dots, y_K)^\top \in \{0, 1\}^K : \sum_{i=1}^K y_i = 1\}$ is the one-hot encoded output label (for instance, the indicator of the class of the image: building, vehicle, etc).

We consider a probabilistic classifier f mapping feature space to probability distributions over K classes. Formally, the output space is the $(K - 1)$ -dimensional simplex Δ_{K-1} ,

$$\Delta_{K-1} := \{\mathbf{z} = (z_1, \dots, z_K)^\top \in [0, 1]^K : z_1 + \dots + z_K = 1\},$$

i.e., $f : \mathcal{X} \rightarrow \Delta_{K-1}$. For any $k \in \{1, \dots, K\}$, the individual component $[f(X)]_k$ denotes the predicted probability of the k -th class. Thus, f is also referred to as a probability predictor. The probability predictor f is assumed to be pre-trained on data that are independent of our calibration data at hand.

We assume that the feature-label pair (X, Y) has an unknown joint probability distributed P on $\mathcal{X} \times \mathcal{Y}$. Calibration requires that the predicted probabilities of correctness are equal to the true probabilities. For an integer $d \geq 1$, and a vector $\mathbf{v} \in \mathbb{R}^d$, we refer to the coordinates of \mathbf{v} as both $[\mathbf{v}]_1, \dots, [\mathbf{v}]_d$ and v_1, \dots, v_d . Thus, given that we predicted the probabilities $f(X) = \mathbf{z}$, and thus $[f(X)]_k = [\mathbf{z}]_k$, the true probability that $[Y]_k = 1$ should be equal to $[f(X)]_k = [\mathbf{z}]_k$. Thus, for almost every \mathbf{z} , calibration requires that for all $k = 1, \dots, K$,

$$P[[Y]_k = 1 \mid f(X) = \mathbf{z}] = [\mathbf{z}]_k.$$

We can reformulate this in a way that is more convenient to study. The map $(\mathbf{x}, \mathbf{y}) \mapsto (f(\mathbf{x}), \mathbf{y})$ induces a probability distribution on $\Delta_{K-1} \times \mathcal{Y}$; where we can think of (\mathbf{x}, \mathbf{y}) as a realization of (X, Y) . As will be discussed shortly, calibration only depends on the joint distribution of $(f(X), Y)$. For this reason, we also denote the joint distribution of $(f(X), Y)$ by P when there is no confusion. We write $Z := f(X)$ for the predicted probabilities corresponding to X .

We define the *regression function* $\text{reg}_f : \Delta_{K-1} \rightarrow \Delta_{K-1}$ as

$$\text{reg}_f(\mathbf{z}) := \mathbb{E}[Y \mid f(X) = \mathbf{z}] = \mathbb{E}[Y \mid Z = \mathbf{z}],$$

where the expectation is conditioned on the score Z with $(Z, Y) \sim P$. Note that each component, for $k = 1, \dots, K$, has the form $\mathbb{E}[[Y]_k = 1 \mid f(X) = \mathbf{z}] = P[[Y]_k = 1 \mid f(X) = \mathbf{z}]$. Especially for binary classification, this is also referred to as the *calibration curve* of the probabilistic classifier f (Harrell, 2015). Since we are particularly interested in continuous probability predictors, we assume that the marginal distribution P_Z of Z has a density with respect to the uniform measure on Δ_{K-1} . Then, this expectation is well defined almost everywhere.

In this language, the probabilistic classifier f is *perfectly calibrated* if $\text{reg}_f(Z) = Z$ almost everywhere.¹ Further, it turns out that it is important to study *the deviations from calibration*. For this reason, we define the *residual function* $\text{res}_f : \Delta_{K-1} \rightarrow \mathbb{R}^K$ as

$$\text{res}_f(\mathbf{z}) := \text{reg}_f(\mathbf{z}) - \mathbf{z},$$

so that perfect calibration amounts to $\text{res}_f(Z) = 0$ almost everywhere. When (Z, Y) have a joint distribution P , we sometimes write $\text{res}_f = \text{res}_{f,P}$ to display the dependence of the mis-calibration curve on P . As we will see, the structure of the residual function crucially determines our ability to detect mis-calibration. In analogy to the notion of calibration curves mentioned above, we may also call res_f the *mis-calibration curve* of the probabilistic classifier f .

We observe calibration data $(Z_i, Y_i) \in \Delta_{K-1} \times \mathcal{Y}$, $i \in \{1, \dots, n\}$, sampled i.i.d. from P , and denote their joint product distribution as P^n . Our goal is to rigorously test if f is perfectly calibrated based on this finite calibration dataset. The calibration properties of the probabilistic classifier f can be expressed equivalently in terms of the distribution P of $(f(X), Y) = (Z, Y)$. Therefore, we will sometimes refer to testing the calibration of the distribution P , and the probabilistic classifier will be implicit.

Expected calibration error. For any $p \geq 1$, and for an integer $K \geq 2$, we denote the ℓ_p -norm of $\mathbf{x} = (x_1, \dots, x_K)^\top \in \mathbb{R}^K$ by $\|\mathbf{x}\|_p := (\sum_{i=1}^K |x_i|^p)^{1/p}$. The ℓ_p -ECE (Expected Calibration Error) for the distribution P , also known as the mean calibration error (e.g., Harrell, 2015, p. 105), is

$$\ell_p\text{-ECE}(f) = \ell_p\text{-ECE}_P(f) = \mathbb{E}_{Z \sim P_Z} [\|\text{reg}_f(Z) - Z\|_p^p]^{\frac{1}{p}} = \mathbb{E}_{Z \sim P_Z} \left[\sum_{k=1}^K |[\text{res}_f(Z)]_k|^p \right]^{\frac{1}{p}}. \quad (1)$$

In words, this quantity measures the average over all classes $k = 1, \dots, K$ and over the data distribution $X \sim P_X$ of the per-class error $[\text{res}_f(\mathbf{z})]_k = \mathbb{E}[[Y]_k \mid f(X) = \mathbf{z}] - [\mathbf{z}]_k$ between the predicted probability of class k for input X —i.e., $[\mathbf{z}]_k = [f(X)]_k$ —and the actual probability $\mathbb{E}[[Y]_k \mid f(X) = \mathbf{z}] = P[[Y]_k = 1 \mid f(X) = \mathbf{z}]$ of that class. For instance, when the number of classes is $K = 2$, and the power is $p = 1$, we have $\ell_1\text{-ECE}(f) = \mathbb{E}_{X \sim P_X} \sum_{k=1}^2 |P[[Y]_k = 1 \mid f(X)] - [f(X)]_k| = 2\mathbb{E}_{X \sim P_X} |P[[Y]_1 = 1 \mid f(X)] - [f(X)]_1|$.

¹In the binary case ($K = 2$), we identify Δ_{K-1} with $[0, 1]$ via the map $(z, 1-z)^\top \mapsto z$ and use $\mathcal{Y} = \{0, 1\}$ instead of the one-hot encoded output space. We say f is perfectly calibrated if $\text{reg}_f(z) := P(Y = 1 \mid f(X) = z) = z$ almost everywhere.

Hölder continuity. We describe the notion of Hölder continuity for functions defined on Δ_{K-1} . For simple description, we only provide the definition for $K = 2$. See Section 8.2.1 for the complete definition for general K .

Identifying Δ_1 with $[0, 1]$ via the map $(z, 1 - z)^\top \mapsto z$, a function $g : \Delta_1 \rightarrow \mathbb{R}$ can be equivalently understood as a function $g : [0, 1] \rightarrow \mathbb{R}$. For an integer $d \geq 0$ and a function $g : [0, 1] \rightarrow \mathbb{R}$, let $g^{(d)}$ be the d -th derivative of the function g . For a real number s , we denote the smallest integer greater than or equal to s by $\lceil s \rceil$.

For a Hölder smoothness parameter $s > 0$ and a Hölder constant $L > 0$, let $\mathcal{H}_K(s, L)$ be the class of (s, L) -Hölder continuous functions $g : [0, 1] \rightarrow \mathbb{R}$ satisfying, for all $x_1, x_2 \in [0, 1]$

$$\left| g^{(\lceil s \rceil - 1)}(x_1) - g^{(\lceil s \rceil - 1)}(x_2) \right| \leq L |x_1 - x_2|^{s - \lceil s \rceil + 1}. \quad (2)$$

In particular, $\mathcal{H}_K(1, L)$ denotes all L -Lipschitz functions. We consider $L > 0$ as an arbitrary fixed constant, and we do not display the dependence of our results on its value. For instance, when the Lipschitz constant is $L = 1$, and the Hölder smoothness parameter is $s = 1.5$, this is the set of real-valued functions g defined on $[0, 1]$ such that for all $x_1, x_2 \in [0, 1]$, $|g'(x_1) - g'(x_2)| \leq L|x_1 - x_2|^{0.5}$.

Goal. Our goal is to test the null hypothesis of perfect calibration, i.e., $\text{res}_f = 0$, against the alternative hypothesis that the model is mis-calibrated. To quantify mis-calibration, we use the notion of the ℓ_p -ECE(f) from (1). We study the signal strength needed so that reliable mis-calibration detection is possible. Further, we assume that the mis-calibration curves are Hölder continuous, because we will show that by only assuming continuity, reliable detection of mis-calibration is impossible.

For a Hölder smoothness parameter s and a Hölder constant L , let $\mathcal{P}_{s, L, K}$ be the family of probability distributions P over the predictions and labels $(f(X), Y) = (Z, Y) \in \Delta_{K-1} \times \mathcal{Y}$ under which the residual map $\mathbf{z} \mapsto [\text{res}_{f, P}(\mathbf{z})]_k$ (i.e., the map res_f under the distribution $(Z, Y) \sim P$) belongs to the class of (s, L) -Hölder continuous functions $\mathcal{H}_K(s, L)$ for every $k \in \{1, \dots, K\}$. Define the collection \mathcal{P}_0 of joint distributions P of (Z, Y) under which the probability predictor f is perfectly calibrated:

$$\mathcal{P}_0 := \{P \in \mathcal{P}_{s, L, K} : \text{res}_{f, P}(Z) = 0, P_{Z\text{-a.s.}}\}.$$

For a separation rate $\varepsilon > 0$, define the collection $\mathcal{P}_1(\varepsilon, p, s)$ of joint distributions P of (Z, Y) under which the ℓ_p -ECE of f is at least ε :

$$\mathcal{P}_1(\varepsilon, p, s) := \{P \in \mathcal{P}_{s, L, K} : \ell_p\text{-ECE}_P(f) \geq \varepsilon\}. \quad (3)$$

We will also refer to these distributions as ε -*miscalibrated*. Our goal is to test the *null hypothesis* of calibration against the *alternative* of an ε -calibration error:

$$H_0 : P \in \mathcal{P}_0 \quad \text{versus} \quad H_1 : P \in \mathcal{P}_1(\varepsilon, p, s). \quad (4)$$

Hypothesis testing. We recall some notions from hypothesis testing (e.g., Lehmann and Romano, 2005; Ingster and Suslina, 2012, etc) that we use to formulate our problem. A *test* ξ is a function² $\xi : (\Delta_{K-1} \times \mathcal{Y})^n \rightarrow \{0, 1\}$ of the data, given a dataset $S = \{(X_i, Y_i)\}_{i=1}^n \in (\Delta_{K-1} \times \mathcal{Y})^n$, the decision $\xi(S)$ of rejecting the null hypothesis. In other words, for a given dataset S , $\xi(S) = 1$ means that we detect mis-calibration, and $\xi(S) = 0$ means that we do not detect mis-calibration.

Denote the set of all *level* $\alpha \in (0, 1)$ tests, which have a *false detection rate* (or, *false positive rate*; *type I error*) bounded by α , as

$$\Phi_n(\alpha) := \left\{ \xi : \sup_{P \in \mathcal{P}_0} P(\xi = 1) \leq \alpha \right\}.$$

The probability $P(\xi = 1)$ is taken with respect to the distribution of the sample. For $\varepsilon > 0$ and $P \in \mathcal{P}_1(\varepsilon, p, s)$ from (3), we want to minimize the *false negative rate* (*type II error*) $P(\xi = 0)$, the probability of not detecting mis-calibration. We consider the worst possible value (maximum or rather supremum) $\sup_{P \in \mathcal{P}_1(\varepsilon, p, s)} P(\xi = 0)$ of the type II error, over all distributions $P \in \mathcal{P}_1(\varepsilon, p, s)$. We then want to minimize

²To be rigorous, a Borel measurable function.

this over all tests $\xi \in \Phi_n(\alpha)$ that appropriately control the level, leading to the *minimax risk* (minimax type II error)

$$R_n(\varepsilon, p, s) := \inf_{\xi \in \Phi_n(\alpha)} \sup_{P \in \mathcal{P}_1(\varepsilon, p, s)} P(\xi = 0).$$

In words, among all tests that have a false detection rate of $\alpha < 1$ using a sample of size n , we want to find the one with the best possible (smallest) mis-detection rate over all ε -miscalibrated distributions.

We consider $\alpha \in (0, 1)$ as a fixed constant, and we do not display the dependence of our results on its value. We want to understand how large the ℓ_p ECE (as measured by ε in $\mathcal{P}_1(\varepsilon, p, s)$) needs to be to ensure reliable detection of mis-calibration. This amounts to finding ε' such that the best possible worst-case risk $R_n(\varepsilon', p, s)$ is small. For a fixed $\beta \in (0, 1 - \alpha)$, the minimum separation (signal strength) for s -Hölder functions, in the ℓ_p -norm, needed for a minimax type II error of at most β is defined as

$$\varepsilon_n(\beta; p, s) := \varepsilon_n(p, s) = \inf\{\varepsilon' : R_n(\varepsilon', p, s) \leq \beta\}.$$

Since $\beta \in (0, 1 - \alpha)$ is fixed, we usually omit the dependence of ε_n on this value.

3 An adaptive debiased calibration test

Here we describe our main test for calibration. This relies on a debiased plug-in estimator for ℓ_2 -ECE(f)². We prove that the test is minimax optimal and discuss why debiasing is necessary. We also provide an adaptive plug-in test, which can adapt to an unknown Hölder smoothness parameter s .

3.1 Debiasing

The calibration error of a continuous probability predictor f is often estimated by a discretized plug-in estimator associated with a partition (or binning) of the simplex Δ_{K-1} (e.g., Cox, 1958; Harrell, 2015). The early work of Cox (1958) already recommended grouping together similar probability forecasts. More recently, Guo et al. (2017) divide the interval $[0, 1]$ into bins of equal width and compute (the top-1) ECE by averaging the difference between confidence and accuracy in each bin. Vaicenavicius et al. (2019) generalize this idea to K -class classification and data-dependent partitions.

In this work, we use an equal-width partition \mathcal{B}_m of the simplex Δ_{K-1} , which is parametrized by a binning scheme parameter $m \in \mathbb{N}_+$. The partition \mathcal{B}_m consists of m^{K-1} simplices with equal volumes and diameters proportional to m^{-1} . The construction of \mathcal{B}_m is elaborated in Section 8.2.3. The purpose of using an equal-width partition \mathcal{B}_m is only for a simpler description of our results, and any partition with aforementioned properties (equal volumes and $\Theta(m^{-1})$ diameters) can be used.

Let us denote the sets comprising the partition as $\mathcal{B}_m = \{B_1, \dots, B_{m^{K-1}}\}$. For each $i \in \{1, \dots, m^{K-1}\}$, define the indices of data points falling into the bin B_i as $\mathcal{I}_{m,i} := \{j : Z_j \in B_i, 1 \leq j \leq n\}$. Then, for each $i \in \{1, \dots, m^{K-1}\}$, the averaged difference between probability predictions $Z_j = f(X_j)$ and true labels Y_j for the probability predictions in B_i is $|\mathcal{I}_{m,i}|^{-1} \sum_{j \in \mathcal{I}_{m,i}} (Y_j - Z_j)$. This estimates $\mathbb{E}[Y - Z \mid Z \in B_i] = \mathbb{E}[\text{res}_f(Z) \mid Z \in B_i]$. Now, the quantity $\ell_2\text{-ECE}(f)^2 = \mathbb{E}[\|\text{res}_f(Z)\|^2]$ can be approximated by piecewise averaging as $\sum_{1 \leq i \leq m^{K-1}} P_Z(B_i) \mathbb{E}[\text{res}_f(Z) \mid Z \in B_i]^2$. Plugging in the estimate $|\mathcal{I}_{m,i}|^{-1} \sum_{j \in \mathcal{I}_{m,i}} (Y_j - Z_j)^2$ of $\mathbb{E}[\text{res}_f(Z) \mid Z \in B_i]^2$, we can define a plug-in estimator of $\ell_2\text{-ECE}(f)^2$ as follows:

$$T_{m,n}^b := \sum_{\substack{1 \leq i \leq m^{K-1} \\ |\mathcal{I}_{m,i}| \geq 1}} \frac{|\mathcal{I}_{m,i}|}{n} \left\| \frac{1}{|\mathcal{I}_{m,i}|} \sum_{j \in \mathcal{I}_{m,i}} (Y_j - Z_j) \right\|^2. \quad (5)$$

Above, the sum is taken over bins B_i containing at least one datapoint. As will be discussed in Section 3.3, the plug-in estimator is biased in the sense that its expectation is not zero under perfectly calibrated distributions. Moreover, it does not lead to an optimal test statistic. Informally, this happens because we are estimating both $\mathbb{E}[Y \mid Z \in B_i]$ and $\mathbb{E}[Z \mid Z \in B_i]$ with the same sample $(Z_i, Y_i), i \in \{1, \dots, n\}$. We hence define the *Debiased Plug-in Estimator* (DPE):

Algorithm 1 T-Cal: an optimal test for calibration (based on debiased plug-in estimation of the calibration error)

Input: Probability predictor $f : \mathcal{X} \rightarrow \Delta_{K-1}$; i.i.d. sample $\{(X_i, Y_i) \in \mathcal{X} \times \mathcal{Y} : i \in \{1, \dots, n\}\}$; false detection rate $\alpha \in (0, 1)$; true detection rate $\beta \in (0, 1 - \alpha)$; Hölder smoothness s

Initialize: $m^* \leftarrow \lfloor n^{2/(4s+K-1)} \rfloor$; $T_{m^*, n}^d \leftarrow 0$; $Z_i \leftarrow f(X_i)$ for $\forall 1 \leq i \leq n$; define $\{B_1, \dots, B_{m^{K-1}}\}$ as in Section 8.2.3

for $i = 1$ **to** $(m^*)^{K-1}$ **do**

$\mathcal{I}_{m^*, i} \leftarrow \{j : Z_j \in B_i, 1 \leq j \leq n\}$

$T_{m^*, n}^d \leftarrow T_{m^*, n}^d + \frac{|\mathcal{I}_{m^*, i}|}{n} \left[\left\| \frac{1}{|\mathcal{I}_{m^*, i}|} \sum_{j \in \mathcal{I}_{m^*, i}} (Y_j - Z_j) \right\|^2 - \frac{1}{|\mathcal{I}_{m^*, i}|^2} \sum_{j \in \mathcal{I}_{m^*, i}} \|Y_j - Z_j\|^2 \right]$

end for

if $(m^*)^{K-1} \leq n$ **then**

$\xi_{m^*, n} \leftarrow I \left(T_{m^*, n}^d \geq \sqrt{\frac{2K}{\alpha}} (m^*)^{\frac{K-1}{2}} n^{-1} \right)$

else

$\xi_{m^*, n} \leftarrow I \left(T_{m^*, n}^d \geq \sqrt{\frac{2K}{\alpha}} (m^*)^{-\frac{K-1}{2}} \right)$

end if

Output: Reject H_0 if $\xi_{m^*, n} = 1$

$$T_{m, n}^d := \sum_{\substack{1 \leq i \leq m^{K-1} \\ |\mathcal{I}_{m, i}| \geq 1}} \frac{|\mathcal{I}_{m, i}|}{n} \left[\left\| \frac{1}{|\mathcal{I}_{m, i}|} \sum_{j \in \mathcal{I}_{m, i}} (Y_j - Z_j) \right\|^2 - \frac{1}{|\mathcal{I}_{m, i}|^2} \sum_{j \in \mathcal{I}_{m, i}} \|Y_j - Z_j\|^2 \right]. \quad (6)$$

The debiasing term in (6) ensures that $T_{m, n}^d$ has mean zero under a distribution $P \in \mathcal{P}_0$ under which f is a calibrated probability predictor. Due to the discretization, the mean of $T_{m, n}^d$ is not exactly ℓ_2 -ECE(f)² under $P \in \mathcal{P}_1(\varepsilon, p, s)$, but the debiasing makes it comparable to ℓ_2 -ECE(f)². This will be a crucial step when proving the optimality of $T_{m, n}^d$.

In the following theorem, we prove that $T_{m, n}^d$ can be used as a minimax optimal statistic when the number of bins is chosen in a specific way, namely $m \asymp n^{2/(4s+K-1)}$.³ Crucially, the number of bins required decreases with the smoothness parameter s . In this sense, our result parallels the well known results on optimal choices of the number of bins for testing probability distributions and densities (Mann and Wald, 1942; Ingster and Suslina, 2012).

The guarantee on the power (or, Type II error control) requires the following mild condition, stated in Assumption 3.1. This ensures that probability of each bin is proportional to the inverse of the number of bins up to some absolute constant. In particular, this holds if the density of the probabilities predicted is close to uniform. This assumption is necessary when extending the results of Arias-Castro et al. (2018); Kim et al. (2022) to a general base probability measure μ of the probability predictions over the simplex. See Section 8.2.2 for more discussion.

Assumption 3.1 (Bounded marginal density). *Let ν be the uniform probability measure on the simplex Δ_{K-1} . There exist constants $\nu_l, \nu_u > 0$ such that $\nu_l \leq dP_Z/d\nu \leq \nu_u$ almost everywhere.*

The theorem requires some additional notations. For an event A , we denote by $I(A)$ its indicator random variable, where $I(A) = 1$ if event A happens, and $I(A) = 0$ otherwise. For a real number x , we denote by $\lfloor x \rfloor$ its *floor*, i.e., the largest integer that is smaller than or equal to x .

Theorem 3.1 (Calibration test via debiased plug-in estimation). *Suppose $p \leq 2$ and assume that the Hölder*

³For two sequences $(a_i)_{i \geq 1}, (b_i)_{i \geq 1}$ of positive numbers, we say that $a_i \asymp b_i$ if there are constants $0 < c < C$ such that $ca_i \leq b_i \leq Ca_i$, for all $i \geq 1$.

smoothness parameter s is known. For a binning scheme parameter $m \in \mathbb{N}_+$, let

$$\xi_{m,n}(\alpha) = \xi_{m,n} := \begin{cases} I\left(T_{m,n}^d \geq \sqrt{\frac{2K}{\alpha}} m^{\frac{K-1}{2}} n^{-1}\right) & \text{if } m^{K-1} \leq n, \\ I\left(T_{m,n}^d \geq \sqrt{\frac{2K}{\alpha}} m^{-\frac{K-1}{2}}\right) & \text{if } m^{K-1} > n. \end{cases}$$

Under Assumption 3.1 and for $m^* = \lfloor n^{2/(4s+K-1)} \rfloor$, we have

1. **False detection rate control.** For every P for which f is perfectly calibrated, i.e., for $P \in \mathcal{P}_0$, the probability of falsely claiming mis-calibration is at most α , i.e., $P(\xi_{m^*,n} = 1) \leq \alpha$.
2. **True detection rate control.** There exists $c > 0$ depending only on $(s, L, K, \nu_l, \nu_u, \alpha, \beta)$ such that when

$$\varepsilon \geq cn^{-2s/(4s+K-1)},$$

then for every $P \in \mathcal{P}_1(\varepsilon, p, s)$ —i.e., when f is mis-calibrated with an ℓ_p -ECE of ε —the power (true positive rate) is bounded as $P(\xi_{m^*,n} = 1) \geq 1 - \beta$.

The proof can be found in Section 8.1.1. Combined with our lower bound in Theorem 5.2, this result shows the desired property that our test is *minimax optimal*. This holds for all $p \leq 2$, so that the test is minimax optimal even when the mis-calibration is measured in the ℓ_p norm with $p < 2$. This is consistent with experimental findings such as those of Nixon et al. (2019), where the empirical ℓ_2 -ECE performs better than the empirical ℓ_1 -ECE as a measure of calibration error. Also see Section 4.1 for a comparison of the empirical ℓ_1 -ECE and ℓ_2 -ECE as a test statistic.

Although we present explicit critical values in Theorem 3.1, they can be conservative in practice, as in other works in nonparametric testing (Ingster, 1987; Arias-Castro et al., 2018; Kim et al., 2022). Therefore, we recommend choosing the critical values via a version of bootstrap: consistency resampling (Bröcker and Smith, 2007; Vaicenavicius et al., 2019). See Section 4.2 for further details.

3.2 An adaptive test

The binning scheme used in our plug-in test requires knowing the smoothness parameter s to be minimax optimal. However, in practice this parameter is usually unknown. Can we design an adaptive test that does not require knowing this parameter? Here we answer this question in the affirmative. As in prior works in non-parametric hypothesis testing, e.g., Ingster (2000); Arias-Castro et al. (2018); Kim et al. (2022), we propose an *adaptive test* that can adapt to an unknown Hölder smoothness parameter s . The idea is to evaluate the plug-in test over a variety of partitions, and thus be able to detect mis-calibration at various different scales.

In more detail, we evaluate the test with a number of bins ranging over a dyadic grid $2, 2^2, \dots, 2^B$. In addition, to make sure that we control the false detection rate, we need to divide the level α by the number of tests performed. Thus, for a number $B = \lceil \frac{2}{K-1} \log_2(n/\sqrt{\log n}) \rceil$ of tests performed, we let the adaptive test

$$\xi_n^{\text{ad}} := \max_{1 \leq b \leq B} \xi_{2^b,n} \left(\frac{\alpha}{B} \right) \quad (7)$$

detect mis-calibration if any of the debiased plug-in tests $\xi_{2^b,n}(\alpha/B)$, with the number of bins 2^b , $b \in \{1, \dots, B\}$, detects mis-calibration at level α/B . We summarize the procedure in Algorithm 2.

Theorem 3.2 (Adaptive plug-in test). *Suppose $p \leq 2$. Under Assumption 3.1, the adaptive test from (7) enjoys*

1. **False detection rate control.** For every P for which f is perfectly calibrated, i.e., for $P \in \mathcal{P}_0$, the probability of falsely claiming mis-calibration is at most α , i.e., $P(\xi_n^{\text{ad}} = 1) \leq \alpha$.
2. **True detection rate control.** There exists $c_{\text{ad}} > 0$ depending on $(s, L, K, \nu_l, \nu_u, \alpha, \beta)$ such that the power (true positive rate) is lower bounded as $P(\xi_n^{\text{ad}} = 1) \geq 1 - \beta$ for every $P \in \mathcal{P}_1(\varepsilon, p, s)$ —i.e., when f is mis-calibrated with an ℓ_p -ECE of at least $\varepsilon \geq c_{\text{ad}}(n/\sqrt{\log n})^{-2s/(4s+K-1)}$.

Algorithm 2 Adaptive T-Cal: an adaptive test for calibration

Input: Probability predictor $f : \mathcal{X} \rightarrow \Delta_{K-1}$; i.i.d. sample $\{(X_i, Y_i) \in \mathcal{X} \times \mathcal{Y} : i \in \{1, \dots, n\}\}$; false detection rate $\alpha \in (0, 1)$; true detection rate $\beta \in (0, 1 - \alpha)$

Initialize: $B \leftarrow \lceil \frac{2}{K-1} \log_2(n/\sqrt{\log n}) \rceil$; $Z_i \leftarrow f(X_i)$ for $\forall 1 \leq i \leq n$; $\xi_n^{\text{ad}} \leftarrow 0$

for $b = 1$ **to** B **do**

- Compute $\xi_{2^b, n}(\frac{\alpha}{B})$ as in Algorithm 1
- if** $\xi_{2^b, n}(\frac{\alpha}{B}) = 1$ **then**

 - $\xi_n^{\text{ad}} \leftarrow 1$
 - break**

- end if**

end for

Output: Reject H_0 if $\xi_n^{\text{ad}} = 1$

See Section 8.1.2 for the proof. Compared to the non-adaptive test, this test requires a mild additional factor of $(\log n)^{s/(4s+K-1)}$ in the separation rate ε to guarantee detection. It is well understood in the area of non-parametric hypothesis testing that some adaptation cost is unavoidable, see for instance Spokoiny (1996); Ingster (2000). For more discussion, see Remark 1.

3.3 Necessity of debiasing

Recall from (5) that $T_{m,n}^b$ is the plug-in estimator of $\ell_2\text{-ECE}(f)^2$ without the debiasing term in (6). We argue that this biased estimator is not an optimal test statistic, even for $m = m^* = \lfloor n^{2/(4s+K-1)} \rfloor$ from Theorem 3.1 (which is optimal for the debiased test), by presenting a failure case in the following example.

Example 3.3 (Failure of naive plug-in). *Consider binary classification problem with $K = 2$, $m^* = \lfloor n^{2/(4s+1)} \rfloor$ (assumed to be divisible by 4), and the partition*

$$\mathcal{B}_{m^*} = \{B_1, \dots, B_{m^*}\} = \left\{ \left[0, \frac{1}{m^*}\right), \dots, \left[\frac{m^*-1}{m^*}, 1\right] \right\}.$$

Let P_0 be the distribution over $(Z, Y) \in [0, 1] \times \{0, 1\}$ given by $Z \stackrel{P_0}{\sim} \text{Unif}([0, 1])$ and $Y | Z = z \stackrel{P_0}{\sim} \text{Ber}(z)$ for all $z \in [0, 1]$. Under P_0 , the probability predictor f is perfectly calibrated, i.e., $P_0 \in \mathcal{P}_0$. Let $\zeta : \mathbb{R} \rightarrow \mathbb{R}$ be the function defined by

$$\zeta(x) := e^{-\frac{1}{x(1-x)}} \mathbb{1}_{(0,1)}(x). \quad (8)$$

Let $g : [0, 1] \rightarrow [0, 1]$ be the function (corresponding to the calibration curve of the probability predictor f)

$$g(z) := z - \rho(m^*)^{-s} \sum_{j=0}^{\frac{m^*}{4}-1} \zeta\left(m^*z - \frac{m^*}{4} - j\right) + \rho(m^*)^{-s} \sum_{j=\frac{m^*}{4}}^{\frac{m^*}{2}-1} \zeta\left(m^*z - \frac{m^*}{4} - j\right) \quad (9)$$

for $s \in (\frac{1}{4}, \frac{1}{2})$, $\rho > 0$, and ζ defined in (8). Define the distribution P_1 over (Z, Y) by

$$Z \stackrel{P_1}{\sim} \text{Unif}([0, 1]) \text{ and } Y | Z = z \stackrel{P_1}{\sim} \text{Ber}(g(z))$$

for all $z \in [0, 1]$. As we will show in the proof of Theorem 5.2, (1) the mis-calibration curve $g(z) - z = \text{res}_f(z)$ is s -Hölder and (2) $\ell_2\text{-ECE}_{P_1}(f) = \Theta(n^{-2s/(4s+1)})$.

As can be seen in Figure 2a, the probability predictor f under P_1 is an example of a mis-calibrated predictor, as $f(X)$ is smaller than $\mathbb{E}[Y | f(X)]$ when $f(X)$ is above 0.5; and vice versa. However, the mean of $T_{m^, n}^b$ under the mis-calibrated distribution P_1 is surprisingly smaller than the mean under the calibrated distribution P_0 when n is large enough (Proposition 3.4).*

That is, the statistic $T_{m^, n}^b$ does not capture the amount of mis-calibration, and therefore the calibration test based on it will not perform well. Figure 2b confirms this finding, and Figure 2c displays that this effect can be removed by using the debiased statistic $T_{m^*, n}^d$.*

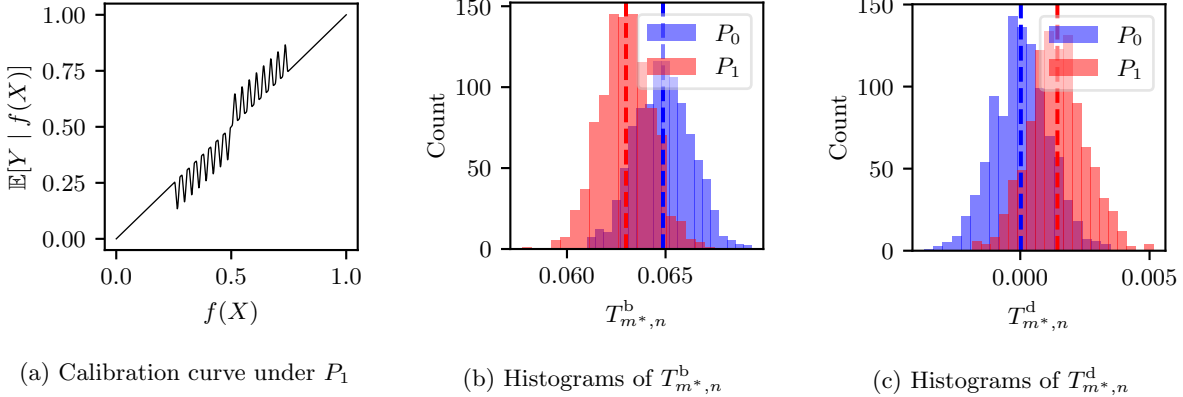


Figure 2: (a) A graph of the calibration curve $z \mapsto g(z) = \mathbb{E}_{P_1}[Y | f(X) = z]$ defined in (9). When the true label probability is above/below 0.5, the model outputs a smaller/larger score. Hence f is a mis-calibrated probability predictor under P_1 . (b) Histograms of $T_{m^*,n}^b$ and $T_{m^*,n}^d$ under P_0 and P_1 are obtained from 1,000 independent observations. We use the parameters $n = 10,000$, $s = 0.3$, and $\rho = 100$. The dashed line indicates the empirical mean of each distribution. Note that the biased estimator $T_{m^*,n}^b$ has a smaller mean under P_1 , which aligns with Proposition 3.4. (c) We see this effect disappears after debiasing and that the mean of $T_{m^*,n}^d$ becomes zero.

Proposition 3.4 (Failure of naive plug-in test). *Let P_0 and P_1 be the distributions defined in Example 3.3, and $m^* = \lfloor n^{2/(4s+1)} \rfloor$. Then $\mathbb{E}_{P_0}[T_{m^*,n}^b] \geq \mathbb{E}_{P_1}[T_{m^*,n}^b]$ for all large enough $n \in \mathbb{N}_+$.*

See Section 8.1.3 for the proof. We remark that it is possible to avoid the phenomenon in Proposition 3.4, by choosing a different m . However, the statistic $T_{m,n}^b$ still cannot achieve the optimal detection rate presented in Theorem 3.1, for any choice of m . Proposition 3.4 is only to highlight the effect of the bias in $T_{m,n}^b$ can be extreme in certain cases, and we do not claim that $m = m^*$ is also the optimal choice for the biased statistic.

We finally comment on the related results of Bröcker (2012); Ferro and Fricker (2012); Kumar et al. (2019). In Bröcker (2012); Ferro and Fricker (2012), the plug-in estimator of the squared ℓ_2 -ECE is decomposed into terms related to reliability and resolution. Based on this observation, Kumar et al. (2019) propose a debiased estimator for the squared ℓ_2 -ECE and show an improved sample complexity for estimation. However, their analysis is restricted to the binary classification case, and to probability predictors with only finitely many output values. It is not clear how to adapt their method to predictors with continuous outputs, because this would require discretizing the outputs. Our debiased plug-in estimator $T_{m,n}^d$ is more general, as it can be used for multi-class problems and continuous probability predictors f . Also, our reason to introduce $T_{m,n}^d$ (testing) differs from theirs (estimation).

4 Experiments

We perform experiments on both synthetic and empirical datasets to support our theoretical results. These experiments suggest that T-Cal is in general superior to state-of-the-art methods.

4.1 Synthetic data: Power analysis

Let $P_0 \in \mathcal{P}_0$ be the distribution defined in Example 3.3—a distribution under which f is perfectly calibrated. For $m \in \mathbb{N}_+$, $s > 0$, $\rho > 0$, and $\zeta : \mathbb{R} \rightarrow \mathbb{R}$ from (8), define $g_m : [0, 1] \rightarrow [0, 1]$ by

$$g_m(z) := z + \rho m^{-s} \sum_{j=0}^{m-1} (-1)^j \zeta \left(2mz - \frac{m}{2} - j \right). \quad (10)$$

This function oscillates strongly, as shown in Figure 3a. Let $P_{1,m}$ be the distribution over $(Z, Y) \in [0, 1] \times \{0, 1\}$ given by $Z \stackrel{P_{1,m}}{\sim} \text{Unif}([0, 1])$ and $Y | Z = z \stackrel{P_{1,m}}{\sim} \text{Ber}(z)$ for all $z \in [0, 1]$. Under $P_{1,m}$, the probability predictor f is mis-calibrated with an ℓ_p -ECE of at least $\varepsilon = \rho \|\zeta\|_{L^p} m^{-s}$. However, since the mis-calibration curve g_m oscillates strongly, mis-calibration can be challenging to detect.

We study the type II error of tests against the alternative where the mis-calibration is specified as $H_1 : (Z, Y) \sim P_{1,m}$. This gives a lower bound on the worst-case type II error over the alternative hypothesis $\mathcal{P}_1(\varepsilon, p, s)$. We repeat the experiment for different values of m to obtain a plot of ℓ_2 -ECE versus type II error.

We compare the test $\xi_{m^*,n}$ with classical calibration tests dating back to Cox (1958), and discussed in Harrell (2015); Vaicenavicius et al. (2019). Harrell (2015) refits a logistic model

$$P(Y = 1 | Z) = \frac{1}{1 + \exp\left(-\left(\gamma_0 + \gamma_1 \log \frac{Z}{1-Z}\right)\right)}$$

on the sample $\{(Z_i, Y_i) : i \in \{1, \dots, n\}\}$ and test the null hypothesis of $\gamma_0 = 0$ and $\gamma_1 = 1$. Especially, we perform the score test (Rao, 1948; Silvey, 1959) in which we use a test statistic derived from the gradient of log-likelihood with respect to the tested parameters and the Fisher information. There are several approaches to set the critical values, including by using the asymptotic distribution theory of sampling statistics under the null hypothesis, or by data reuse methods such as the bootstrap. We estimate the critical values via 1000 Monte Carlo simulations.

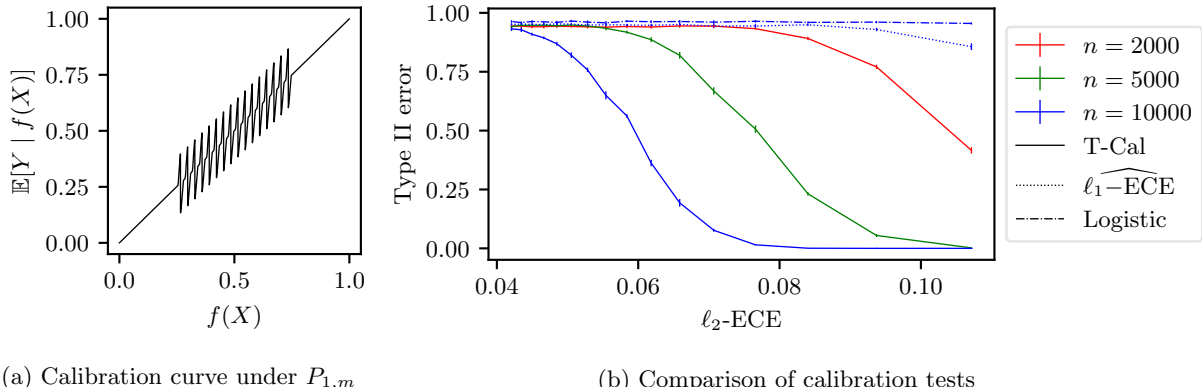


Figure 3: **(a)** A graph of the calibration curve $z \mapsto g_m(z) = \mathbb{E}_{P_{1,m}}[Y | f(X) = z]$ defined in (10). The mis-calibration curve alternates between negative and positive values, making detection challenging. **(b)** We compare our test $\xi_{m^*,n}$ with other commonly used calibration tests. Since our test optimally adjust the number of bins $m^* = \lfloor n^{2/(4s+K-1)} \rfloor$ according to the sample size n , it can detect mis-calibration over smaller and smaller intervals as n grows. On the other hand, the plug-in test $\xi_{m,n}$, with a fixed-in- n binning scheme parameter m , fails to detect mis-calibration over intervals smaller than the bin width. This issue remains when the sample size n increases. The test based on the calibration slope and intercept also suffers from the same issue. Standard error bars are plotted over 10 repetitions.

Vaicenavicius et al. (2019) use $\widehat{\ell_1\text{-ECE}}$, the plug-in estimator for $\ell_1\text{-ECE}$, as their test statistic. They approximate the distribution of $\widehat{\ell_1\text{-ECE}}$ by a bootstrapping procedure called consistency resampling (in which both the probability predictions and the labels are resampled) and compute a p -value based on this approximation. This test also uses a plug-in estimator as the test statistic, but differs from T-Cal because it is not debiased or adaptive. Since the data-generating distribution is known in this synthetic experiment, we set the critical value via 1000 Monte Carlo simulations.

We control the false detection rate at a level $\alpha = 0.05$ and run experiments for $n = 2,000, 5,000$, and $10,000$. We find that our proposed test achieves the lowest type II error, see Figure 3b. We also find that other tests do not leverage the growing sample size n . For this reason, we only display $n = 10,000$ for the other two tests. As can be seen in Figure 3b, T-Cal outperforms other testing methods in true detection rate by a large margin.

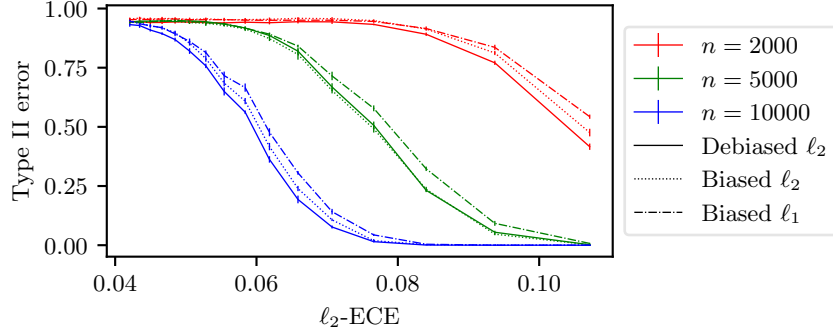


Figure 4: Type II error comparison for $T_{m^*,n}^d$ (T-Cal), $T_{m^*,n}^b$, and $T_{m^*,n}^{\ell_1}$. Using ℓ_2 is better than ℓ_1 , and debiased ℓ_2 (T-Cal) is better than biased ℓ_2 . Standard error bars are plotted over 10 repetitions.

Finally, to confirm the effectiveness of using the ℓ_2 -ECE estimator $T_{m^*,n}^d$, we compare it with a plug-in ℓ_1 -ECE estimator defined as

$$T_{m,n}^{\ell_1} := \sum_{\substack{1 \leq i \leq m^{K-1} \\ |\mathcal{I}_{m,i}| \geq 1}} \frac{|\mathcal{I}_{m,i}|}{n} \left\| \frac{1}{|\mathcal{I}_{m,i}|} \sum_{j \in \mathcal{I}_{m,i}} (Y_j - Z_j) \right\|_1.$$

At the moment, it is unknown how to debias this. We use the optimal binning parameter $m = m^* = \lfloor n^{2/(4s+K-1)} \rfloor$ for both ℓ_1 and ℓ_2 estimators; because it is unknown what the ℓ_1 -optimal binning scheme is. Also, to isolate the effect of debiasing, we compare the biased ℓ_2 estimator $T_{m^*,n}^b$ as well, with the same number of bins. In Figure 4, we see the ℓ_2 estimators consistently outperform the ℓ_1 estimator, regardless of debiasing. While it is a common practice to use a plug-in estimator of ℓ_1 -ECE, our result suggests T-Cal compares favorably to it.

4.2 Results on empirical datasets

	DenseNet 121		ResNet 50		VGG-19	
	$\widehat{\ell_1\text{-ECE}}$	Calibrated?	$\widehat{\ell_1\text{-ECE}}$	Calibrated?	$\widehat{\ell_1\text{-ECE}}$	Calibrated?
No Calibration	2.02%	reject	2.23%	reject	2.13%	reject
Platt Scaling	2.32%	reject	1.78%	reject	1.71%	reject
Poly. Scaling	1.71%	reject	1.29%	reject	0.90%	accept
Isot. Regression	1.16%	reject	0.62%	reject	1.13%	accept
Hist. Binning	0.97%	reject	1.12%	reject	1.28%	reject
Scal. Binning	1.94%	reject	1.21%	reject	1.67%	reject

Table 1: The values of the empirical ℓ_1 -ECE (Guo et al., 2017) and the testing results, via adaptive T-Cal and multiple binomial testing, of models trained on CIFAR-10.

To verify the performance of adaptive T-Cal empirically, we apply it to the probability predictions output by deep neural networks trained on several datasets. Since our goal is to test calibration, we calculate the probabilities predicted by pre-trained models on the test sets. As in (Guo et al., 2017; Kumar et al., 2019; Nixon et al., 2019, etc), we binarize the test labels by taking the top-1 confidence as the new probability prediction, and the labels as the results of the top-1 classification, i.e., $\tilde{Z} = \max_{1 \leq k \leq K} [Z]_k$ and $\tilde{Y} = I(\text{correctly classified by the top-1 prediction})$. This changes the problem of detecting the full-class miscalibration to testing the mis-calibration of a binary classifier. Hence, we choose $K = 2$ for adaptive T-Cal in the experiments below. We refer readers to (Gupta and Ramdas, 2021) for more details about binarization via the top-1 prediction.

CIFAR-10. For the CIFAR-10 dataset, the models are DenseNet 121, ResNet 50, and VGG-19. We first apply the adaptive test directly to the 10,000 uncalibrated probability predictions output by each model, with the false detection rate controlled at the level $\alpha = 0.05$.

For every choice of the number of bins m , we estimate the critical value by taking the upper 5% quantile of the values of the test statistic over 3,000 bootstrap re-samples of the probability predictions. The labels are also chosen randomly, following Bernoulli distributions with the probability prediction as the success probability. We also provide the values of the standard empirical ℓ_1 -ECE calculated with Guo et al. (2017)’s approach for the reader’s reference, and with 15 equal-width bins.

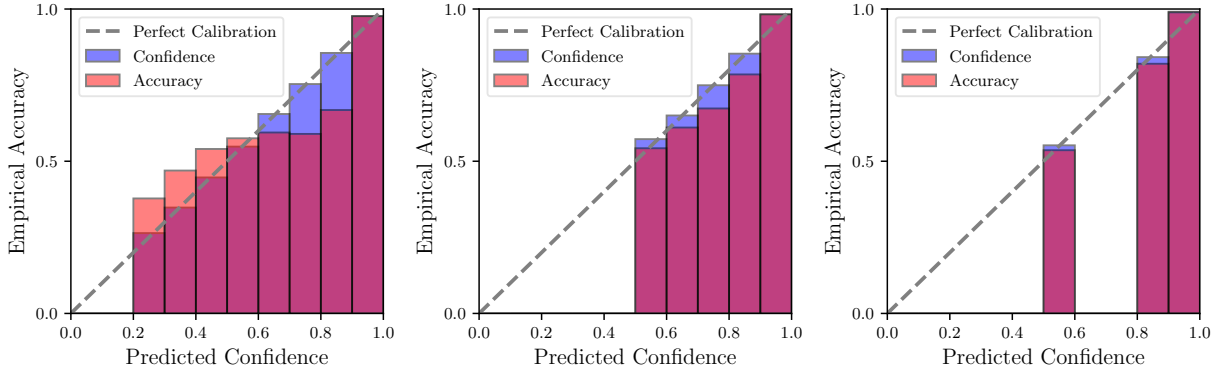


Figure 5: The reliability diagrams for VGG-19, trained on CIFAR-10, calibrated by Platt scaling (left), polynomial scaling (middle), and histogram binning (right). The bins (bars) containing less than 10 data points, where the sample noise dominates, are omitted for clarity.

We then test the probability predictions of these three models calibrated by several post-calibration methods: Platt scaling (Platt, 1999), polynomial scaling, isotonic regression (Zadrozny and Elkan, 2002), histogram binning (Zadrozny and Elkan, 2001), and scaling-binning (Kumar et al., 2019). To this end, we split the original dataset of 10,000 images into 2 sets—of sizes 2,000 and 8,000. The first set is used to calibrate the model, and the second is used to perform adaptive T-Cal and calculate the empirical ℓ_1 -ECE. In polynomial scaling, we use polynomials of order 3 to do regression on all the prediction-label pairs (Z_i, Y_i) , and truncate the calibrated prediction values into the interval $[0, 1]$. We set the binning scheme in both histogram binning and scaling-binning as 15 equal-mass bins. Our implementation is adapted from Kumar et al. (2019).

Since the recalibrated probability predictions output by the latter two methods belong to a finite set, we use a test based on the binomial distribution. See Section 8.2.4 for details. For completeness, we also provide the debiased empirical ℓ_2 -ECE values (Kumar et al., 2019) for models calibrated by the two discrete methods, see the details in Table 4, Section 8.3.

The results are listed in Table 1, where we use “accept” to denote that the test does not reject. The models with smaller empirical ℓ_1 -ECE are more likely to be accepted, by adaptive T-Cal and by multiple binomial testing, as perfectly calibrated. This can be further illustrated by the three empirical reliability diagrams given in Figure 5, where the model’s predictions calibrated by Platt scaling (left) are visually more “mis-calibrated” than those calibrated by polynomial scaling (middle) and histogram binning (right).

CIFAR-100. We perform the same experimental procedure for three models pre-trained on the CIFAR-100 dataset: MobileNet-v2, ResNet 56, and ShuffleNet-v2 (Chen, 2021). The test set provided by CIFAR-100 is split into two parts, containing 2,000 and 8,000 images, respectively. Since the regression functions reg_f of models trained on the larger CIFAR-100 dataset can be more complicated than those of models trained on CIFAR-10, we set the polynomial degree as 5 in polynomial scaling.

The results are listed in Table 2. The values of the debiased empirical ℓ_2 -ECE (Kumar et al., 2019) for the two discrete calibration methods are provided in Table 5, Section 8.3. The results roughly align with the magnitude of the empirical ECE value.

	MobileNet-v2		ResNet 56		ShuffleNet-v2	
	$\widehat{\ell_1\text{-ECE}}$	Calibrated?	$\widehat{\ell_1\text{-ECE}}$	Calibrated?	$\widehat{\ell_1\text{-ECE}}$	Calibrated?
No Calibration	11.87%	reject	15.2%	reject	9.08%	reject
Platt Scaling	1.40%	accept	1.84%	accept	1.34%	accept
Poly. Scaling	1.69%	reject	1.91%	reject	1.81%	accept
Isot. Regression	1.76%	accept	2.33%	reject	1.38%	accept
Hist. Binning	1.66%	reject	2.44%	reject	2.77%	reject
Scal. Binning	1.85%	reject	1.57%	reject	1.65%	accept

Table 2: The values of the empirical ℓ_1 -ECE (Guo et al., 2017) and the testing results, via adaptive T-Cal and multiple binomial testing, of models trained on CIFAR-100.

However, as can be observed in the column corresponding to ResNet 56, this trend is certainly *not* monotone. The calibrated ResNet 56 with the empirical ECE 1.84% is accepted while the calibrated ResNet 56 with a smaller value 1.57% is rejected. Furthermore, the test results reveal that models with relatively large (or small) empirical ℓ_1 -ECE values may not necessarily be poorly (or well) calibrated since the ℓ_1 -ECE values measured can be highly dominated by the sample noise.

ImageNet. We repeat the above experiments on models pre-trained on the ImageNet dataset. We examine three pre-trained models provided in the torchvision package in PyTorch: DenseNet 161, ResNet 152, and EfficientNet-b7. We split the validation set of 50,000 images into a calibration set and a test set—of sizes 10,000 and 40,000, respectively. We use polynomials of degree 5 in polynomial scaling.

The results are listed in Table 3. The values of the debiased empirical ℓ_2 -ECE (Kumar et al., 2019) are provided in Table 6, in Section 8.3. As can be seen, the test results here generally align with the empirical ECE values.

	DenseNet 161		ResNet 152		EfficientNet-b7	
	$\widehat{\ell_1\text{-ECE}}$	Calibrated?	$\widehat{\ell_1\text{-ECE}}$	Calibrated?	$\widehat{\ell_1\text{-ECE}}$	Calibrated?
No Calibration	5.67%	reject	4.99%	reject	2.82%	reject
Platt Scaling	1.58%	reject	1.41%	reject	1.90%	reject
Poly. Scaling	0.62%	accept	0.64%	accept	0.71%	accept
Isot. Regression	0.63%	reject	0.80%	reject	1.06%	reject
Hist. Binning	0.46%	reject	1.26%	reject	0.88%	reject
Scal. Binning	1.55%	reject	1.40%	reject	1.97%	reject

Table 3: The values of the empirical ℓ_1 -ECE (Guo et al., 2017) and the testing results, via adaptive T-Cal and multiple binomial testing, of models trained on ImageNet.

5 Lower bounds for detecting mis-calibration

To complement our results on the performance of the plug-in tests proposed earlier, we now show some fundamental lower bounds for detecting mis-calibration. We also provide a reduction that allows us to test calibration via two-sample tests and sample splitting. We show that this has a minimax optimal performance, but empirically does not perform as well as our previous test.

5.1 Impossibility for general continuous mis-calibration curves

In Proposition 5.1, we show that detecting mis-calibration is impossible, even when the sample size n is arbitrarily large, unless the mis-calibration curve res_f has some level of smoothness. Intuitively, if the mis-

calibration curve can be arbitrarily non-smooth, then it can oscillate between positive and negative values with arbitrarily high frequency, and these oscillations cannot be detected from a finite sample.

In this regard, one needs to be careful when drawing conclusions about the quality of calibration from a finite sample. If we only assume that the mis-calibration curve is a continuous function of the probability predictions, then it is impossible to tell apart calibrated and mis-calibrated models. Further, for more complex models such as deep neural networks, one expects the predicted probabilities to be able to capture larger and larger classes of functions; thus this result is even more relevant for modern large-scale machine learning.

Let $\mathcal{P}_1^{\text{cont}}(\varepsilon, p)$ be the family of probability distributions P over (Z, Y) such that $\ell_p\text{-ECE}_P(f) \geq \varepsilon$ and every entry of the mis-calibration curve $\text{res}_{f,P}$ is continuous. This is a larger set of distributions than $\mathcal{P}_1(\varepsilon, p, s)$ in (3), because we only assume continuity, not Hölder smoothness. Denote the corresponding minimax type II error by $R_n^{\text{cont}}(\varepsilon, p)$, namely

$$R_n^{\text{cont}}(\varepsilon, p) := \inf_{\xi \in \Phi_n(\alpha)} \sup_{P \in \mathcal{P}_1^{\text{cont}}(\varepsilon, p)} P(\xi = 0).$$

This has the same interpretation as before, namely it is the best possible false negative rate for detecting mis-calibration for data distributions belonging to $\mathcal{P}_1^{\text{cont}}(\varepsilon, p)$, in a worst-case sense.

Proposition 5.1 (Detecting mis-calibration is impossible for general continuous mis-calibration curves). *Let $\varepsilon_0 = 0.1$. For any level $\alpha \in (0, 1)$, the minimax type II error $R_n^{\text{cont}}(\varepsilon_0, p)$ for testing the null hypothesis of calibration at level α against the hypothesis $P \in \mathcal{P}_1^{\text{cont}}(\varepsilon_0, p)$ of general continuous mis-calibration curves satisfies $R_n^{\text{cont}}(\varepsilon_0, p) \geq 1 - \alpha$ for all n .*

In words, this result shows that for a certain fixed ℓ_p calibration error ε_0 , and for a fixed false positive rate $\alpha > 0$, the false negative rate is as large as is can possibly be, namely at least $1 - \alpha$. Thus, it is not possible to detect mis-calibration in this setting. The choice of the constant $\varepsilon_0 = 0.1$ is arbitrary and can be replaced by any other constant; the result holds with minor modifications to the proof.

The proof can be found in Section 8.1.4. We make a few remarks on related results. While Example 3.2 of Kumar et al. (2019) demonstrates that—related to earlier results on probability distribution and density estimation (Mann and Wald, 1942)—using a binned estimator of ECE can arbitrarily underestimate the calibration error, we show a fundamental failure not due to binning, but instead due to the finite sample size. Also, our result echoes Theorem 3 of Gupta et al. (2020a) which states that asymptotically perfect calibration is only possible for probability predictors with a countable support; but this does not overlap with Proposition 5.1 as our conclusion is about the impossibility of detecting mis-calibration.

5.2 Hölder alternatives

As is customary in nonparametric statistics (Ingster, 1987; Low, 1997; Györfi et al., 2002; Ingster and Suslina, 2012), we consider testing against Hölder continuous alternatives; or, differently put, detecting mis-calibration when the mis-calibration curves are Hölder continuous. This excludes the pathological examples where the mis-calibration curves oscillate widely that were discussed in Section 5.1; but still allow a very rich class of possible mis-calibration curves, including non-smooth ones.

Theorem 5.2 states that, for a K -class classification problem and for alternatives with a Hölder smoothness parameter s , the mis-calibration of a model can be detected only when the calibration error is of order $\Omega(n^{-2s/(4s+K-1)})$.⁴ In other words, the smallest possible calibration error that can be detected using a sample of size n is of order $n^{-2s/(4s+K-1)}$.

Testing calibration of a probability predictor in our nonparametric model leads to rates that are slower than the parametric case $n^{-1/2}$. This is because $2s/(4s+K-1) < 1/2$ for $s > 0$ and $K \geq 2$. The rate becomes even slower as the number of classes K grows. This indicates that evaluating model calibration on a small-sized dataset can be problematic. Further, it suggests that multi-class calibration may be even harder to achieve.

This rate is what one may expect based on results for similar problems in nonparametric hypothesis testing (Ingster and Suslina, 2012), with $K-1$ interpreted as the dimension. Specifically, the rate is equal to

⁴For two sequences $(a_i)_{i \geq 1}, (b_i)_{i \geq 1}$ of positive numbers, we say that $a_i = \Omega(b_i)$ if there is a constant $c > 0$ such that $a_i \geq cb_i$, for all $i \geq 1$.

the minimum separation rate in two-sample goodness-of-fit testing for densities on Δ_{K-1} . This connection to two-sample testing will be made clear in Section 6.

Theorem 5.2 (Lower bound for detecting mis-calibration). *Given a level $\alpha \in (0, 1)$ and $\beta \in (0, 1 - \alpha)$, consider the hypothesis testing problem (4), in which we test the calibration of the K -class probability predictor f assuming (s, L) -Hölder continuity of mis-calibration curves as defined in (58). There exists $c_{\text{lower}} > 0$ depending only on $(p, s, L, K, \alpha, \beta)$ such that, for any $p > 0$, the minimum ℓ_p -ECE of f , i.e. $\varepsilon_n(p, s)$, required to have a test with a false positive rate (type I error) at most α and with a true positive rate (power) at least $1 - \beta$ satisfies $\varepsilon_n(p, s) \geq c_{\text{lower}} n^{-2s/(4s+K-1)}$ for all n .*

See Section 8.1.5 for the proof. The proofs of both Proposition 5.1 and Theorem 5.2 are based on Ingster's method, also known as the chi-squared or Ingster-Suslina method (Ingster, 1987; Ingster and Suslina, 2012). Informally, Ingster's method states that if we can select alternative distributions with an average likelihood ratio to a null distribution close to unity, then no test with a fixed level can control the minimax type II error below a certain threshold. For completeness and reader's convenience, we list the well known result below:

Lemma 5.3 (Ingster's method for the lower bound). *Let $P_0 \in \mathcal{P}_0$ and $P_1, \dots, P_M \in \mathcal{P}_1(\varepsilon, p, s)$ be probability distributions on $\Delta_{K-1} \times \mathcal{Y}$, and suppose that P_1, \dots, P_M are absolutely continuous with respect to P_0 . For an i.i.d. sample $\{(Z_i, Y_i) : i \in \{1, \dots, n\}\}$ from P_0 , define the average likelihood ratio between P_1, \dots, P_M and P_0 as*

$$L_n := \frac{1}{M} \sum_{i=1}^M \prod_{j=1}^n \frac{dP_i}{dP_0}(Z_j, Y_j).$$

If $\mathbb{E}_{P_0}[L_n^2] \leq 1 + (1 - \alpha - \beta)^2$, then the minimax type II error (false negative rate) for testing $H_0 : P \in \mathcal{P}_0$ against $H_1 : P \in \mathcal{P}_1(\varepsilon, p, s)$ at level α satisfies $R_n(\varepsilon, p, s) \geq \beta$ and the minimum separation rate to ensure type II error at most β obeys $\varepsilon_n(\beta; p, s) \geq \varepsilon$.

See Section 8.1.6 for the proof of this lemma, provided again for completeness and reader's convenience. Therefore, the main steps in the proofs of Proposition 5.1 and Theorem 5.2 are choosing P_0, P_1, \dots, P_M and bounding the expected value of L_n^2 .

6 Reduction to two-sample goodness-of-fit testing

To further put our work in context in the literature on non-parametric hypothesis testing, in this section we carefully examine the connections between the problem of testing calibration, and a well-known problem in that area. Specifically, we describe a novel randomization scheme that allows us to reduce the null hypothesis of perfect calibration to a hypothesis of equality of two distributions—making a strong connection to the problem of *two-sample goodness of fit testing*. In other words, we can use a calibrated probabilistic classifier and randomization to generate two samples from an identical distribution. For a mis-calibrated classifier the same scheme will generally result in two samples from two different distributions.

If a classifier is perfectly calibrated, then its class probability predictions will match the true prediction-conditional class probabilities. Therefore, randomly sampling labels according to the classifier's probability predictions will yields a sample from the empirical distribution. We rely on sample splitting to obtain two samples: the empirical and the generated one. Then we can use any classical test to check if the two samples are generated from the same distribution. As we will show, the resulting test has a theoretically optimal detection rate. However, due to the sample splitting step, its empirical performance is inferior to the test based on the debiased plug-in estimator from Section 3.

We split our sample into two parts. For $i \in \{\lfloor n/2 \rfloor + 1, \dots, n\}$, we generate random variables \tilde{Y}_i following the categorical distribution $\text{Cat}(Z_i)$ over classes $\mathcal{Y} = \{1, \dots, K\}$, with a K -class probability distribution $Z_i = f(X_i)$ predicted by the classifier f . These \tilde{Y}_i are independent of each other and of $Y_1, \dots, Y_{\lfloor n/2 \rfloor}$, due to the sample splitting step. For each $k \in \{1, \dots, K\}$, define

$$\mathcal{V}_k := \left\{ Z_i : [Y_i]_k = 1, 1 \leq i \leq \left\lfloor \frac{n}{2} \right\rfloor \right\}$$

and

$$\mathcal{W}_k := \left\{ Z_i : [\tilde{Y}_i]_k = 1, \left\lfloor \frac{n}{2} \right\rfloor + 1 \leq i \leq n \right\}.$$

By construction, \mathcal{V}_k is an i.i.d. sample from the distribution on the simplex Δ_{K-1} with a density⁵

$$\pi_k^{\mathcal{V}}(\mathbf{z}) := \frac{[\text{reg}_f(\mathbf{z})]_k}{\int_{\Delta_{K-1}} [\text{reg}_f(\mathbf{z})]_k dP_Z(\mathbf{z})} = \frac{[\text{reg}_f(\mathbf{z})]_k}{\mathbb{E}[Y]_k}$$

with respect to P_Z . Similarly, \mathcal{W}_k is an i.i.d. sample from the distribution on Δ_{K-1} with a density

$$\pi_k^{\mathcal{W}}(\mathbf{z}) := \frac{[\mathbf{z}]_k}{\int_{\Delta_{K-1}} [\mathbf{z}]_k dP_Z(\mathbf{z})} = \frac{[\mathbf{z}]_k}{\mathbb{E}[Z]_k}.$$

Now we consider testing the null hypothesis

$$H_0 : \pi_k^{\mathcal{V}} = \pi_k^{\mathcal{W}} \text{ for all } k \in \{1, \dots, K\}$$

against the complement of H_0 . We claim that if we use an appropriate test for this null hypothesis, with an additional procedure to rule out “easily detectable” alternatives, then we can obtain a test that attains the optimal rate specified in Theorem 5.2.

We describe the main idea of this reduction. A formal result can be found in Theorem 6.1. Let $P \in \mathcal{P}_1(\varepsilon, p, s)$ and assume $\varepsilon = \tilde{\Omega}(n^{-2s/(4s+K-1)})$.⁶ The squared distance between $\pi_k^{\mathcal{V}}$ and $\pi_k^{\mathcal{W}}$ in $L^2(P_Z)$ is

$$\begin{aligned} \int_{\Delta_{K-1}} \left(\frac{[\text{reg}_f(\mathbf{z})]_k}{\mathbb{E}[Y]_k} - \frac{[\mathbf{z}]_k}{\mathbb{E}[Z]_k} \right)^2 dP_Z(\mathbf{z}) &= \int_{\Delta_{K-1}} \left(\frac{[\text{res}_f(\mathbf{z})]_k}{\mathbb{E}[Y]_k} + \frac{[\mathbf{z}]_k}{\mathbb{E}[Y]_k} - \frac{[\mathbf{z}]_k}{\mathbb{E}[Z]_k} \right)^2 dP_Z(\mathbf{z}) \\ &\geq \frac{1}{(\mathbb{E}[Y]_k)^2} \int_{\Delta_{K-1}} [\text{res}_f(\mathbf{z})]_k^2 dP_Z(\mathbf{z}) + \frac{2\mathbb{E}[Z-Y]_k}{(\mathbb{E}[Y]_k)^2 \mathbb{E}[Z]_k} \int_{\Delta_{K-1}} [\mathbf{z}]_k [\text{res}_f(\mathbf{z})]_k dP_Z(\mathbf{z}). \end{aligned} \quad (11)$$

Further,

$$\int_{\Delta_{K-1}} [\mathbf{z}]_k [\text{res}_f(\mathbf{z})]_k dP_Z(\mathbf{z}) = \mathbb{E}_P[[Z]_k \mathbb{E}[Y - Z|Z]_k] = \mathbb{E}_P[[Z]_k [Y - Z]_k]. \quad (12)$$

Since $\mathbb{E}[Y - Z]_k = \mathbb{E}[[Z]_k [Y - Z]_k] = 0$ and $\text{Var}([Y - Z]_k), \text{Var}([Z]_k [Y - Z]_k) \leq 1$ under H_0 , we can detect mis-calibration for the alternatives $P \in \mathcal{P}_1(\varepsilon, p, s)$ such that $\mathbb{E}_P[Y - Z]_k = \Omega(n^{-1/2})$ or $\mathbb{E}_P[[Z]_k [Y - Z]_k] = \Omega(n^{-1/2})$ by rejecting the null hypothesis H_0 of calibration if $\frac{1}{n} \sum_{i=1}^n [Y_i - Z_i]_k \geq cn^{-1/2}$ or $\frac{1}{n} \sum_{i=1}^n [Z_i]_k [Y_i - Z_i]_k \geq cn^{-1/2}$ for some $c > 0$. For the remaining alternatives, choose $k_0 \in \{1, \dots, K\}$ such that

$$\frac{1}{(\mathbb{E}[Y]_{k_0})^2} \int_{\Delta_{K-1}} [\text{res}_f(\mathbf{z})]_{k_0}^2 dP_Z(\mathbf{z}) \geq \frac{\varepsilon^2}{K(\mathbb{E}[Y]_{k_0})^2} = \tilde{\Omega}(n^{-\frac{4s}{4s+K-1}}).$$

Then, $\|\pi_k^{\mathcal{V}} - \pi_k^{\mathcal{W}}\|_{L^2(P_Z)}^2$ is at least

$$\tilde{\Omega}(n^{-\frac{4s}{4s+K-1}}) + \frac{2\mathbb{E}[Z-Y]_{k_0} \mathbb{E}[[Z]_{k_0} [Y - Z]_{k_0}]}{(\mathbb{E}[Y]_{k_0})^2 \mathbb{E}[Z]_{k_0}} = \tilde{\Omega}(n^{-\frac{4s}{4s+K-1}}).$$

Since $|\mathcal{V}_{k_0}|, |\mathcal{W}_{k_0}| = \Theta(n)$ with high probability, the power of the test can be controlled using standard results on two sample testing. The full procedure is described in Algorithm 3.

To be general, for a positive integer $d > 0$, we allow using an arbitrary deterministic two-sample testing procedure $\text{TS}_{\alpha, \beta} : ([0, 1]^d)^{n_1} \times ([0, 1]^d)^{n_2} \rightarrow \{0, 1\}$, which takes in two d -dimensional samples $\{V_1, \dots, V_{n_1}\}, \{W_1, \dots, W_{n_2}\}$ and outputs “1” if and only if the null hypothesis is rejected. The two samples $\{V_1, \dots, V_{n_1}\}$ and $\{W_1, \dots, W_{n_2}\}$ are sampled i.i.d. from distributions with densities f_1 and f_2 , respectively, with respect

⁵We assume that the densities $\pi_k^{\mathcal{V}}$ and $\pi_k^{\mathcal{W}}$ are well defined, and in particular that $\mathbb{E}[Y]_k > 0$ and $\mathbb{E}[Z]_k > 0$ for every $k \in \{1, \dots, K\}$. This follows by Assumption 6.1, which will be introduced later in the section.

⁶Here we use the notation $\tilde{\Omega}(\cdot)$ to include the adaptive case. The $\tilde{\Omega}$ notation allows for additional logarithmic factors and is defined precisely in the appendix. See Corollary 6.2 and Remark 1 for further details.

Algorithm 3 Sample splitting calibration test ξ_n^{split}

Input: Probability predictor $f : \mathcal{X} \rightarrow \Delta_{K-1}$; i.i.d. sample $\{(X_i, Y_i) \in \mathcal{X} \times \mathcal{Y} : i \in \{1, \dots, n\}\}$; false detection rate $\alpha \in (0, 1)$; true detection rate $\beta \in (0, 1 - \alpha)$; Hölder smoothness s ; minimax optimal two-sample density test TS

Procedure: $Z_i \leftarrow f(X_i)$ for $i \in \{1, \dots, n\}$; independently sample $\tilde{Y}_i \sim \text{Cat}(Z_i)$ for $i \in \{\lfloor \frac{n}{2} \rfloor + 1, \dots, n\}$

for $k = 1$ **to** K **do**

$T_{1,k} \leftarrow \frac{1}{n} \sum_{i=1}^n [Y_i - Z_i]_k$, $T_{2,k} \leftarrow \frac{1}{n} \sum_{i=1}^n [Z_i]_k [Y_i - Z_i]_k$

$\mathcal{V}_k \leftarrow \{Z_i : [Y_i]_k = 1, 1 \leq i \leq \lfloor \frac{n}{2} \rfloor\}$, $\mathcal{W}_k \leftarrow \{Z_i : [\tilde{Y}_i]_k = 1, \lfloor \frac{n}{2} \rfloor + 1 \leq i \leq n\}$

$b_k \leftarrow I(|T_{1,k}| \geq \sqrt{\frac{3K}{\alpha n}}) \vee I(|T_{2,k}| \geq \sqrt{\frac{3K}{\alpha n}}) \vee \text{TS}_{\frac{\alpha}{3K}, \frac{\beta}{2}}(\mathcal{V}_k, \mathcal{W}_k)$

end for

Output: Reject H_0 if $\xi_n^{\text{split}} := \max\{b_k : k \in \{1, \dots, K\}\} = 1$

to an appropriate probability measure μ on $[0, 1]^d$. Further, it is assumed that $f_1 - f_2$ is (s, L) -Hölder continuous for a Hölder smoothness parameter $s > 0$ and a Hölder constant $L > 0$. Given $\alpha \in (0, 1)$ and $\beta \in (0, 1 - \alpha)$, the two-sample test is required to satisfy, for some $c_{\text{ts}} > 0$ depending on (s, L, d, α, β) and on ν_l, ν_u from Assumption 3.1 to be introduced next,

$$\begin{aligned} P(\text{TS}_{\alpha, \beta}(V_1, \dots, V_{n_1}, W_1, \dots, W_{n_2}) = 1) &\leq \alpha \quad \text{if } f_1 = f_2, \\ P(\text{TS}_{\alpha, \beta}(V_1, \dots, V_{n_1}, W_1, \dots, W_{n_2}) = 0) &\leq \beta \quad \text{if } \|f_1 - f_2\|_{L^2(\mu)} \geq c_{\text{ts}}(n_1 \wedge n_2)^{-\frac{2s}{4s+d}}. \end{aligned} \quad (13)$$

There are a number of such tests proposed in prior work, see e.g., Ingster and Suslina (2012); Arias-Castro et al. (2018); Kim et al. (2022) and Section 8.2.2. Our general approach allows using any of these. It is also known that there are *adaptive* tests TS^{ad} that do not require knowing the Hölder smoothness parameter s . In the adaptive setting, the best known minimum required separation in this general dimensional situation is

$$\|f_1 - f_2\|_{L^2(\mu)} \geq c_{\text{ad}} \left(\frac{n_1 \wedge n_2}{\log \log(n_1 \wedge n_2)} \right)^{-\frac{2s}{4s+d}} \quad (14)$$

for some $c_{\text{ad}} > 0$. See Section 8.2.2 for examples of TS and TS^{ad} .

Next we state an additional assumption required in our theorem. See Section 8.2.2 for more discussion. Assumption 6.1 guarantees that every class appears in the dataset. This is reasonable in many practical settings, as classes that do not appear can be omitted.

Assumption 6.1 (Lower bounded class probability). *There exists a constant $d_c > 0$ such that $\mathbb{E}[Y]_k > d_c$ for all $k \in \{1, \dots, K\}$.*

Our result is as follows.

Theorem 6.1 (Optimal calibration test via sample splitting). *Suppose $p \leq 2$ and let ξ_n^{split} be the test described in Algorithm 3. Assume the Hölder smoothness parameter s is known. Under Assumption 3.1 and 6.1, we have*

1. **False detection rate control.** *For every P for which f is perfectly calibrated, i.e., for $P \in \mathcal{P}_0$, the probability of falsely claiming mis-calibration is at most α , i.e., $P(\xi_n^{\text{split}} = 1) \leq \alpha$.*
2. **True detection rate control.** *There exists $c_{\text{split}} > 0$ depending on $(s, L, K, \nu_l, \nu_u, d_c, \alpha, \beta)$ such that the power (true positive rate) is bounded as $P(\xi_n^{\text{split}} = 1) \geq 1 - \beta$ for every $P \in \mathcal{P}_1(\varepsilon, p, s)$ —i.e., when f is mis-calibrated with an ℓ_p -ECE of at least $\varepsilon \geq c_{\text{split}} n^{-2s/(4s+K-1)}$.*

The proof is in Section 8.1.7. Theorem 5.2 and Theorem 6.1 together imply that the minimax optimal detection rate for calibration is $\varepsilon_n(p, s) \asymp n^{-2s/(4s+K-1)}$. By replacing TS with an adaptive test TS^{ad} , we obtain an adaptive version of the test ξ_n^{split} .

Corollary 6.2 (Adaptive test via sample splitting). *Suppose $p \leq 2$ and let $\xi_n^{\text{ad-s}}$ be the test described in Algorithm 3 with TS replaced by an adaptive two-sample test TS^{ad} . Under Assumption 3.1 and 6.1, we have*

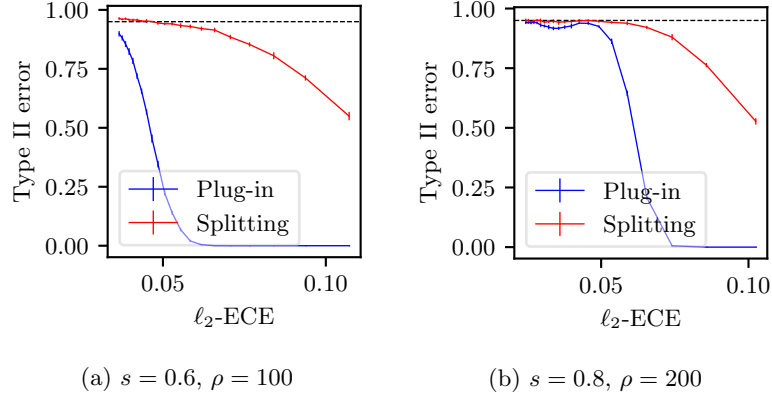


Figure 6: Type II error comparison for $\xi_{m^*,n}$ and ξ_n^{split} . The horizontal dashed line indicates a type II error of $1 - \alpha = 0.95$. Since ξ_n^{split} relies on sampling splitting, its effective sample size is much smaller than that of the plug-in test. This results in higher type II errors as can be seen in the figure. Standard error bars are plotted over 10 repetitions.

1. **False detection rate control.** For every P for which f is perfectly calibrated, i.e., for $P \in \mathcal{P}_0$, the probability of falsely claiming mis-calibration is at most α , i.e., $P(\xi_n^{\text{ad-s}} = 1) \leq \alpha$.
2. **True detection rate control.** There exists $c_{\text{ad-s}} > 0$ depending on $(s, L, K, \nu_l, \nu_u, d_c, \alpha, \beta)$ such that the power (true positive rate) is bounded as $P(\xi_n^{\text{ad-s}} = 1) \geq 1 - \beta$ for every $P \in \mathcal{P}_1(\varepsilon, p, s)$ —i.e., when f is mis-calibrated with an ℓ_p -ECE of at least $\varepsilon \geq c_{\text{ad-s}}(n/\log \log n)^{-2s/(4s+K-1)}$.

Remark 1 (Adaptation cost). Spokoiny (1996); Ingster (2000) develop an adaptive chi-squared test for one-dimensional goodness-of-fit testing which can adapt to an unknown Hölder smoothness parameter s while only losing a $(\log \log n)^{s/(4s+1)}$ factor in the separation rate. The test was proven to be minimax optimal in the adaptive setting. Arias-Castro et al. (2018) extend the adaptive test to a general dimension d and attain an adaptive test at the cost of $\sqrt{\log n}$ factor. Kim et al. (2022) provide a stronger analysis for their permutation test and reduce the adaptation cost to $(\log \log n)^{2s/(4s+d)}$. To our knowledge, the minimax optimality of these adaptive tests in general dimensions is so far not established.

While the adaptive test in Corollary 6.2 requires an additional factor of $(\log \log n)^{2s/(4s+K-1)}$ in the separation rate, Theorem 3.2 requires a factor of $(\log n)^{s/(4s+K-1)}$. This gap comes from the requirement (14) which we borrow from Kim et al. (2022). Theorem 6.1 and Lemma C.1 of Kim et al. (2022) develops combinatorial concentration inequalities to improve a polynomial dependency on α in the separation rate to a logarithmic dependency. This results in the $(\log \log n)^{2s/(4s+K-1)}$ factor in their adaptive test. Since our proof of Theorem 3.1 uses a quadratic tail bound from Chebyshev's inequality, the adaptation cost in Theorem 3.2 is $(\log n)^{s/(4s+K-1)}$. Currently, it appears challenging to improve the polynomial dependence for $T_{m,n}^d$, due to its complicated conditional structure.

Remark 2 (Connection to testing the ℓ_p norm). Our task here is different from the classical problem of testing that the ℓ_p -norm of a function is zero against the alternative that it is nonzero (Berman et al., 2014), where we are provided with noisy observations of the function values. In our problem, we have a different data generating mechanism and are not provided independent noisy observations of the function res_f .

6.1 Comparison with the debiased plug-in test

We compare the empirical performances of the debiased plug-in test $\xi_{m^*,n}$ and the sample splitting test ξ_n^{split} . As described in Section 4.1, we study the type II error against the fixed alternative where the mis-calibration is specified as $H_1 : (Z, Y) \sim P_{1,m}$, for various values of m . We use a sample size of $n = 20,000$ and pairs of Hölder smoothness and scaling parameter indicated in Figure 6. The critical value for $\alpha = 0.05$ and the corresponding type II error are estimated via 1,000 Monte Carlo simulations. For the sample splitting test ξ_n^{split} , we use the chi-squared two-sample test of Arias-Castro et al. (2018).

Since ξ_n^{split} relies on sample splitting and discards some of the observations, its effective sample size is smaller than that of the debiased plug-in test. For this reason, we find that T-Cal outperforms the sample splitting test by a large margin. While the sample splitting test reveals a theoretically interesting connection to two-sample density testing, it appears empirically suboptimal.

7 Conclusion

This paper studied the problem of testing model calibration from a finite sample. We analyzed the plug-in estimator of $\ell_2\text{-ECE}(f)^2$ as a test statistic for calibration testing. We discovered that the estimator needs debiasing and becomes minimax optimal when the number of bins is chosen appropriately. We also provided an adaptive version of the test, which can be used without knowing the Hölder smoothness parameter s . We tested T-Cal with a broad range of experiments, including with several neural net architectures and post-hoc calibration methods.

In the theory side, we provided an impossibility result for testing calibration against general continuous alternatives. Assuming that the calibration curve is s -Hölder-smooth, we derived a lower bound of $\Omega(n^{-2s/(4s+K-1)})$ on the calibration error required for a model to be distinguished from a perfectly calibrated one. We also discussed a reduction to two-sample testing and showed that the resulting test also matches the lower bound.

Interesting future directions include (1) developing a testing framework for comparing calibration of predictive models, (2) extending the theoretical result to other calibration concepts such as top(- k), within- k , and marginal calibration, and (3) developing a minimax estimation theory for calibration errors.

Acknowledgements

This work was supported in part by the NSF TRIPODS 1934960, NSF DMS 2046874 (CAREER), ARO W911NF-20-1-0080, DCIST, and NSF CAREER award CIF-1943064, and Air Force Office of Scientific Research Young Investigator Program (AFOSR-YIP) #FA9550-20-1-0111 award.

8 Appendix

Notations. For completeness and to help the reader, we present (and in some cases recall) some notations. We will use the symbols $:=$ or $=:$ to define quantities in equations. We will occasionally use bold font for vectors. For an integer $d \geq 1$, we denote $[d] := \{1, \dots, d\}$ and $\mathbf{1}_d := (1, 1, \dots, 1)^\top \in \mathbb{R}^d$. For a vector $\mathbf{v} \in \mathbb{R}^d$, we will sometimes write $[\mathbf{v}]_i$ for the i -th coordinate of \mathbf{v} , for any $i \in [d]$. The minimum of two scalars $a, b \in \mathbb{R}$ is denoted by $\min(a, b)$ or $a \wedge b$; their maximum is denoted by $\max(a, b)$ or $a \vee b$. We denote the d -dimensional Lebesgue measure by Leb_d . For a function $h : \mathbb{R}^d \rightarrow \mathbb{R}$, $1 \leq p < \infty$, and a measure μ on \mathbb{R}^d , we let $\|h\|_{L^p(\mu)} := (\int |h|^p d\mu)^{1/p}$. When $\mu = \text{Leb}_d$, we omit μ and write $\|h\|_{L^p}$. If $p = \infty$, then $\|h\|_{L^p} := \text{ess sup}_{x \in \mathbb{R}^d} |h(x)|$. We denote the ℓ_p -norm of $\mathbf{x} = (x_1, \dots, x_d)^\top \in \mathbb{R}^d$ by $\|\mathbf{x}\|_p := (\sum_{i=1}^d |x_i|^p)^{1/p}$. When p is unspecified, $\|\cdot\|$ stands for $\|\cdot\|_2$.

For two sequences $(a_n)_{n \geq 1}$ and $(b_n)_{n \geq 1}$ with $b_n \neq 0$, we write $a_n \asymp b_n$ if $0 < \liminf_n a_n/b_n \leq \limsup_n a_n/b_n < \infty$. When the index n is self-evident, we may omit it above. We use the Bachmann-Landau asymptotic notations $\Omega(\cdot), \Theta(\cdot)$ to hide constant factors in inequalities and use $\tilde{\Omega}(\cdot), \tilde{\Theta}(\cdot)$ to also hide logarithmic factors. For a Lebesgue measurable set $A \subseteq \mathbb{R}^d$, we denote by $\mathbf{1}_A : \mathbb{R}^d \rightarrow \{0, 1\}$ its indicator function where $\mathbf{1}_A(\mathbf{x}) = 1$ if $\mathbf{x} \in A$ and $\mathbf{1}_A(\mathbf{x}) = 0$ otherwise. For a real number $s \in \mathbb{R}$, we denote the largest integer less than or equal to s by $\lfloor s \rfloor$. Also, the smallest integer greater than or equal to s is denoted by $\lceil s \rceil$.

For an integer $d \geq 1$, a vector $\boldsymbol{\gamma} = (\gamma_1, \dots, \gamma_d)^\top \in \mathbb{N}^d$ is called a multi-index. We write $|\boldsymbol{\gamma}| := \gamma_1 + \dots + \gamma_d$. For a vector $\mathbf{x} = (x_1, \dots, x_d) \in \mathbb{R}^d$ and a multi-index $\boldsymbol{\gamma} = (\gamma_1, \dots, \gamma_d)^\top \in \mathbb{N}^d$, we write $\mathbf{x}^{\boldsymbol{\gamma}} := x_1^{\gamma_1} \cdots x_d^{\gamma_d}$. For a sufficiently smooth function $f : \mathbb{R}^d \rightarrow \mathbb{R}$, we denote its partial derivative of order $\boldsymbol{\gamma} = (\gamma_1, \dots, \gamma_d)^\top$ by $f^{(\boldsymbol{\gamma})} := \partial_1^{\gamma_1} \cdots \partial_d^{\gamma_d} f$. A pure partial derivative with respect to an individual coordinate $i \in [d]$ is also denoted as $\partial_i f$. For two sets S, T , a map $f : S \rightarrow T$, and a subset $S' \subseteq S$, we denote by $f(S')$ the image of S' under f . The support of a function $f : S \rightarrow \mathbb{R}$ is the set of points $\text{supp}(f) := \{a \in S : f(a) \neq 0\}$.

The uniform distribution on a compact set $S \subseteq \mathbb{R}^d$ is denoted by $\text{Unif}(S)$. The binomial distribution with $n \in \mathbb{N}$ trials and success probability $p \in [0, 1]$ is denoted by $\text{Bin}(n, p)$, and write $\text{Ber}(p) := \text{Bin}(1, p)$. For an integer $d \geq 2$, we let $\Delta_{d-1} := \{\mathbf{z} = (z_1, \dots, z_d)^\top \in [0, 1]^d : z_1 + \dots + z_d = 1\}$ be the $(d-1)$ -dimensional simplex. We denote the multinomial distribution with $n \in \mathbb{N}$ trials and class probability vector $\mathbf{p} \in \Delta_{d-1}$ by $\text{Multi}(n, \mathbf{p})$, and write $\text{Cat}(\mathbf{p}) := \text{Multi}(1, \mathbf{p})$. For a joint distribution $(X, Y) \sim P$, we will write P_X, P_Y for the marginal distributions of X, Y , respectively. For a distribution Q and a random variable $Z \sim Q$, we will denote expectations of functions of Z with respect to Q as $\mathbb{E}f(Z)$, $\mathbb{E}_Z f(Z)$, $\mathbb{E}_Q f(Z)$, or $\mathbb{E}_{Z \sim Q} f(Z)$. We abbreviate almost surely by “a.s.”, and almost everywhere by “a.e.”

8.1 Proofs

8.1.1 Proof of Theorem 3.1

We state some lemmas used in the proof. See Section 3.2.2 of Ingster and Suslina (2012) for a discussion of how such results connected to geometric notions such as Kolmogorov diameters.

Lemma 8.1. *For $m \in \mathbb{N}_+$, let $\mathcal{B}_m = \{B_1, \dots, B_{m^{K-1}}\}$ be the partition of Δ_{K-1} defined in Section 8.2.3 and μ be a probability measure on Δ_{K-1} such that $\mu(B_i) > 0$ for all $i \in [m^{K-1}]$. For any continuous function $h : \Delta_{K-1} \rightarrow \mathbb{R}$, define*

$$W_m[h] := \sum_{i=1}^{m^{K-1}} \frac{\int_{B_i} h(\mathbf{z}) d\mu(\mathbf{z})}{\mu(B_i)} \mathbb{1}_{B_i}.$$

There are $b_1, b_2 > 0$ depending on (K, s, L) such that for every $h \in \mathcal{H}_K(s, L)$

$$\|W_m[h]\|_{L^2(\mu)} \geq b_1 \|h\|_{L^2(\mu)} - b_2 m^{-s}.$$

In other words,

$$\left(\sum_{i=1}^{m^{K-1}} \frac{\mathbb{E}_\mu[h(Z)I(Z \in B_i)]^2}{\mu(B_i)} \right)^{\frac{1}{2}} \geq b_1 \mathbb{E}_\mu[h(Z)^2]^{\frac{1}{2}} - b_2 m^{-s}.$$

Proof. This lemma is a generalization of Lemma 3 in Arias-Castro et al. (2018). We state and prove two facts:

1. Fix $h \in \mathcal{H}_K(s, L)$ and $\mathbf{z}_0 \in \Delta_{K-1}$. Let u be the $(\lceil s \rceil - 1)$ -th order Taylor series of h at \mathbf{z}_0 . There is L' depending on (K, s, L) such that

$$|h(\mathbf{z}) - u(\mathbf{z})| \leq L' \|\mathbf{z} - \mathbf{z}_0\|^s \quad (15)$$

for all $\mathbf{z} \in \Delta_{K-1}$.

Proof of Fact 1. Let $\psi = \pi_{-K}$ as in (58). Recall that for a multi-index $\gamma = (\gamma_1, \dots, \gamma_{K-1})^\top \in \mathbb{N}^{K-1}$, we write $(\psi(\mathbf{z}) - \psi(\mathbf{z}_0))^\gamma = \prod_{j \in [K-1]} (\psi_j(\mathbf{z}) - \psi_j(\mathbf{z}_0))^{\gamma_j}$. By a Taylor series expansion, there exists $t \in [0, 1]$ such that

$$\begin{aligned} h(\mathbf{z}) &= (h \circ \psi^{-1})(\psi(\mathbf{z})) = \sum_{\substack{\gamma \in \mathbb{N}^{K-1} \\ 0 \leq |\gamma| \leq \lceil s \rceil - 2}} \frac{(h \circ \psi^{-1})^{(\gamma)}(\psi(\mathbf{z}_0))}{|\gamma|!} (\psi(\mathbf{z}) - \psi(\mathbf{z}_0))^\gamma \\ &\quad + \sum_{\substack{\gamma \in \mathbb{N}^{K-1} \\ |\gamma| = \lceil s \rceil - 1}} \frac{(h \circ \psi^{-1})^{(\gamma)}(t\psi(\mathbf{z}) + (1-t)\psi(\mathbf{z}_0))}{|\gamma|!} (\psi(\mathbf{z}) - \psi(\mathbf{z}_0))^\gamma. \end{aligned}$$

Then,

$$\begin{aligned}
h(\mathbf{z}) - u(\mathbf{z}) &= h(\mathbf{z}) - \sum_{\substack{\gamma \in \mathbb{N}^{K-1} \\ 0 \leq |\gamma| \leq \lceil s \rceil - 1}} \frac{(h \circ \psi^{-1})^{(\gamma)}(\psi(\mathbf{z}_0))}{|\gamma|!} (\psi(\mathbf{z}) - \psi(\mathbf{z}_0))^\gamma \\
&= \sum_{\substack{\gamma \in \mathbb{N}^{K-1} \\ |\gamma| = \lceil s \rceil - 1}} \frac{(h \circ \psi^{-1})^{(\gamma)}(t\psi(\mathbf{z}) + (1-t)\psi(\mathbf{z}_0)) - (h \circ \psi^{-1})^{(\gamma)}(\psi(\mathbf{z}_0))}{|\gamma|!} (\psi(\mathbf{z}) - \psi(\mathbf{z}_0))^\gamma.
\end{aligned}$$

By the triangle inequality and the s -Hölder continuity of h ,

$$\begin{aligned}
|h(\mathbf{z}) - u(\mathbf{z})| &\leq \sum_{\substack{\gamma \in \mathbb{N}^{K-1} \\ |\gamma| = \lceil s \rceil - 1}} \frac{|(h \circ \psi^{-1})^{(\gamma)}(t\psi(\mathbf{z}) + (1-t)\psi(\mathbf{z}_0)) - (h \circ \psi^{-1})^{(\gamma)}(\psi(\mathbf{z}_0))|}{|\gamma|!} |(\psi(\mathbf{z}) - \psi(\mathbf{z}_0))^\gamma| \\
&\leq \sum_{\substack{\gamma \in \mathbb{N}^{K-1} \\ |\gamma| = \lceil s \rceil - 1}} \frac{L(t\|\psi(\mathbf{z}) - \psi(\mathbf{z}_0)\|)^{s - \lceil s \rceil + 1}}{|\gamma|!} \|\psi(\mathbf{z}) - \psi(\mathbf{z}_0)\|^{\lceil s \rceil - 1} \leq L' \|\psi(\mathbf{z}) - \psi(\mathbf{z}_0)\|^s \leq L' \|\mathbf{z} - \mathbf{z}_0\|^s.
\end{aligned}$$

□

2. Let \mathcal{P}_q^K be the class of polynomials on \mathbb{R}^K of degree at most q . There are $a_1, a_2 > 0$ depending on (K, q) such that

$$\|W_m[v]\|_{L^2(\mu)} \geq a_1 \|v\|_{L^2(\mu)} \quad (16)$$

for every $v \in \mathcal{P}_q^K$ and $m \geq a_2$.

Proof of Fact 2. If (16) does not hold, then we can find a sequence $\{m_l\}_{l=1}^\infty$ increasing to infinity and a sequence of polynomials $\{v_l\}_{l=1}^\infty \subseteq \mathcal{P}_q^K$ such that $\|W_{m_l}[v_l]\|_{L^2(\mu)} < \frac{1}{l} \|v_l\|_{L^2(\mu)}$. Dividing v_l by $\|v_l\|_{L^2(\mu)}$, we may assume $\|v_l\|_{L^2(\mu)} = 1$. Now $\{v \in \mathcal{P}_q^K : \|v\|_{L^2(\mu)} = 1\}$ is compact in the topology induced by the norm $\|\cdot\|_{L^2(\mu)}$, due to the Heine-Borel theorem, because it is closed and bounded. Thus, we can find a convergent subsequence $\{v_{l_k}\}_{k=1}^\infty$. Denote the limit by v_∞ . On one hand,

$$\|W_{m_{l_k}}[v_\infty]\|_{L^2(\mu)} \leq \|W_{m_{l_k}}[v_\infty - v_{l_k}]\|_{L^2(\mu)} + \|W_{m_{l_k}}[v_{l_k}]\|_{L^2(\mu)} \leq \|v_\infty - v_{l_k}\|_{L^2(\mu)} + \frac{1}{l_k} \rightarrow 0.$$

Here, we used that

$$\|W_m[v]\|_{L^2(\mu)}^2 = \sum_{i=1}^{m^{K-1}} \frac{\left(\int_{B_i} v(\mathbf{z}) d\mu(\mathbf{z})\right)^2}{\mu(B_i)} \leq \sum_{i=1}^{m^{K-1}} \int_{B_i} v(\mathbf{z})^2 d\mu(\mathbf{z}) = \|v\|_{L^2(\mu)}^2. \quad (17)$$

On the other hand, $\|W_{m_{l_k}}[v_\infty]\|_{L^2(\mu)} \rightarrow \|v_\infty\|_{L^2(\mu)} = 1$ since $W_{m_{l_k}}[v_\infty] \rightarrow v_\infty$ a.e. μ and $\|W_{m_{l_k}}[v_\infty]\|_{L^\infty} \leq \|v_\infty\|_{L^\infty}$. The proof is done by contradiction.

□

Choose $r > 0$ such that $\text{diam}(\mathcal{B}_r(\Delta_{K-1})) \leq a_1$, where a_1 is defined in (16). Since a_1 does not depend on m , for sufficiently large m , we can choose r such that m/r is an integer. Partition Δ_{K-1} into $\mathcal{M} := (m/r)^{K-1}$ simplices as described in Section 8.2.3 and call them $\tilde{B}_1, \dots, \tilde{B}_{|\mathcal{M}|}$. Each \tilde{B}_j , $j \in [\mathcal{M}]$, consists of r^{K-1} different simplices B_i (also defined in Section 8.2.3). For $j \in [\mathcal{M}]$, let u_j be the $(\lceil s \rceil - 1)$ -th order Taylor expansion of h at an arbitrary vertex of \tilde{B}_j . Define $u := \sum_{j=1}^{\mathcal{M}} u_j \mathbf{1}_{\tilde{B}_j}$. By equation (15),

$$|h(\mathbf{z}) - u(\mathbf{z})| \leq L' \left(\frac{r}{m}\right)^s =: b m^{-s} \quad (18)$$

for all $\mathbf{z} \in \Delta_{K-1}$. Therefore,

$$\begin{aligned} \|W_m[h]\|_{L^2(\mu)} &\geq \|W_m[u]\|_{L^2(\mu)} - \|W_m[u-h]\|_{L^2(\mu)} \\ &\geq \|W_m[u]\|_{L^2(\mu)} - \|u-h\|_{L^2(\mu)} \geq \|W_m[u]\|_{L^2(\mu)} - bm^{-s}. \end{aligned}$$

The second inequality is from (17). Note that

$$\|W_m[u]\|_{L^2(\mu)}^2 = \sum_{j=1}^M \|W_m[u_j \mathbf{1}_{\tilde{B}_j}]\|_{L^2(\mu)}^2,$$

and that equation (16) can be applied to $\|W_m[u_j \mathbf{1}_{\tilde{B}_j}]\|_{L^2(\mu)}$ by scaling \tilde{B}_j by r . Thus,

$$\|W_m[u]\|_{L^2(\mu)}^2 \geq \sum_{j=1}^M a_1^2 \|u_j \mathbf{1}_{\tilde{B}_j}\|_{L^2(\mu)}^2 = a_1^2 \|u\|_{L^2(\mu)}^2.$$

In conclusion, by (18)

$$\|W_m[h]\|_{L^2(\mu)} \geq a_1 \|u\|_{L^2(\mu)} - bm^{-s} \geq a_1 (\|h\|_{L^2(\mu)} - bm^{-s}) - bm^{-s} =: b_1 \|h\|_{L^2(\mu)} - b_2 m^{-s}.$$

This finishes the proof of Lemma 8.1. \square

Overview of the proof We compute the mean and variance of $T_{m^*,n}^d$ under null distributions $P_0 \in \mathcal{P}_1$ and alternative distributions $P_1 \in \mathcal{P}(\varepsilon, p, s)$. Using Lemma 8.1, we can find a lower bound for $\mathbb{E}_{P_1}[T_{m^*,n}^d] - \mathbb{E}_{P_0}[T_{m^*,n}^d]$. The variances $\text{Var}_{P_0}(T_{m^*,n}^d)$ and $\text{Var}_{P_1}(T_{m^*,n}^d)$ can be also upper bounded. We argue that the mean difference $\mathbb{E}_{P_1}[T_{m^*,n}^d] - \mathbb{E}_{P_0}[T_{m^*,n}^d]$ is significantly larger than the square root of the variances $\text{Var}_{P_0}(T_{m^*,n}^d)$ and $\text{Var}_{P_1}(T_{m^*,n}^d)$. The conclusion follows from Chebyshev's inequality.

Proof of Theorem 3.1. Let $N_i := |\mathcal{I}_{m^*,i}|$ for each $i \in [(m^*)^{K-1}]$ and $\mathcal{I} := \{i \in [(m^*)^{K-1}] : N_i \geq 1\}$. Also write $\mathbf{N} := (N_1, \dots, N_{(m^*)^{K-1}})^\top$, $\mathbf{Z} := (Z_1, \dots, Z_n)^\top$, $\bar{Y} := Y - Z$, and $\bar{Y}_j := Y_j - Z_j$ for all $j \in [n]$. By Assumption 3.1,

$$\int_{\Delta_{K-1}} \|\text{res}_f(\mathbf{z})\|^2 dP_Z(\mathbf{z}) \leq \nu_u \int_{\Delta_{K-1}} \|\text{res}_f(\mathbf{z})\|^2 d\mathbf{z},$$

where the latter integral is with respect to the uniform measure $\text{Unif}(\Delta_{K-1})$. Therefore, we may assume $P_Z = \text{Unif}(\Delta_{K-1})$ by merging ν_u with c . We prove the theorem for $p = 2$. Then, the general case follows since $\mathcal{P}_1(\varepsilon, p, s) \subseteq \mathcal{P}_1(\varepsilon, 2, s)$ for all $p \leq 2$.

Let $P_0 \in \mathcal{P}_0$ and $P_1 \in \mathcal{P}_1(\varepsilon, p, s)$ be a null and an alternative distribution over (Z, Y) , respectively. Under P_0 and conditioned on \mathbf{Z} ,

$$\mathbb{E}_{P_0}[T_{m^*,n}^d \mid \mathbf{Z}] = \frac{1}{n} \sum_{i \in \mathcal{I}} \frac{1}{N_i} \sum_{j_1 \neq j_2 \in \mathcal{I}_{m^*,i}} \mathbb{E}_{P_0} [\bar{Y}_{j_1}^\top \bar{Y}_{j_2} \mid \mathbf{Z}] = 0$$

because $\mathbb{E}_{P_0}[\bar{Y}_{j_1}^\top \bar{Y}_{j_2} \mid \mathbf{Z}] = \mathbb{E}_{P_0}[\bar{Y}_{j_1} \mid \mathbf{Z}]^\top \mathbb{E}_{P_0}[\bar{Y}_{j_2} \mid \mathbf{Z}] = 0$ for all $j_1 \neq j_2 \in \mathcal{I}_{m^*,i}$. Therefore,

$$\mathbb{E}_{P_0}[T_{m^*,n}^d] = \mathbb{E}_{P_0}[\mathbb{E}_{P_0}[T_{m^*,n}^d \mid \mathbf{Z}]] = 0 \tag{19}$$

Also,

$$\begin{aligned} \text{Var}_{P_0}(T_{m^*,n}^d \mid \mathbf{Z}) &= \frac{1}{n^2} \sum_{i \in \mathcal{I}} \frac{1}{N_i^2} \text{Var}_{P_0} \left(2 \sum_{j_1 < j_2 \in \mathcal{I}_{m^*,i}} \bar{Y}_{j_1}^\top \bar{Y}_{j_2} \mid \mathbf{Z} \right) \\ &= \frac{1}{n^2} \sum_{i \in \mathcal{I}} \frac{4}{N_i^2} \sum_{j_1 < j_2 \in \mathcal{I}_{m^*,i}} \text{Var}_{P_0} (\bar{Y}_{j_1}^\top \bar{Y}_{j_2} \mid \mathbf{Z}). \end{aligned}$$

The cross terms in the expansion of $\text{Var}_{P_0}(\sum_{j_1 < j_2 \in \mathcal{I}_{m^*,i}} \bar{Y}_{j_1} \bar{Y}_{j_2} \mid \mathbf{Z})$ vanish since for $j_1, j_2, j_3 \in \mathcal{I}_{m^*,i}$ that are pairwise different,

$$\begin{aligned} \text{Cov}_{P_0}(\bar{Y}_{j_1}^\top \bar{Y}_{j_2}, \bar{Y}_{j_1}^\top \bar{Y}_{j_3} \mid \mathbf{Z}) &= \mathbb{E}_{P_0}[\bar{Y}_{j_2}^\top \bar{Y}_{j_1} \bar{Y}_{j_1}^\top \bar{Y}_{j_3} \mid \mathbf{Z}] - \mathbb{E}_{P_0}[\bar{Y}_{j_1}^\top \bar{Y}_{j_2} \mid \mathbf{Z}] \mathbb{E}_{P_0}[\bar{Y}_{j_1}^\top \bar{Y}_{j_3} \mid \mathbf{Z}] \\ &= \mathbb{E}_{P_0}[\bar{Y}_{j_2} \mid \mathbf{Z}]^\top \mathbb{E}_{P_0}[\bar{Y}_{j_1} \bar{Y}_{j_1}^\top \mid \mathbf{Z}] \mathbb{E}_{P_0}[\bar{Y}_{j_3} \mid \mathbf{Z}] - \mathbb{E}_{P_0}[\bar{Y}_{j_1} \mid \mathbf{Z}]^\top \mathbb{E}_{P_0}[\bar{Y}_{j_2} \mid \mathbf{Z}] \mathbb{E}_{P_0}[\bar{Y}_{j_1} \mid \mathbf{Z}]^\top \mathbb{E}_{P_0}[\bar{Y}_{j_3} \mid \mathbf{Z}] \\ &= 0, \end{aligned}$$

and for $j_1, j_2, j_3, j_4 \in \mathcal{I}_{m^*,i}$ that are pairwise different, $\text{Cov}_{P_0}(\bar{Y}_{j_1}^\top \bar{Y}_{j_2}, \bar{Y}_{j_3}^\top \bar{Y}_{j_4} \mid \mathbf{Z}) = 0$ by the independence of $\bar{Y}_{j_1}, \bar{Y}_{j_2}, \bar{Y}_{j_3}, \bar{Y}_{j_4}$ given \mathbf{Z} . Further, since $\text{Var}_{P_0}(\bar{Y}_{j_1}^\top \bar{Y}_{j_2} \mid \mathbf{Z}) \leq K^2$ for all $j_1 < j_2 \in \mathcal{I}_{m^*,i}$,

$$\text{Var}_{P_0}(T_{m^*,n}^d \mid \mathbf{Z}) \leq \frac{1}{n^2} \sum_{i \in \mathcal{I}} \frac{2K^2 N_i(N_i - 1)}{N_i^2} \leq 2K^2 n^{-2} \sum_{i=1}^{(m^*)^{K-1}} I(N_i \geq 2).$$

Thus, by the law of total variance,

$$\begin{aligned} \text{Var}_{P_0}(T_{m^*,n}^d) &= \mathbb{E}_{P_0}[\text{Var}_{P_0}(T_{m^*,n}^d \mid \mathbf{Z})] + \text{Var}_{P_0}(\mathbb{E}_{P_0}[T_{m^*,n}^d \mid \mathbf{Z}]) \leq 2K^2 n^{-2} \sum_{i=1}^{(m^*)^{K-1}} P_0(N_i \geq 2) \\ &= 2K^2 (m^*)^{K-1} n^{-2} P_0(N_1 \geq 2). \end{aligned}$$

Since $(1-x)^{n-1} \geq 1 - (n-1)x$ for any $x \in [0, 1]$, we see

$$P_0(N_1 \geq 2) = 1 - \left(1 - \frac{1}{(m^*)^{K-1}}\right)^{n-1} \left(1 + \frac{n-1}{(m^*)^{K-1}}\right) \leq 1 \wedge \frac{n^2}{(m^*)^{2(K-1)}} \quad (20)$$

Therefore, defining τ^2 below,

$$\text{Var}_{P_0}(T_{m^*,n}^d) \leq 2K^2 \left((m^*)^{K-1} n^{-2} \wedge (m^*)^{-(K-1)}\right) =: \tau^2. \quad (21)$$

Under P_1 , we have

$$\mathbb{E}_{P_1}[T_{m^*,n}^d \mid \mathbf{Z}] = \frac{1}{n} \sum_{i \in \mathcal{I}} \frac{1}{N_i} \sum_{j_1 \neq j_2 \in \mathcal{I}_{m^*,i}} \mathbb{E}_{P_1}[\bar{Y}_{j_1}^\top \bar{Y}_{j_2} \mid \mathbf{Z}] = \frac{1}{n} \sum_{i \in \mathcal{I}} \frac{1}{N_i} \sum_{j_1 \neq j_2 \in \mathcal{I}_{m^*,i}} \text{res}_f(Z_{j_1})^\top \text{res}_f(Z_{j_2})$$

since, for each $i \in \mathcal{I}$, $\mathbb{E}_{P_1}[\bar{Y}_{j_1}^\top \bar{Y}_{j_2} \mid \mathbf{Z}] = \mathbb{E}_{P_1}[\bar{Y}_{j_1} \mid \mathbf{Z}]^\top \mathbb{E}_{P_1}[\bar{Y}_{j_2} \mid \mathbf{Z}] = \text{res}_f(Z_{j_1})^\top \text{res}_f(Z_{j_2})$ for all $j_1 \neq j_2 \in \mathcal{I}_{m^*,i}$. Moreover,

$$\begin{aligned} \mathbb{E}_{P_1}[T_{m^*,n}^d \mid \mathbf{N}] &= \mathbb{E}_{P_1}[\mathbb{E}_{P_1}[T_{m^*,n}^d \mid \mathbf{Z}] \mid \mathbf{N}] = \frac{1}{n} \sum_{i \in \mathcal{I}} \frac{N_i(N_i - 1)}{N_i} \mathbb{E}_{P_1}[\text{res}_f(Z) \mid Z \in B_i]^\top \mathbb{E}_{P_1}[\text{res}_f(Z) \mid Z \in B_i] \\ &= \frac{1}{n} \sum_{i \in \mathcal{I}} (N_i - 1) \|\mathbb{E}_{P_1}[\text{res}_f(Z) \mid Z \in B_i]\|^2 \end{aligned}$$

and

$$\mathbb{E}_{P_1}[T_{m^*,n}^d] = \mathbb{E}_{P_1}[\mathbb{E}_{P_1}[T_{m^*,n}^d \mid \mathbf{N}]] = \frac{1}{n} \sum_{i=1}^{(m^*)^{K-1}} \mathbb{E}_{P_1}[I(N_i \geq 1)(N_i - 1)] \|\mathbb{E}_{P_1}[\text{res}_f(Z) \mid Z \in B_i]\|^2.$$

For any $x \in [0, 1]$, we have $1 - nx + \binom{n}{2}x^2 - \binom{n}{3}x^3 \leq (1-x)^n \leq 1 - nx + \binom{n}{2}x^2$. Applying the inequality for $x = (m^*)^{-(K-1)}$, we derive

$$\begin{aligned} \frac{1}{4} \left(\frac{n}{(m^*)^{K-1}} \wedge \frac{n^2}{(m^*)^{2(K-1)}} \right) &\leq \mathbb{E}_{P_1}[I(N_i \geq 1)(N_i - 1)] = \frac{n}{(m^*)^{K-1}} - 1 + \left(1 - \frac{1}{(m^*)^{K-1}}\right)^n \\ &\leq \frac{n}{(m^*)^{K-1}} \wedge \frac{n^2}{(m^*)^{2(K-1)}} \end{aligned} \quad (22)$$

for all large enough n .

By Lemma 8.1, and because $\varepsilon^2 = \sum_{k=1}^K \mathbb{E}_{P_1}[[\text{res}_f(Z)]_k^2] \geq K^{-1}(\sum_{k=1}^K \mathbb{E}_{P_1}[[\text{res}_f(Z)]_k^2])^2$ by the Cauchy-Schwarz inequality,

$$\begin{aligned} \sum_{i=1}^{(m^*)^{K-1}} (m^*)^{-(K-1)} \|\mathbb{E}_{P_1}[\text{res}_f(Z)I(Z \in B_i)]\|^2 &= \sum_{i=1}^{(m^*)^{K-1}} \sum_{k=1}^K (m^*)^{-(K-1)} \mathbb{E}_{P_1}[[\text{res}_f(Z)]_k I(Z \in B_i)]^2 \\ &\geq \sum_{k=1}^K \left(b_1 \mathbb{E}_{P_1}[[\text{res}_f(Z)]_k^2]^{\frac{1}{2}} - b_2 (m^*)^{-s} \right)^2 \geq \sum_{k=1}^K \left(b_1^2 \mathbb{E}_{P_1}[[\text{res}_f(Z)]_k^2] - 2b_1 b_2 \mathbb{E}_{P_1}[[\text{res}_f(Z)]_k^2]^{\frac{1}{2}} (m^*)^{-s} \right) \\ &\geq b_1^2 \varepsilon^2 - 2\sqrt{K} b_1 b_2 (m^*)^{-s} n \varepsilon. \end{aligned} \quad (23)$$

By (22) and (23), defining δ below,

$$\mathbb{E}_{P_1}[T_{m^*,n}^d] \geq \frac{1}{4} (b_1^2 \varepsilon^2 - 2\sqrt{K} b_1 b_2 (m^*)^{-s} \varepsilon) \left(1 \wedge \frac{n}{(m^*)^{K-1}} \right) =: \delta \quad (24)$$

Moreover, we find

$$\begin{aligned} \text{Var}_{P_1}(T_{m^*,n}^d \mid \mathbf{N}) &= \frac{1}{n^2} \sum_{i \in \mathcal{I}} \frac{1}{N_i^2} \text{Var}_{P_1} \left(2 \sum_{j_1 < j_2 \in \mathcal{I}_{m^*,i}} \bar{Y}_{j_1}^\top \bar{Y}_{j_2} \mid \mathbf{N} \right) \\ &= \frac{1}{n^2} \sum_{i \in \mathcal{I}} \frac{1}{N_i^2} \left[2N_i(N_i-1) \text{Var}_{P_1} \left(\bar{Y}_1^\top \bar{Y}_2 \mid Z_1, Z_2 \in B_i \right) \right. \\ &\quad \left. + 4N_i(N_i-1)(N_i-2) \text{Cov}_{P_1} \left(\bar{Y}_1^\top \bar{Y}_2, \bar{Y}_1^\top \bar{Y}_3 \mid Z_1, Z_2, Z_3 \in B_i \right) \right] \\ &\leq \frac{1}{n^2} \sum_{i \in \mathcal{I}} \left(\frac{2K^2 N_i(N_i-1)}{N_i^2} + \frac{4K^2 N_i(N_i-1)(N_i-2)}{N_i^2} \|\mathbb{E}_{P_1}[\text{res}_f(Z) \mid Z \in B_i]\|^2 \right). \end{aligned}$$

Further by equations (20), (22) and since $\|\mathbb{E}_{P_1}[\text{res}_f(Z) \mid Z \in B_i]\|^2 \leq \mathbb{E}_{P_1}[\|\text{res}_f(Z)\|^2 \mid Z \in B_i]$,

$$\begin{aligned} \mathbb{E}_{P_1}[\text{Var}_{P_1}(T_{m^*,n}^d \mid \mathbf{N})] &\leq \frac{1}{n^2} \sum_{i=1}^{(m^*)^{K-1}} (2K^2 \mathbb{E}_{P_1}[(N_i \geq 2)] + 4K^2 \mathbb{E}_{P_1}[(N_i-1)I(N_i \geq 1)] \|\mathbb{E}_{P_1}[\text{res}_f(Z) \mid Z \in B_i]\|^2) \\ &\leq \tau^2 + 4K^2 (m^*)^{K-1} n^{-2} \mathbb{E}_{P_1}[(N_1-1)I(N_i \geq 1)] \sum_{i=1}^{(m^*)^{K-1}} \mathbb{E}_{P_1}[\|\text{res}_f(Z)\|^2 I(Z \in B_i)] \\ &\leq \tau^2 + 4K^2 \varepsilon^2 (n^{-1} \wedge (m^*)^{-(K-1)}). \end{aligned} \quad (25)$$

Also,

$$\text{Var}_{P_1}(\mathbb{E}_{P_1}[T_{m^*,n}^d \mid \mathbf{N}]) \leq K^2 \varepsilon^2 (n^{-1} \wedge (m^*)^{-(K-1)}) \quad (26)$$

for all large enough n . By equations (25), (26), and the total law of variance, defining σ^2 below,

$$\begin{aligned} \text{Var}_{P_1}(T_{m^*,n}^d) &= \text{Var}_{P_1}(\mathbb{E}_{P_1}[T_{m^*,n}^d \mid \mathbf{N}]) + \mathbb{E}_{P_1}[\text{Var}_{P_1}(T_{m^*,n}^d \mid \mathbf{N})] \\ &\leq \tau^2 + 5K^2 \varepsilon^2 (n^{-1} \wedge (m^*)^{-(K-1)}) =: \sigma^2. \end{aligned} \quad (27)$$

We choose $c > 0$ such that $\varepsilon \geq cn^{-2s/(4s+K-1)}$ implies

$$\sqrt{\frac{2}{\alpha}} K (m^*)^{\frac{K-1}{2}} n^{-1} + \sqrt{\frac{7}{\beta}} K (m^*)^{\frac{K-1}{2}} n^{-1} \leq \frac{1}{4} (b_1^2 \varepsilon^2 - 2\sqrt{K} b_1 b_2 (m^*)^{-s} \varepsilon)$$

for all large enough n . For τ , δ , and σ from (21), (24), and (27), this gives

$$\frac{\tau}{\sqrt{\alpha}} + \frac{\sigma}{\sqrt{\beta}} \leq \delta. \quad (28)$$

By equations (19), (21), and Chebyshev's inequality,

$$P_0(\xi_{m^*,n} = 1) \leq P_0\left(T_{m^*,n}^d \geq \frac{\tau}{\sqrt{\alpha}}\right) \leq \frac{\text{Var}_{P_0}(T_{m^*,n}^d)}{\tau^2/\alpha} \leq \alpha.$$

By equations (24), (27), (28), and Chebyshev's inequality,

$$\begin{aligned} P_1\left(T_{m^*,n}^d < \frac{\tau}{\sqrt{\alpha}}\right) &\leq P_1\left(T_{m^*,n}^d - \mathbb{E}_{P_1}[T_{m^*,n}^d] \leq \frac{\tau}{\sqrt{\alpha}} - \delta\right) \\ &\leq P_1\left(\left|T_{m^*,n}^d - \mathbb{E}_{P_1}[T_{m^*,n}^d]\right| \geq \frac{\sigma}{\sqrt{\beta}}\right) \leq \frac{\text{Var}_{P_1}(T_{m^*,n}^d)}{\sigma^2/\beta} \leq \beta. \end{aligned}$$

By the above arguments, Theorem 3.1 holds for all $n \geq N$, where $N \in \mathbb{N}_+$ depends on $(s, L, K, \nu_l, \nu_u, \alpha, \beta)$. If we require c to further satisfy $c \geq N^{2s/(4s+K-1)}$, then the family $\mathcal{P}_1(\varepsilon, p, s)$ is empty for $n < N$ given $\varepsilon \geq cn^{-2s/(4s+K-1)} > 1$. Therefore, Theorem 3.1 becomes vacuously true for $n < N$, and thereby true for all n . This finishes the proof. \square

8.1.2 Proof of Theorem 3.2

By the union bound, for $P \in \mathcal{P}_0$,

$$P(\xi_n^{\text{ad}} = 1) \leq \sum_{b=1}^B P\left(\xi_{2^b,n}\left(\frac{\alpha}{B}\right) = 1\right) \leq \sum_{b=1}^B \frac{\alpha}{B} = \alpha.$$

There exists $b_0 \in \{1, \dots, B\}$ such that $2^{b_0-1} < (n/\sqrt{\log n})^{2/(4s+K-1)} \leq 2^{b_0}$. Let $m_0 = 2^{b_0}$ and repeat the argument in the proof of Theorem 3.1. The condition (28) for type II error control is now changed to

$$\sqrt{\frac{2}{\alpha}} K m_0^{\frac{K-1}{2}} n^{-1} \sqrt{\log n} + \sqrt{\frac{7}{\beta}} K m_0^{\frac{K-1}{2}} n^{-1} \leq \frac{1}{4} (b_1^2 \varepsilon^2 - 2\sqrt{K} b_1 b_2 m_0^{-s} \varepsilon),$$

which is satisfied when $\varepsilon \geq c_{\text{ad}}(n/\sqrt{\log n})^{-2s/(4s+K-1)}$ for a sufficiently large $c_{\text{ad}} > 0$. Assuming $\varepsilon \geq c_{\text{ad}}(n/\sqrt{\log n})^{-2s/(4s+K-1)}$ and $P \in \mathcal{P}_1(\varepsilon, p, s)$, we have

$$P(\xi_n^{\text{ad}} = 1) \geq P(\xi_{m_0,n} = 1) \geq 1 - \beta.$$

This finishes the proof.

8.1.3 Proof of Proposition 3.4

Overview of the proof We repeat the computation in Section 8.1.1. However, due to the bias term, now the mean difference $\mathbb{E}_{P_1}[T_{m^*,n}^b] - \mathbb{E}_{P_0}[T_{m^*,n}^b]$ cannot be lower bounded by a positive number. Instead, we prove that $\mathbb{E}_{P_0}[T_{m^*,n}^b] \geq \mathbb{E}_{P_1}[T_{m^*,n}^b]$ holds for all large enough n .

We use the same notations as in Section 8.1.1. Since

$$\begin{aligned} \mathbb{E}_{P_0}[T_{m^*,n}^b \mid \mathbf{Z}] &= \frac{1}{n} \sum_{i \in \mathcal{I}} \frac{1}{N_i} \left[\sum_{j \in \mathcal{I}_{m^*,i}} \mathbb{E}_{P_0}[\bar{Y}_j^2 \mid \mathbf{Z}] + \sum_{j_1 \neq j_2 \in \mathcal{I}_{m^*,i}} \mathbb{E}_{P_0}[\bar{Y}_{j_1} \bar{Y}_{j_2} \mid \mathbf{Z}] \right] \\ &= \frac{1}{n} \sum_{i \in \mathcal{I}} \frac{1}{N_i} \sum_{j \in \mathcal{I}_{m^*,i}} (Z_j - Z_j^2), \end{aligned}$$

we have

$$\mathbb{E}_{P_0}[T_{m^*,n}^b \mid \mathbf{N}] = \mathbb{E}_{P_0}[\mathbb{E}_{P_0}[T_{m^*,n}^b \mid \mathbf{Z}] \mid \mathbf{N}] = \frac{1}{n} \sum_{i \in \mathcal{I}} \mathbb{E}_{P_0}[Z - Z^2 \mid Z \in B_i]. \quad (29)$$

Similarly,

$$\begin{aligned}\mathbb{E}_{P_1}[T_{m^*,n}^b \mid \mathbf{Z}] &= \frac{1}{n} \sum_{i \in \mathcal{I}} \frac{1}{N_i} \left[\sum_{j \in \mathcal{I}_{m^*,i}} \mathbb{E}_{P_1} [\bar{Y}_j^2 \mid \mathbf{Z}] + \sum_{j_1 \neq j_2 \in \mathcal{I}_{m^*,i}} \mathbb{E}_{P_1} [\bar{Y}_{j_1} \bar{Y}_{j_2} \mid \mathbf{Z}] \right] \\ &= \frac{1}{n} \sum_{i \in \mathcal{I}} \frac{1}{N_i} \left[\sum_{j \in \mathcal{I}_{m^*,i}} (\text{reg}_f(Z_j) - \text{reg}_f(Z_j)^2 + \text{res}_f(Z_j)^2) + \sum_{j_1 \neq j_2 \in \mathcal{I}_{m^*,i}} \text{res}_f(Z_{j_1}) \text{res}_f(Z_{j_2}) \right],\end{aligned}$$

and thus

$$\begin{aligned}\mathbb{E}_{P_1}[T_{m^*,n}^b \mid \mathbf{N}] &= \mathbb{E}_{P_1}[\mathbb{E}_{P_1}[T_{m^*,n}^b \mid \mathbf{Z}] \mid \mathbf{N}] \\ &= \frac{1}{n} \sum_{i \in \mathcal{I}} \left(\mathbb{E}_{P_1} [\text{reg}_f(Z) - \text{reg}_f(Z)^2 + \text{res}_f(Z)^2 \mid Z \in B_i] + (N_i - 1) \mathbb{E}_{P_1} [\text{res}_f(Z) \mid Z \in B_i]^2 \right).\end{aligned}\quad (30)$$

Since $Z \sim \text{Unif}([0, 1])$ under both P_0 and P_1 , the equations (29) and (30) imply

$$\begin{aligned}\mathbb{E}_{P_0}[T_{m^*,n}^b \mid \mathbf{N}] - \mathbb{E}_{P_1}[T_{m^*,n}^b \mid \mathbf{N}] &= \frac{1}{n} \sum_{i \in \mathcal{I}} (\mathbb{E}[\text{res}_f(Z)(2Z - 1) \mid Z \in B_i] - (N_i - 1) \mathbb{E}[\text{res}_f(Z) \mid Z \in B_i]^2) \\ &\geq \frac{1}{n} \sum_{i \in \mathcal{I}} \mathbb{E}[\text{res}_f(Z)(2Z - 1) \mid Z \in B_i] - \rho^2 \|\zeta\|_{L^1}^2 (m^*)^{-2s}.\end{aligned}$$

Here we used that $\mathbb{E}[\text{res}_f(Z) \mid Z \in B_i]^2 \leq \rho^2 \|\zeta\|_{L^1}^2 (m^*)^{-2s}$ for all $i \in [m^*]$ and $\sum_{i \in \mathcal{I}} (N_i - 1) \leq n$. Taking total expectation,

$$\begin{aligned}\mathbb{E}_{P_0}[T_{m^*,n}^b] - \mathbb{E}_{P_1}[T_{m^*,n}^b] &\geq \frac{1}{n} \mathbb{E} \left[\sum_{i \in \mathcal{I}} \mathbb{E}[\text{res}_f(Z)(2Z - 1) \mid Z \in B_i] \right] - \rho^2 \|\zeta\|_{L^1}^2 (m^*)^{-2s} \\ &= \frac{1}{n} \sum_{i=1}^{m^*} P(N_i \geq 1) \mathbb{E}[\text{res}_f(Z)(2Z - 1) \mid Z \in B_i] - \rho^2 \|\zeta\|_{L^1}^2 (m^*)^{-2s} \\ &= \frac{1}{n} P(N_1 \geq 1) \sum_{i=1}^{m^*} \mathbb{E}[\text{res}_f(Z)(2Z - 1) \mid Z \in B_i] - \rho^2 \|\zeta\|_{L^1}^2 (m^*)^{-2s}.\end{aligned}\quad (31)$$

From (9), we see that $\mathbb{E}[\text{res}_f(Z)(2Z - 1) \mid Z \in B_i] \geq 0$ for all $i \in [m^*]$. Thus,

$$\begin{aligned}\sum_{i=1}^{m^*} \mathbb{E}[\text{res}_f(Z)(2Z - 1) \mid Z \in B_i] &\geq \sum_{i=\frac{m^*}{4}+1}^{\frac{m^*}{8}} \mathbb{E}[\text{res}_f(Z)(2Z - 1) \mid Z \in B_i] \\ &\geq \frac{1}{4} \sum_{i=\frac{m^*}{4}+1}^{\frac{m^*}{8}} \mathbb{E}[-\text{res}_f(Z) \mid Z \in B_i] = \frac{\rho}{32} \|\zeta\|_{L^1} (m^*)^{1-s}.\end{aligned}\quad (32)$$

Combining (31) and (32), we find

$$\mathbb{E}_{P_0}[T_{m^*,n}^b] - \mathbb{E}_{P_1}[T_{m^*,n}^b] \geq \frac{\rho}{32} P(N_1 \geq 1) \|\zeta\|_{L^1} (m^*)^{1-s} n^{-1} - \rho^2 \|\zeta\|_{L^1}^2 (m^*)^{-2s}.\quad (33)$$

Since $m^* = \lfloor n^{2/(4s+1)} \rfloor$ and $\frac{2}{4s+1} < 1$, we find

$$\lim_{n \rightarrow \infty} P(N_1 \geq 1) = \lim_{n \rightarrow \infty} 1 - \left(1 - \frac{1}{m^*}\right)^n = 1.$$

Also, we have $(m^*)^{1-s} n^{-1} \asymp n^{(1-6s)/(4s+1)}$ and $(m^*)^{-2s} \asymp n^{-4s/(4s+1)}$ with $\frac{1-6s}{4s+1} > \frac{-4s}{4s+1}$. In conclusion, the RHS of (33) is positive for all large enough n .

8.1.4 Proof of Proposition 5.1

Overview of the proof We construct distributions P_1, \dots, P_M over (Z, Y) under which the predictor f has an ℓ_p -ECE of at least $\varepsilon_0 = 0.1$. We can choose the mis-calibration curves of P_1, \dots, P_M to be orthogonal in L^2 , so that the cross terms in the expansion of $\mathbb{E}_{P_0}[L_n^2]$ cancel out. By choosing M sufficiently large, we can ensure that $\mathbb{E}_{P_0}[L_n^2]$ is at most $1 + (1 - \alpha - \beta)^2$. The conclusion follows from Lemma 5.3.

We prove Proposition 5.1 for the binary case. The generalization to the multi-class case follows the same argument and is omitted. The construction in this proof is inspired by Ingster (1987, 2000); Burnashev (1979). Let P_0 be a null distribution over $(Z, Y) \in [0, 1] \times \{0, 1\}$ defined as follows: the distribution of the predicted probabilities follows $Z \stackrel{P_0}{\sim} \text{Unif}([0, 1])$ and $P_0(Y = 1 \mid Z = z) = z$ for all $z \in [0, 1]$. Under P_0 , the probability predictor f is perfectly calibrated. For each $i \in [M]$, let

$$g_i(u) := \begin{cases} u + \sqrt{\frac{u(1-u)}{3}} \sin(2i\pi(u - \frac{1}{4})) & u \in [\frac{1}{4}, \frac{3}{4}], \\ u & u \notin [\frac{1}{4}, \frac{3}{4}], \end{cases}$$

and define P_i as follows: $Z \stackrel{P_i}{\sim} \text{Unif}([0, 1])$ and $P_i(Y = 1 \mid Z = z) = g_i(z)$ for all $z \in [0, 1]$.

It can be verified that $0 \leq g_i(u) \leq 1$ for all $u \in [0, 1]$. Since $p \geq 1$, for all $i \in [M]$, the ℓ_p -ECE of the probability predictor f under P_i is lower bounded as

$$\ell_p\text{-ECE}_{P_i}(f) \geq \ell_1\text{-ECE}_{P_i}(f) = 2 \int_0^1 |g_i(u) - u| du = 2 \int_{\frac{1}{4}}^{\frac{3}{4}} \sqrt{\frac{u(1-u)}{3}} \left| \sin\left(2i\pi\left(u - \frac{1}{4}\right)\right) \right| du \geq 0.1.$$

Thus we know that $P_i \in \mathcal{P}_1^{\text{cont}}(\varepsilon_0, p)$ for all $i \in [M]$. Now, observe that

$$L_n = \frac{1}{M} \sum_{i=1}^M \prod_{j=1}^n \frac{dP_i}{dP_0}(Z_j, Y_j) = \frac{1}{M} \sum_{i=1}^M \prod_{j=1}^n \frac{1 - Y_j + (2Y_j - 1)g_i(Z_j)}{1 - Y_j + (2Y_j - 1)Z_j}$$

and thus, for a random variable $(Z, Y) \sim P_0$, and defining $A_{a,b}$ below

$$\begin{aligned} \mathbb{E}_{P_0}[L_n^2] &= \frac{1}{M^2} \sum_{a,b \in [M]} \mathbb{E}_{P_0} \left[\prod_{j=1}^n \frac{1 - Y_j + (2Y_j - 1)g_a(Z_j)}{1 - Y_j + (2Y_j - 1)Z_j} \cdot \frac{1 - Y_j + (2Y_j - 1)g_b(Z_j)}{1 - Y_j + (2Y_j - 1)Z_j} \right] \\ &= \frac{1}{M^2} \sum_{a,b \in [M]} \mathbb{E}_{P_0} \left[\frac{1 - Y + (2Y - 1)g_a(Z)}{1 - Y + (2Y - 1)Z} \cdot \frac{1 - Y + (2Y - 1)g_b(Z)}{1 - Y + (2Y - 1)Z} \right]^n \\ &=: \frac{1}{M^2} \sum_{a,b \in [M]} \mathbb{E}_{P_0} [A_{a,b}]^n. \end{aligned}$$

In the second line, we have used the independence of the observations. If $a = b$, then

$$\begin{aligned} \mathbb{E}_{P_0} [A_{a,b}] &= \int_0^1 u \frac{g_a(u)^2}{u^2} + (1-u) \frac{(1-g_a(u))^2}{(1-u)^2} du = 1 + \int_0^1 \frac{(g_a(u) - u)^2}{u(1-u)} du \\ &= 1 + \int_{\frac{1}{4}}^{\frac{3}{4}} \frac{1}{3} \sin^2 \left(2a\pi \left(u - \frac{1}{4} \right) \right) du = \frac{13}{12}. \end{aligned}$$

If $a \neq b$, then

$$\begin{aligned} \mathbb{E}_{P_0} [A_{a,b}] &= \int_0^1 u \frac{g_a(u)g_b(u)}{u^2} + (1-u) \frac{(1-g_a(u))(1-g_b(u))}{(1-u)^2} du \\ &= 1 + \int_0^1 \frac{(g_a(u) - u)(g_b(u) - u)}{u(1-u)} du = 1 + \int_{\frac{1}{4}}^{\frac{3}{4}} \frac{1}{3} \sin \left(2a\pi \left(u - \frac{1}{4} \right) \right) \sin \left(2b\pi \left(u - \frac{1}{4} \right) \right) du = 1. \end{aligned}$$

Therefore,

$$\mathbb{E}_{P_0}[L_n^2] = \frac{1}{M^2} \left(M \left(\frac{13}{12} \right)^n + (M^2 - M) \right).$$

Choose a large enough $M \in \mathbb{N}_+$ such that $M \geq [(13/12)^n - 1]/(1 - \alpha - \beta)^2$. Then,

$$\frac{1}{M^2} \left(M \left(\frac{13}{12} \right)^n + (M^2 - M) \right) \leq 1 + (1 - \alpha - \beta)^2,$$

and the result follows by Lemma 5.3.

8.1.5 Proof of Theorem 5.2

Overview of the proof We construct m^{K-1} distributions under which the predictor f has an ℓ_p -ECE of $\Omega(n^{-2s/(4s+K-1)})$. The mis-calibration curves are constructed by linearly combining bump functions with disjoint supports. By properly scaling them, we can guarantee Hölder continuity. Also, the mis-calibration curves are chosen to be ‘‘almost’’ orthogonal in L^2 , so that the cross terms in the expansion of $\mathbb{E}_{P_0}[L_n^2]$ are small. We use Lemma 5.3 to conclude.

The proof is inspired by the lower bound arguments in Arias-Castro et al. (2018). For $m := \lceil n^{2/(4s+K-1)} \rceil$ and $\boldsymbol{\eta} \in \{\pm 1\}^{[m]^{K-1}}$, we define alternative distributions $P_{\boldsymbol{\eta}} \in \mathcal{P}_1(\varepsilon, p, s)$ with $\varepsilon := c_{\text{lower}} n^{-2s/(4s+K-1)}$ and use Lemma 5.3 to prove $\varepsilon_n(p, s) \geq c_{\text{lower}} n^{-2s/(4s+K-1)}$. Let $\zeta : \mathbb{R} \rightarrow \mathbb{R}$ be the function from (8). It can be verified that ζ is infinitely differentiable and its derivatives of every order are bounded. For $\psi = \pi_{-K} : (z_1, \dots, z_K)^\top \mapsto (z_1, \dots, z_{K-1})^\top$, we see that $[\frac{1}{2K}, \frac{1}{K}]^{K-1} \subseteq \psi(\Delta_{K-1} \cap [\frac{1}{2K}, 1]^K)$. For each $\mathbf{j} = (j_1, \dots, j_{K-1})^\top \in [m]^{K-1}$, define $\Psi_{\mathbf{j}} : \mathbb{R}^{K-1} \rightarrow \mathbb{R}$ by

$$\Psi_{\mathbf{j}}(x_1, \dots, x_{K-1}) := m^{-s} \prod_{k=1}^{K-1} \zeta(m(2Kx_k - 1) - j_k + 1). \quad (34)$$

Then, each $\Psi_{\mathbf{j}}$ is supported on the cube

$$\text{supp}(\Psi_{\mathbf{j}}) = \prod_{k=1}^{K-1} \left(\frac{j_k - 1 + m}{2Km}, \frac{j_k + m}{2Km} \right).$$

The sets $\text{supp}(\Psi_{\mathbf{j}})$ are disjoint for different indices $\mathbf{j} \in [m]^{K-1}$, and we have

$$\bigcup_{\mathbf{j} \in [m]^{K-1}} \text{supp}(\Psi_{\mathbf{j}}) \subseteq \left[\frac{1}{2K}, \frac{1}{K} \right]^{K-1} \subseteq \psi \left(\Delta_{K-1} \cap \left[\frac{1}{2K}, 1 \right]^K \right).$$

Let $c_{\alpha, \beta} := (\log(1 + (1 - \alpha - \beta)^2))^{1/4}$ and

$$\rho := \left(\max_{t \in \{0, \dots, \lceil s \rceil\}} \left\| \zeta^{(t)} \right\|_{L^\infty}^{K-1} \right)^{-1} \left(\frac{1}{2K} \wedge \frac{L(2K)^{-\lceil s \rceil}}{2\sqrt{K-1}} \wedge \frac{L(2K)^{-\lceil s \rceil+1}}{4} \wedge \frac{c_{\alpha, \beta}(2K)^{\frac{K-1}{2}}}{2\sqrt{K!}} \right). \quad (35)$$

By the definition of ρ in (35), we see that

$$\rho \left\| \zeta \right\|_{L^\infty}^{K-1} \leq \frac{1}{2K}, \quad (36)$$

$$\rho \sqrt{K-1} (2K)^{\lceil s \rceil} \left(\max_{t \in \{0, \dots, \lceil s \rceil\}} \left\| \zeta^{(t)} \right\|_{L^\infty}^{K-1} \right) \leq \frac{L}{2}, \quad (37)$$

$$2\rho (2K)^{\lceil s \rceil-1} \left(\max_{t \in \{0, \dots, \lceil s \rceil-1\}} \left\| \zeta^{(t)} \right\|_{L^\infty}^{K-1} \right) \leq \frac{L}{2}, \quad (38)$$

and

$$4\rho^2 K! (2K)^{-K+1} \left\| \zeta \right\|_{L^2}^{2(K-1)} \leq c_{\alpha, \beta}^2 \leq 1. \quad (39)$$

For each $\boldsymbol{\eta} \in \{\pm 1\}^{[m]^{K-1}}$, define $g_{\boldsymbol{\eta}} : \Delta_{K-1} \rightarrow \mathbb{R}^K$ by

$$g_{\boldsymbol{\eta}}(\mathbf{z}) := \mathbf{z} + \rho \left(\sum_{\mathbf{j} \in [m]^{K-1}} \boldsymbol{\eta}_{\mathbf{j}} (\Psi_{\mathbf{j}} \circ \psi)(\mathbf{z}) \right) (1, -1, 0, \dots, 0)^{\top}.$$

Then we have $g_{\boldsymbol{\eta}}(\Delta_{K-1}) \subseteq \Delta_{K-1}$ for all $\boldsymbol{\eta} \in \{\pm 1\}^{[m]^{K-1}}$. This is because

$$\sum_{k=1}^K [g_{\boldsymbol{\eta}}(\mathbf{z})]_k = \sum_{k=1}^K [\mathbf{z}]_k + \rho \left(\sum_{\mathbf{j} \in [m]^{K-1}} \boldsymbol{\eta}_{\mathbf{j}} (\Psi_{\mathbf{j}} \circ \psi)(\mathbf{z}) \right) - \rho \left(\sum_{\mathbf{j} \in [m]^{K-1}} \boldsymbol{\eta}_{\mathbf{j}} (\Psi_{\mathbf{j}} \circ \psi)(\mathbf{z}) \right) = 1$$

for all $\mathbf{z} \in \Delta_{K-1}$ and

$$[g_{\boldsymbol{\eta}}(\mathbf{z})]_k = \begin{cases} [\mathbf{z}]_k \geq 0 & \text{if } \mathbf{z} \notin [\frac{1}{2K}, 1]^K \text{ or } k \notin \{1, 2\}, \\ [\mathbf{z}]_k \pm \rho \sum_{\mathbf{j} \in [m]^{K-1}} \boldsymbol{\eta}_{\mathbf{j}} (\Psi_{\mathbf{j}} \circ \psi)(\mathbf{z}) \geq \frac{1}{2K} - \rho m^{-s} \|\zeta\|_{L^\infty}^{K-1} \geq 0 & \text{if } \mathbf{z} \in [\frac{1}{2K}, 1]^K \text{ and } k \in \{1, 2\} \end{cases}$$

for all $\mathbf{z} \in \Delta_{K-1}$ and $k \in \{1, \dots, K\}$ by (36).

Next, we claim that each coordinate function of the mapping $\mathbf{z} \mapsto g_{\boldsymbol{\eta}}(\mathbf{z}) - \mathbf{z}$ belongs to $\mathcal{H}_K(s, L)$, i.e., for all multi-indices $\boldsymbol{\gamma} \in \mathbb{N}^{K-1}$ with $|\boldsymbol{\gamma}| = \lceil s \rceil - 1$ and $\mathbf{x}_1, \mathbf{x}_2 \in \psi(\Delta_{K-1})$,

$$\rho \left| \sum_{\mathbf{j} \in [m]^{K-1}} \boldsymbol{\eta}_{\mathbf{j}} (\Psi_{\mathbf{j}}^{(\boldsymbol{\gamma})}(\mathbf{x}_1) - \Psi_{\mathbf{j}}^{(\boldsymbol{\gamma})}(\mathbf{x}_2)) \right| \leq L \|\mathbf{x}_1 - \mathbf{x}_2\|^{s - \lceil s \rceil + 1}. \quad (40)$$

If $m \|\mathbf{x}_1 - \mathbf{x}_2\| \leq 1$, then from the mean value theorem

$$\rho \left| \Psi_{\mathbf{j}}^{(\boldsymbol{\gamma})}(\mathbf{x}_1) - \Psi_{\mathbf{j}}^{(\boldsymbol{\gamma})}(\mathbf{x}_2) \right| \leq \rho \sqrt{K-1} \max_{\substack{\boldsymbol{\gamma} \in \mathbb{N}^{K-1} \\ |\boldsymbol{\gamma}'| = \lceil s \rceil}} \left\| \Psi_{\mathbf{j}}^{(\boldsymbol{\gamma}')} \right\|_{L^\infty} \|\mathbf{x}_1 - \mathbf{x}_2\|. \quad (41)$$

By the definition of $\Psi_{\mathbf{j}}$ in (34), for any $\boldsymbol{\gamma}' = (\gamma'_1, \dots, \gamma'_{K-1})^{\top} \in \mathbb{N}^{K-1}$ with $|\boldsymbol{\gamma}'| = \lceil s \rceil$,

$$\left\| \Psi_{\mathbf{j}}^{(\boldsymbol{\gamma}')} \right\|_{L^\infty} = m^{|\boldsymbol{\gamma}'|-s} (2K)^{|\boldsymbol{\gamma}'|} \prod_{k=1}^{K-1} \left\| \zeta^{(\gamma'_k)} \right\|_{L^\infty} \leq m^{\lceil s \rceil - s} (2K)^{\lceil s \rceil} \max_{t \in \{0, \dots, \lceil s \rceil\}} \left\| \zeta^{(t)} \right\|_{L^\infty}^{K-1}. \quad (42)$$

Plugging (42) into (41), and using (37), we reach

$$\begin{aligned} \rho \left| \Psi_{\mathbf{j}}^{(\boldsymbol{\gamma})}(\mathbf{x}_1) - \Psi_{\mathbf{j}}^{(\boldsymbol{\gamma})}(\mathbf{x}_2) \right| &\leq \rho \sqrt{K-1} m^{\lceil s \rceil - s} (2K)^{\lceil s \rceil} \left(\max_{t \in \{0, \dots, \lceil s \rceil\}} \left\| \zeta^{(t)} \right\|_{L^\infty}^{K-1} \right) \|\mathbf{x}_1 - \mathbf{x}_2\| \\ &\leq \frac{L}{2} m^{\lceil s \rceil - s} \|\mathbf{x}_1 - \mathbf{x}_2\| \leq \frac{L}{2} \|\mathbf{x}_1 - \mathbf{x}_2\|^{s - \lceil s \rceil + 1}. \end{aligned}$$

If $m \|\mathbf{x}_1 - \mathbf{x}_2\| > 1$, using (38), we similarly get

$$\begin{aligned} \rho \left| \Psi_{\mathbf{j}}^{(\boldsymbol{\gamma})}(\mathbf{x}_1) - \Psi_{\mathbf{j}}^{(\boldsymbol{\gamma})}(\mathbf{x}_2) \right| &\leq 2\rho \max_{|\boldsymbol{\gamma}'| = \lceil s \rceil - 1} \left\| \Psi_{\mathbf{j}}^{(\boldsymbol{\gamma}')} \right\|_{L^\infty} \leq 2\rho m^{\lceil s \rceil - s - 1} (2K)^{\lceil s \rceil - 1} \left(\max_{t \in \{0, \dots, \lceil s \rceil - 1\}} \left\| \zeta^{(t)} \right\|_{L^\infty}^{K-1} \right) \\ &\leq \frac{L}{2} m^{\lceil s \rceil - s - 1} \leq \frac{L}{2} \|\mathbf{x}_1 - \mathbf{x}_2\|^{s - \lceil s \rceil + 1}. \end{aligned}$$

Thus, for any $\mathbf{j} \in [m]^{K-1}$ and $\mathbf{x}_1, \mathbf{x}_2 \in \psi(\Delta_{K-1})$, it holds that

$$\rho \left| \Psi_{\mathbf{j}}^{(\boldsymbol{\gamma})}(\mathbf{x}_1) - \Psi_{\mathbf{j}}^{(\boldsymbol{\gamma})}(\mathbf{x}_2) \right| \leq \frac{L}{2} \|\mathbf{x}_1 - \mathbf{x}_2\|^{s - \lceil s \rceil + 1}. \quad (43)$$

Given $\mathbf{x}_1, \mathbf{x}_2 \in \psi(\Delta_{K-1})$, there can be two cases: (1) there exists $\mathbf{j}_1 \in [m]^{K-1}$ such that

$$\rho \left(\sum_{\mathbf{j} \in [m]^{K-1}} \boldsymbol{\eta}_{\mathbf{j}} (\Psi_{\mathbf{j}}^{(\boldsymbol{\gamma})}(\mathbf{x}_1) - \Psi_{\mathbf{j}}^{(\boldsymbol{\gamma})}(\mathbf{x}_2)) \right) = \rho \boldsymbol{\eta}_{\mathbf{j}_1} (\Psi_{\mathbf{j}_1}^{(\boldsymbol{\gamma})}(\mathbf{x}_1) - \Psi_{\mathbf{j}_1}^{(\boldsymbol{\gamma})}(\mathbf{x}_2));$$

or (2) there exist distinct $\mathbf{j}_1, \mathbf{j}_2 \in [m]^{K-1}$ such that $\mathbf{x}_1 \in \text{supp}(\Psi_{\mathbf{j}_1})$ and $\mathbf{x}_2 \in \text{supp}(\Psi_{\mathbf{j}_2})$. In the first case, (40) directly follows from (43). In the second case, choose a point \mathbf{x}_3 on the line segment connecting \mathbf{x}_1 and \mathbf{x}_2 such that $\mathbf{x}_3 \notin \text{supp}(\Psi_{\mathbf{j}_1}) \cup \text{supp}(\Psi_{\mathbf{j}_2})$. Such a point exists since $\text{supp}(\Psi_{\mathbf{j}_1})$, $\text{supp}(\Psi_{\mathbf{j}_2})$ are open and $\text{supp}(\Psi_{\mathbf{j}_1}) \cap \text{supp}(\Psi_{\mathbf{j}_2}) = \emptyset$. For any $\gamma \in \mathbb{N}^{K-1}$ with $|\gamma| = \lceil s \rceil - 1$, we have

$$\begin{aligned} \rho \left| \sum_{\mathbf{j} \in [m]^{K-1}} \boldsymbol{\eta}_{\mathbf{j}} \left(\Psi_{\mathbf{j}}^{(\gamma)}(\mathbf{x}_1) - \Psi_{\mathbf{j}}^{(\gamma)}(\mathbf{x}_2) \right) \right| &= \rho \left| \boldsymbol{\eta}_{\mathbf{j}_1} \Psi_{\mathbf{j}_1}^{(\gamma)}(\mathbf{x}_1) - \boldsymbol{\eta}_{\mathbf{j}_2} \Psi_{\mathbf{j}_2}^{(\gamma)}(\mathbf{x}_2) \right| \\ &= \rho \left| \boldsymbol{\eta}_{\mathbf{j}_1} \Psi_{\mathbf{j}_1}^{(\gamma)}(\mathbf{x}_1) - \boldsymbol{\eta}_{\mathbf{j}_1} \Psi_{\mathbf{j}_1}^{(\gamma)}(\mathbf{x}_3) + \boldsymbol{\eta}_{\mathbf{j}_2} \Psi_{\mathbf{j}_2}^{(\gamma)}(\mathbf{x}_3) - \boldsymbol{\eta}_{\mathbf{j}_2} \Psi_{\mathbf{j}_2}^{(\gamma)}(\mathbf{x}_2) \right| \\ &\leq \rho \left| \Psi_{\mathbf{j}_1}^{(\gamma)}(\mathbf{x}_1) - \Psi_{\mathbf{j}_1}^{(\gamma)}(\mathbf{x}_3) \right| + \rho \left| \Psi_{\mathbf{j}_2}^{(\gamma)}(\mathbf{x}_3) - \Psi_{\mathbf{j}_2}^{(\gamma)}(\mathbf{x}_2) \right| \\ &\leq \frac{L}{2} \|\mathbf{x}_1 - \mathbf{x}_3\|^{s - \lceil s \rceil + 1} + \frac{L}{2} \|\mathbf{x}_3 - \mathbf{x}_2\|^{s - \lceil s \rceil + 1} \leq L \|\mathbf{x}_1 - \mathbf{x}_2\|^{s - \lceil s \rceil + 1}. \end{aligned}$$

The second inequality holds because of (43), and the last inequality holds because $\|\mathbf{x}_1 - \mathbf{x}_3\|, \|\mathbf{x}_3 - \mathbf{x}_2\| \leq \|\mathbf{x}_1 - \mathbf{x}_2\|$ and $s - \lceil s \rceil + 1 > 0$. This finishes the proof of (40).

Now, let P_0 and $P_{\boldsymbol{\eta}}$, $\boldsymbol{\eta} \in \{\pm 1\}^{[m]^{K-1}}$, be the distributions of $(Z, Y) \in \Delta_{K-1} \times \mathcal{Y}$ characterized by

$$Z \xrightarrow{P_0} \text{Unif}(\Delta_{K-1}), \quad Y \mid Z = \mathbf{z} \xrightarrow{P_0} \text{Cat}(\mathbf{z}) \text{ for all } \mathbf{z} \in \Delta_{K-1},$$

and

$$Z \xrightarrow{P_{\boldsymbol{\eta}}} \text{Unif}(\Delta_{K-1}), \quad Y \mid Z = \mathbf{z} \xrightarrow{P_{\boldsymbol{\eta}}} \text{Cat}(g_{\boldsymbol{\eta}}(\mathbf{z})) \text{ for all } \mathbf{z} \in \Delta_{K-1}.$$

We have $P_0 \in \mathcal{P}_0$ by definition. For $Z \sim \text{Unif}(\Delta_{K-1})$ and $\mathbf{j}_0 := \mathbf{1}_{K-1} \in [m]^{K-1}$,

$$\begin{aligned} \ell_p\text{-ECE}_{P_{\boldsymbol{\eta}}}(f)^p &= \mathbb{E} \left[\sum_{k=1}^K |[g_{\boldsymbol{\eta}}(Z) - Z]_k|^p \right] = 2\rho^p \mathbb{E} \left[\left| \sum_{\mathbf{j} \in [m]^{K-1}} \boldsymbol{\eta}_{\mathbf{j}} (\Psi_{\mathbf{j}} \circ \psi)(Z) \right|^p \right] \\ &= 2(K-1)! \rho^p m^{K-1} \int_{\mathbb{R}^{K-1}} |\Psi_{\mathbf{j}_0}(\mathbf{x})|^p d\mathbf{x}. \end{aligned}$$

Further,

$$m^{K-1} \int_{\mathbb{R}^{K-1}} |\Psi_{\mathbf{j}_0}(\mathbf{x})|^p d\mathbf{x} = m^{-ps} \prod_{k=1}^{K-1} \left(m \int_{\mathbb{R}} |\zeta(m(2Kx_k - 1))|^p dx_k \right) = m^{-ps} (2K)^{-K+1} \|\zeta\|_{L^p}^{(K-1)p}. \quad (44)$$

Thus, we have

$$\ell_p\text{-ECE}_{P_{\boldsymbol{\eta}}}(f) = (2(2K)^{-K+1}(K-1)!)^{\frac{1}{p}} \rho m^{-s} \|\zeta\|_{L^p}^{K-1} \geq c_{\text{lower}} n^{-\frac{2s}{4s+K-1}} \quad (45)$$

for some $c_{\text{lower}} > 0$ because

$$\lim_{n \rightarrow \infty} \frac{m^{-s}}{n^{-\frac{2s}{4s+K-1}}} = \lim_{n \rightarrow \infty} \left(\lceil n^{\frac{2}{4s+K-1}} \rceil \right)^{-s} n^{-\frac{2s}{4s+K-1}} = 1.$$

From (40) and (45), we see that $P_{\boldsymbol{\eta}} \in \mathcal{P}_1(\varepsilon, p, s)$ with $\varepsilon = c_{\text{lower}} n^{-2s/(4s+K-1)}$ for all $\boldsymbol{\eta} \in \{\pm 1\}^{[m]^{K-1}}$.

The final step is to apply Lemma 5.3. Given n i.i.d. observations $\{(Z_i, Y_i) : i \in [n]\}$, the average likelihood ratio between $P_{\boldsymbol{\eta}}$, $\boldsymbol{\eta} \in \{\pm 1\}^{[m]^{K-1}}$, and P_0 is

$$L_n = \frac{1}{2^{m^{K-1}}} \sum_{\boldsymbol{\eta} \in \{\pm 1\}^{[m]^{K-1}}} \prod_{i=1}^n \frac{[g_{\boldsymbol{\eta}}(Z_i)]_{\text{argmax}_k[Y_i]_k}}{[Z_i]_{\text{argmax}_k[Y_i]_k}}.$$

Let $\boldsymbol{\eta}^1, \boldsymbol{\eta}^2$ be independent random variables uniformly drawn from $\{\pm 1\}^{[m]^{K-1}}$, and $(Z, Y) \sim P_0$. Then,

$$\begin{aligned} \mathbb{E}_{P_0}[L_n^2] &= \mathbb{E}_{\boldsymbol{\eta}^1, \boldsymbol{\eta}^2} \mathbb{E}_{P_0} \prod_{i=1}^n \frac{[g_{\boldsymbol{\eta}^1}(Z_i)]_{\text{argmax}_k[Y_i]_k}}{[Z_i]_{\text{argmax}_k[Y_i]_k}} \cdot \frac{[g_{\boldsymbol{\eta}^2}(Z_i)]_{\text{argmax}_k[Y_i]_k}}{[Z_i]_{\text{argmax}_k[Y_i]_k}} \\ &= \mathbb{E}_{\boldsymbol{\eta}^1, \boldsymbol{\eta}^2} \left(\mathbb{E}_{P_0} \frac{[g_{\boldsymbol{\eta}^1}(Z)]_{\text{argmax}_k[Y]_k} [g_{\boldsymbol{\eta}^2}(Z)]_{\text{argmax}_k[Y]_k}}{[Z]_{\text{argmax}_k[Y]_k}^2} \right)^n. \end{aligned}$$

Moreover,

$$\begin{aligned}
& \mathbb{E}_{P_0} \frac{[g_{\boldsymbol{\eta}^1}(Z)]_{\text{argmax}_k[Y]_k} [g_{\boldsymbol{\eta}^2}(Z)]_{\text{argmax}_k[Y]_k}}{[Z]_{\text{argmax}_k[Y]_k}^2} = \int_{\Delta_{K-1}} \left(\sum_{k=1}^K [\mathbf{z}]_k \frac{[g_{\boldsymbol{\eta}^1}(\mathbf{z})]_k [g_{\boldsymbol{\eta}^2}(\mathbf{z})]_k}{[\mathbf{z}]_k^2} \right) d\mathbf{z} \\
&= 1 + \int_{\Delta_{K-1}} \left(\sum_{k=1}^K \frac{[g_{\boldsymbol{\eta}^1}(\mathbf{z}) - \mathbf{z}]_k [g_{\boldsymbol{\eta}^2}(\mathbf{z}) - \mathbf{z}]_k}{[\mathbf{z}]_k} \right) d\mathbf{z} \\
&= 1 + \rho^2 \int_{\Delta_{K-1}} \left(\sum_{\mathbf{j} \in [m]^{K-1}} \boldsymbol{\eta}_{\mathbf{j}}^1 (\Psi_{\mathbf{j}} \circ \psi)(\mathbf{z}) \right) \left(\sum_{\mathbf{j} \in [m]^{K-1}} \boldsymbol{\eta}_{\mathbf{j}}^2 (\Psi_{\mathbf{j}} \circ \psi)(\mathbf{z}) \right) \left(\frac{1}{[\mathbf{z}]_0} + \frac{1}{[\mathbf{z}]_1} \right) d\mathbf{z}
\end{aligned}$$

where the integral $\int_{\Delta_{K-1}}$ is over $\text{Unif}(\Delta_{K-1})$. Since $\{\text{supp}(\Psi_{\mathbf{j}}) : \mathbf{j} \in [m]^{K-1}\}$ is a collection of pairwise disjoint sets,

$$\begin{aligned}
& \int_{\Delta_{K-1}} \left(\sum_{\mathbf{j} \in [m]^{K-1}} \boldsymbol{\eta}_{\mathbf{j}}^1 (\Psi_{\mathbf{j}} \circ \psi)(\mathbf{z}) \right) \left(\sum_{\mathbf{j} \in [m]^{K-1}} \boldsymbol{\eta}_{\mathbf{j}}^2 (\Psi_{\mathbf{j}} \circ \psi)(\mathbf{z}) \right) \left(\frac{1}{[\mathbf{z}]_0} + \frac{1}{[\mathbf{z}]_1} \right) d\mathbf{z} \\
&= \int_{\Delta_{K-1}} \left(\sum_{\mathbf{j} \in [m]^{K-1}} \boldsymbol{\eta}_{\mathbf{j}}^1 \boldsymbol{\eta}_{\mathbf{j}}^2 (\Psi_{\mathbf{j}} \circ \psi)(\mathbf{z})^2 \right) \left(\frac{1}{[\mathbf{z}]_0} + \frac{1}{[\mathbf{z}]_1} \right) d\mathbf{z}.
\end{aligned}$$

The random variable $(\boldsymbol{\eta}_{\mathbf{j}}^1 \boldsymbol{\eta}_{\mathbf{j}}^2)_{\mathbf{j} \in [m]^{K-1}}$ is also uniformly distributed on $\{\pm 1\}^{[m]^{K-1}}$. Hence,

$$\mathbb{E}_{P_0}[L_n^2] = \mathbb{E}_{\boldsymbol{\eta}^1} \left(1 + \rho^2 \sum_{\mathbf{j} \in [m]^{K-1}} \boldsymbol{\eta}_{\mathbf{j}}^1 \int_{\Delta_{K-1}} (\Psi_{\mathbf{j}} \circ \psi)(\mathbf{z})^2 \left(\frac{1}{[\mathbf{z}]_0} + \frac{1}{[\mathbf{z}]_1} \right) d\mathbf{z} \right)^n. \quad (46)$$

Since $\bigcup_{\mathbf{j} \in [m]^{K-1}} \text{supp}(\Psi_{\mathbf{j}}) \subseteq \psi(\Delta_{K-1} \cap [\frac{1}{2K}, 1]^K)$, we have $\frac{1}{[\mathbf{z}]_0} + \frac{1}{[\mathbf{z}]_1} \leq 4K$ for every $\mathbf{z} \in \Delta_{K-1}$ such that $(\Psi_{\mathbf{j}} \circ \psi)(\mathbf{z}) \neq 0$ for at least one $\mathbf{j} \in [m]^{K-1}$. Thus,

$$\begin{aligned}
& \left| \rho^2 \sum_{\mathbf{j} \in [m]^{K-1}} \boldsymbol{\eta}_{\mathbf{j}} \int_{\Delta_{K-1}} (\Psi_{\mathbf{j}} \circ \psi)(\mathbf{z})^2 \left(\frac{1}{[\mathbf{z}]_0} + \frac{1}{[\mathbf{z}]_1} \right) d\mathbf{z} \right| \leq \rho^2 \sum_{\mathbf{j} \in [m]^{K-1}} \left| \int_{\Delta_{K-1}} (\Psi_{\mathbf{j}} \circ \psi)(\mathbf{z})^2 \left(\frac{1}{[\mathbf{z}]_0} + \frac{1}{[\mathbf{z}]_1} \right) d\mathbf{z} \right| \\
& \leq \rho^2 \sum_{\mathbf{j} \in [m]^{K-1}} 4K \left| \int_{\Delta_{K-1}} (\Psi_{\mathbf{j}} \circ \psi)(\mathbf{z})^2 d\mathbf{z} \right| = 4\rho^2 K! m^{K-1} \int_{\mathbb{R}^{K-1}} \Psi_{\mathbf{j}_0}(\mathbf{x})^2 d\mathbf{x}.
\end{aligned} \quad (47)$$

The last equality is because $\text{Unif}(\Delta_{K-1})$ has density $(K-1)!$ with respect to Leb_{K-1} , when projected to \mathbb{R}^{K-1} . Also, by (39) and (44),

$$4\rho^2 K! m^{K-1} \int_{\mathbb{R}^{K-1}} \Psi_{\mathbf{j}_0}(\mathbf{x})^2 d\mathbf{x} = 4\rho^2 K! m^{-2s} (2K)^{-K+1} \|\zeta\|_{L^2}^{2(K-1)} \leq c_{\alpha, \beta}^2 m^{-2s} \leq 1.$$

By (46) and that $(1+x)^n \leq \exp(nx)$ for all $x \in (-1, 1]$,

$$\mathbb{E}_{P_0}[L_n^2] \leq \mathbb{E}_{\boldsymbol{\eta}^1} \exp \left(n\rho^2 \sum_{\mathbf{j} \in [m]^{K-1}} \boldsymbol{\eta}_{\mathbf{j}}^1 \int_{\Delta_{K-1}} (\Psi_{\mathbf{j}} \circ \psi)(\mathbf{z})^2 \left(\frac{1}{[\mathbf{z}]_0} + \frac{1}{[\mathbf{z}]_1} \right) d\mathbf{z} \right). \quad (48)$$

Since $\{\boldsymbol{\eta}_{\mathbf{j}}^1 : \mathbf{j} \in [m]^{K-1}\}$ is a set of i.i.d. random variables drawn from $\text{Unif}(\{\pm 1\})$, we have, with

$\cosh(x) := [\exp(x) + \exp(-x)]/2$,

$$\begin{aligned}
& \mathbb{E}_{\boldsymbol{\eta}^1} \exp \left(n \rho^2 \sum_{\mathbf{j} \in [m]^{K-1}} \boldsymbol{\eta}_{\mathbf{j}}^1 \int_{\Delta_{K-1}} (\Psi_{\mathbf{j}} \circ \psi)(\mathbf{z})^2 \left(\frac{1}{[\mathbf{z}]_0} + \frac{1}{[\mathbf{z}]_1} \right) d\mathbf{z} \right) \\
&= \prod_{\mathbf{j} \in [m]^{K-1}} \mathbb{E}_{\boldsymbol{\eta}_{\mathbf{j}}^1} \exp \left(n \rho^2 \boldsymbol{\eta}_{\mathbf{j}}^1 \int_{\Delta_{K-1}} (\Psi_{\mathbf{j}} \circ \psi)(\mathbf{z})^2 \left(\frac{1}{[\mathbf{z}]_0} + \frac{1}{[\mathbf{z}]_1} \right) d\mathbf{z} \right) \\
&= \prod_{\mathbf{j} \in [m]^{K-1}} \cosh \left(n \rho^2 \int_{\Delta_{K-1}} (\Psi_{\mathbf{j}} \circ \psi)(\mathbf{z})^2 \left(\frac{1}{[\mathbf{z}]_0} + \frac{1}{[\mathbf{z}]_1} \right) d\mathbf{z} \right).
\end{aligned}$$

Similarly to (47) and (48), we have

$$\left| n \rho^2 \int_{\Delta_{K-1}} (\Psi_{\mathbf{j}} \circ \psi)(\mathbf{z})^2 \left(\frac{1}{[\mathbf{z}]_0} + \frac{1}{[\mathbf{z}]_1} \right) d\mathbf{z} \right| \leq c_{\alpha, \beta}^2 m^{-2s-K+1} n \leq 1 \quad (49)$$

for each $\mathbf{j} \in [m]^{K-1}$. Using that $\cosh(x) \leq 1 + x^2 \leq e^{x^2}$ for $x \in [-1, 1]$,

$$\begin{aligned}
& \prod_{\mathbf{j} \in [m]^{K-1}} \cosh \left(n \rho^2 \int_{\Delta_{K-1}} (\Psi_{\mathbf{j}} \circ \psi)(\mathbf{z})^2 \left(\frac{1}{[\mathbf{z}]_0} + \frac{1}{[\mathbf{z}]_1} \right) d\mathbf{z} \right) \\
& \leq \exp \left(\sum_{\mathbf{j} \in [m]^{K-1}} \left(n \rho^2 \int_{\Delta_{K-1}} (\Psi_{\mathbf{j}} \circ \psi)(\mathbf{z})^2 \left(\frac{1}{[\mathbf{z}]_0} + \frac{1}{[\mathbf{z}]_1} \right) d\mathbf{z} \right)^2 \right).
\end{aligned}$$

Again from (49), it follows that

$$\exp \left(\sum_{\mathbf{j} \in [m]^{K-1}} \left(n \rho^2 \int_{\Delta_{K-1}} (\Psi_{\mathbf{j}} \circ \psi)(\mathbf{z})^2 \left(\frac{1}{[\mathbf{z}]_0} + \frac{1}{[\mathbf{z}]_1} \right) d\mathbf{z} \right)^2 \right) \leq \exp(c_{\alpha, \beta}^4 m^{-4s-K+1} n^2) \leq 1 + (1 - \alpha - \beta)^2.$$

In conclusion, $\varepsilon_n(p, s) \geq c_{\text{lower}} n^{-2s/(4s+K-1)}$ by Lemma 5.3.

8.1.6 Proof of Lemma 5.3

The proof follows from the results of Ingster (1987); Ingster and Suslina (2012); see also Lemma G.1 in Kim et al. (2022) for a very clear statement. By definition, it holds that

$$\begin{aligned}
R_n(\varepsilon, p, s) &= \inf_{\xi \in \Phi_n(\alpha)} \sup_{P \in \mathcal{P}_1(\varepsilon, p, s)} \mathbb{E}_P[1 - \xi] \geq \inf_{\xi \in \Phi_n(\alpha)} \frac{1}{M} \sum_{i=1}^M \mathbb{E}_{P_i}[1 - \xi] \\
&= \inf_{\xi \in \Phi_n(\alpha)} \left(\mathbb{E}_{P_0}[1 - \xi] + \frac{1}{M} \sum_{i=1}^M \mathbb{E}_{P_i}[1 - \xi] - \mathbb{E}_{P_0}[1 - \xi] \right) \\
&\geq 1 - \alpha + \inf_{\xi \in \Phi_n(\alpha)} \left(\frac{1}{M} \sum_{i=1}^M \mathbb{E}_{P_i}[1 - \xi] - \mathbb{E}_{P_0}[1 - \xi] \right).
\end{aligned}$$

where the last inequality holds because $\mathbb{E}_{P_0}[\xi] \leq \alpha$. Further,

$$\begin{aligned}
\left| \frac{1}{M} \sum_{i=1}^M \mathbb{E}_{P_i}[1 - \xi] - \mathbb{E}_{P_0}[1 - \xi] \right| &= \left| \mathbb{E}_{P_0}[\xi] - \frac{1}{M} \sum_{i=1}^M \mathbb{E}_{P_i}[\xi] \right| = |\mathbb{E}_{P_0}[\xi] - \mathbb{E}_{P_0}[\xi L_n]| \\
&\leq \mathbb{E}_{P_0}[|L_n - 1|] \leq \sqrt{\mathbb{E}_{P_0}[L_n^2] - 1} \leq 1 - \alpha - \beta
\end{aligned}$$

by a change of variables and the Cauchy-Schwarz inequality. Therefore, we have $R_n(\varepsilon, p, s) \geq 1 - \alpha - (1 - \alpha - \beta) = \beta$. Finally, since $\varepsilon \mapsto R_n(\varepsilon, p, s)$ is non-increasing, we get $\varepsilon_n(p, s) \geq \varepsilon$.

8.1.7 Proof of Theorem 6.1

Overview of the proof Under $P \in \mathcal{P}_0$, we prove that $T_{1,k}$ and $T_{2,k}$ have zero mean, and their variances are bounded by unity. By rejecting H_0 when $|T_{1,k}| \geq \sqrt{3K/\alpha n}$ or $|T_{2,k}| \geq \sqrt{3K/\alpha n}$, we can filter out distributions $P \in \mathcal{P}_1(\varepsilon, p, s)$ such that $\mathbb{E}_P[T_{1,k}] = \Omega(n^{-1/2})$ or $\mathbb{E}_P[T_{2,k}] = \Omega(n^{-1/2})$. For the remaining cases, we compute $\|\pi_k^{\mathcal{V}} - \pi_k^{\mathcal{W}}\|_{L^2(P_Z)}$ and show it is lower bounded by $\Omega(n^{-2s/(4s+K-1)})$. We conclude using the minimax optimality of the two-sample test **TS**.

We prove the theorem for $p = 2$. Then, the general case follows since $\mathcal{P}_1(\varepsilon, p, s) \subseteq \mathcal{P}_1(\varepsilon, 2, s)$ for all $p \leq 2$. Assume $P \in \mathcal{P}_0$. By the union bound,

$$P(\xi_n^{\text{split}} = 1) \leq \sum_{k=1}^K \left[P\left(|T_{1,k}| \geq \sqrt{\frac{3K}{\alpha n}}\right) + P\left(|T_{2,k}| \geq \sqrt{\frac{3K}{\alpha n}}\right) + P\left(\text{TS}_{\frac{\alpha}{3K}, \frac{\beta}{2}}(\mathcal{V}_k, \mathcal{W}_k) = 1\right) \right].$$

Moreover, for all $k \in \{1, \dots, K\}$,

$$\mathbb{E}_P[Y - Z]_k = \mathbb{E}_P[\mathbb{E}_P[[Y - Z]_k | Z]] = \mathbb{E}_P[[\mathbb{E}_P[Y | Z] - Z]_k] = 0$$

and $\text{Var}_P([Y - Z]_k) = \mathbb{E}_P[[Y - Z]_k^2] \leq 1$. Thus, by Chebyshev's inequality

$$P\left(|T_{1,k}| \geq \sqrt{\frac{3K}{\alpha n}}\right) \leq \frac{\alpha n}{3K} \text{Var}_P(T_{1,k}) = \frac{\alpha}{3K} \text{Var}_P([Y - Z]_k) \leq \frac{\alpha}{3K}.$$

Similarly, we have

$$P\left(|T_{2,k}| \geq \sqrt{\frac{3K}{\alpha n}}\right) \leq \frac{\alpha n}{3K} \text{Var}_P(T_{2,k}) = \frac{\alpha}{3K} \text{Var}_P([Z]_k [Y - Z]_k) \leq \frac{\alpha}{3K}.$$

From (13), we know that $P(\text{TS}_{\frac{\alpha}{3K}, \frac{\beta}{2}}(\mathcal{V}_k, \mathcal{W}_k) = 1) \leq \frac{\alpha}{3K}$. Therefore,

$$P(\xi_n^{\text{split}} = 1) \leq \sum_{k=1}^K \left(\frac{\alpha}{3K} + \frac{\alpha}{3K} + \frac{\alpha}{3K} \right) = \alpha.$$

Let $P \in \mathcal{P}_1(\varepsilon, p, s)$ and suppose that, for some $k \in \{1, \dots, K\}$,

$$|\mathbb{E}_P[T_{1,k}]| = |\mathbb{E}_P[Y - Z]_k| \geq \frac{1}{\sqrt{n}} \left(\sqrt{\frac{3K}{\alpha}} + \frac{1}{\sqrt{\beta}} \right). \quad (50)$$

By Chebyshev's inequality,

$$P\left(|T_{1,k} - \mathbb{E}_P[T_{1,k}]| \leq \frac{1}{\sqrt{\beta n}}\right) \geq 1 - \beta n \text{Var}_P(T_{1,k}) \geq 1 - \beta.$$

Note that (50) and $|T_{1,k} - \mathbb{E}_P[T_{1,k}]| \leq 1/\sqrt{\beta n}$ imply

$$|T_{1,k}| \geq |\mathbb{E}_P[T_{1,k}]| - |T_{1,k} - \mathbb{E}_P[T_{1,k}]| \geq \sqrt{\frac{3K}{\alpha n}}.$$

Therefore,

$$P(\xi_n^{\text{split}} = 1) \geq P\left(|T_{1,k}| \geq \sqrt{\frac{3K}{\alpha n}}\right) \geq P\left(|T_{1,k} - \mathbb{E}_P[T_{1,k}]| \leq \frac{1}{\sqrt{\beta n}}\right) \geq 1 - \beta.$$

The same conclusion can be drawn when

$$|\mathbb{E}_P[T_{2,k}]| = |\mathbb{E}_P[[Z]_k [Y - Z]_k]| \geq \frac{1}{\sqrt{n}} \left(\sqrt{\frac{3K}{\alpha}} + \frac{1}{\sqrt{\beta}} \right)$$

for some $k \in \{1, \dots, K\}$.

Now it remains to prove the claim for $P \in H(\varepsilon, p, s)$ such that

$$|\mathbb{E}_P[Y - Z]_k| \vee |\mathbb{E}_P[[Z]_k[Y - Z]_k]| < \frac{1}{\sqrt{n}} \left(\sqrt{\frac{3K}{\alpha}} + \frac{1}{\sqrt{\beta}} \right) \quad (51)$$

for every $k \in \{1, \dots, K\}$. Since

$$\ell_2\text{-ECE}_P(f)^2 = \sum_{k=1}^K \int_{\Delta_{K-1}} [\text{res}_f(\mathbf{z})]_k^2 dP_Z(\mathbf{z}) \geq \varepsilon^2,$$

we can choose $k_0 \in \{1, \dots, K\}$ such that $\int_{\Delta_{K-1}} [\text{res}_f(\mathbf{z})]_{k_0}^2 dP_Z(\mathbf{z}) \geq \frac{\varepsilon^2}{K}$. Choose $c'_{\text{split}} > 0$ such that, for d_c from Assumption 6.1 and c_{ts} from (13),

$$\frac{(c'_{\text{split}})^2}{K} \geq \frac{4}{d_c^3} \left(\sqrt{\frac{3K}{\alpha}} + \frac{1}{\sqrt{\beta}} \right)^2 + c_{\text{ts}}^2 \left(\frac{d_c}{8} \right)^{-\frac{4s}{4s+K-1}}. \quad (52)$$

There exists $N \in \mathbb{N}_+$ such that for all $n \geq N$,

$$\frac{1}{\sqrt{n}} \left(\sqrt{\frac{3K}{\alpha}} + \frac{1}{\sqrt{\beta}} \right) \leq \frac{d_c}{2}, \quad 2 \left(\frac{2}{e} \right)^{\frac{d_c n}{8}} \leq \frac{\beta}{2}. \quad (53)$$

Let $c_{\text{split}} = c'_{\text{split}} \vee N^{2s/(4s+K-1)}$. If $n < N$, then $\mathcal{P}_1(\varepsilon, p, s)$ is empty since $\varepsilon \geq c_{\text{split}} n^{-2s/(4s+K-1)} > 1$, so the claim is vacuously true. Assume $n \geq N$. By (51), (53), and Assumption 6.1,

$$\mathbb{E}_P[Z]_{k_0} \geq \mathbb{E}_P[Y]_{k_0} - |\mathbb{E}_P[Y - Z]_{k_0}| \geq \frac{d_c}{2}. \quad (54)$$

By (11), (12), (51), and (54), $\|\pi_{k_0}^{\mathcal{V}} - \pi_{k_0}^{\mathcal{W}}\|_{L^2(P_Z)}^2$ is lower bounded by

$$\begin{aligned} & \frac{1}{(\mathbb{E}_P[Y]_{k_0})^2} \int_{\Delta_{K-1}} [\text{res}_f(\mathbf{z})]_{k_0}^2 dP_Z(\mathbf{z}) + \frac{2\mathbb{E}_P[Z - Y]_{k_0} \mathbb{E}_P[[Z]_{k_0}[Y - Z]_{k_0}]}{(\mathbb{E}_P[Y]_{k_0})^2 \mathbb{E}_P[Z]_{k_0}} \\ & \geq \frac{\varepsilon^2}{K} - \frac{4}{d_c^3} \left(\sqrt{\frac{3K}{\alpha}} + \frac{1}{\sqrt{\beta}} \right)^2 n^{-1}. \end{aligned}$$

Further by $\varepsilon \geq c'_{\text{split}} n^{-2s/(4s+K-1)}$ and (52),

$$\frac{\varepsilon^2}{K} - \frac{4}{d_c^3} \left(\sqrt{\frac{3K}{\alpha}} + \frac{1}{\sqrt{\beta}} \right)^2 n^{-1} \geq \left(\frac{(c'_{\text{split}})^2}{K} - \frac{4}{d_c^3} \left(\sqrt{\frac{3K}{\alpha}} + \frac{1}{\sqrt{\beta}} \right)^2 \right) n^{-\frac{4s}{4s+K-1}} \geq c_{\text{ts}}^2 \left(\frac{d_c n}{8} \right)^{-\frac{4s}{4s+K-1}}. \quad (55)$$

In conclusion,

$$\|\pi_{k_0}^{\mathcal{V}} - \pi_{k_0}^{\mathcal{W}}\|_{L^2(P_Z)} \geq c_{\text{ts}} \left(\frac{d_c n}{8} \right)^{-\frac{2s}{4s+K-1}}.$$

Note that $\pi_{k_0}^{\mathcal{V}} - \pi_{k_0}^{\mathcal{W}}$ is s -Hölder since it is a linear combination of two s -Hölder functions $\mathbf{z} \mapsto [\text{res}_f(\mathbf{z})]_{k_0}$ and $\mathbf{z} \mapsto [\mathbf{z}]_{k_0}$, possibly with different Hölder constants. Thus by (13), we have

$$P \left(\text{TS}_{\frac{\alpha}{3K}, \frac{\beta}{2}}(\mathcal{V}_{k_0}, \mathcal{W}_{k_0}) = 1 \mid |\mathcal{V}_{k_0}| = v, |\mathcal{W}_{k_0}| = w \right) \geq 1 - \frac{\beta}{2} \quad (56)$$

given that $v, w \geq \frac{d_c n}{8}$. For convenience, assume that n is even (if required, drop an observation). Since $|\mathcal{V}_{k_0}| \sim \text{Bin}(\frac{n}{2}, \mathbb{E}_P[Y]_{k_0})$ and $|\mathcal{W}_{k_0}| \sim \text{Bin}(\frac{n}{2}, \mathbb{E}_P[Z]_{k_0})$, we find

$$P \left(|\mathcal{V}_{k_0}| < \frac{n\mathbb{E}_P[Y]_{k_0}}{4} \right) \leq \left(\frac{2}{e} \right)^{\frac{n\mathbb{E}_P[Y]_{k_0}}{4}}, \quad P \left(|\mathcal{W}_{k_0}| < \frac{n\mathbb{E}_P[Z]_{k_0}}{4} \right) \leq \left(\frac{2}{e} \right)^{\frac{n\mathbb{E}_P[Z]_{k_0}}{4}}$$

by Chernoff's inequality (Exercise 2.3.2 of Vershynin (2018)). Therefore,

$$\begin{aligned} P\left(|\mathcal{V}_{k_0}| < \frac{d_c n}{8} \text{ or } |\mathcal{W}_{k_0}| < \frac{d_c n}{8}\right) &\leq P\left(|\mathcal{V}_{k_0}| < \frac{d_c n}{8}\right) + P\left(|\mathcal{W}_{k_0}| < \frac{d_c n}{8}\right) \\ &\leq P\left(|\mathcal{V}_{k_0}| < \frac{n\mathbb{E}_P[Y]_{k_0}}{4}\right) + P\left(|\mathcal{W}_{k_0}| < \frac{n\mathbb{E}_P[Z]_{k_0}}{4}\right) \leq \left(\frac{2}{e}\right)^{\frac{n\mathbb{E}_P[Y]_{k_0}}{4}} + \left(\frac{2}{e}\right)^{\frac{n\mathbb{E}_P[Z]_{k_0}}{4}} \leq 2\left(\frac{2}{e}\right)^{\frac{d_c n}{8}} \leq \frac{\beta}{2}, \end{aligned}$$

and thus

$$P\left(|\mathcal{V}_{k_0}|, |\mathcal{W}_{k_0}| \geq \frac{d_c n}{8}\right) \geq 1 - \frac{\beta}{2}. \quad (57)$$

The last inequality is by (52). Finally by (56) and (57),

$$\begin{aligned} &P\left(\text{TS}_{\frac{\alpha}{3K}, \frac{\beta}{2}}(\mathcal{V}_{k_0}, \mathcal{W}_{k_0}) = 1\right) \\ &\geq \int_{\{(v, w) \in \mathbf{z}^2 : v, w \geq \frac{d_c n}{8}\}} P\left(\text{TS}_{\frac{\alpha}{3K}, \frac{\beta}{2}}(\mathcal{V}_{k_0}, \mathcal{W}_{k_0}) = 1 \mid |\mathcal{V}_{k_0}| = v, |\mathcal{W}_{k_0}| = w\right) dP_{|\mathcal{V}_{k_0}|, |\mathcal{W}_{k_0}|}(v, w) \\ &\geq \left(1 - \frac{\beta}{2}\right) P\left(|\mathcal{V}_{k_0}|, |\mathcal{W}_{k_0}| \geq \frac{d_c n}{8}\right) \geq \left(1 - \frac{\beta}{2}\right)^2 \geq 1 - \beta \end{aligned}$$

where the integral is with respect to the joint distribution of $|\mathcal{V}_{k_0}|$ and $|\mathcal{W}_{k_0}|$. This proves that

$$P(\xi_n^{\text{split}} = 1) \geq P\left(\text{TS}_{\frac{\alpha}{3K}, \frac{\beta}{2}}(\mathcal{V}_{k_0}, \mathcal{W}_{k_0}) = 1\right) \geq 1 - \beta.$$

8.1.8 Proof of Corollary 6.2

The proof of Theorem 6.1 can be repeated by replacing (13) with (14). The only difference is (55), where we used $n^{-4s/(4s+K-1)} \geq n^{-1}$. In the adaptive setting, we instead need $(n/\log\log n)^{-4s/(4s+K-1)} \geq n^{-1}$. This inequality holds for all large $n \in \mathbb{N}_+$, say $n \geq N'$. Then, we can define $c_{\text{ad-s}}$ to be larger than $(N'/\log\log N')^{2s/(4s+K-1)}$, so that $\mathcal{P}_1(\varepsilon, p, s)$ becomes empty when $n < N'$.

8.2 Background

8.2.1 Hölder continuity on the simplex

To define derivatives—and thus the class of functions we study—on Δ_{K-1} , a coordinate chart $\psi : \Delta_{K-1} \rightarrow \mathbb{R}^{K-1}$ has to be specified. For example, we can consider the canonical projection $\pi_{-k} : (z_1, \dots, z_K)^\top \mapsto (z_1, \dots, z_{k-1}, z_{k+1}, \dots, z_K)^\top$. The definition of Hölder smoothness below depends on the choice of ψ . We assume $\psi = \pi_{-K}$, but all conclusions and proofs remain the same for any choice of the coordinate chart ψ .

For an integer $d \geq 1$, a vector $\gamma = (\gamma_1, \dots, \gamma_d)^\top \in \mathbb{N}^d$ is called a multi-index. We write $|\gamma| := \gamma_1 + \dots + \gamma_d$. For a sufficiently smooth function $f : \mathbb{R}^d \rightarrow \mathbb{R}$, we denote its partial derivative of order $\gamma = (\gamma_1, \dots, \gamma_d)^\top$ by $f^{(\gamma)} := \partial_1^{\gamma_1} \cdots \partial_d^{\gamma_d} f$. For a Hölder smoothness parameter $s > 0$ and a Hölder constant $L > 0$, let $\mathcal{H}_K(s, L)$ be the class of (s, L) -Hölder continuous functions $g : \Delta_{K-1} \rightarrow \mathbb{R}$ satisfying, for all $\mathbf{x}_1, \mathbf{x}_2 \in \psi(\Delta_{K-1})$ and multi-indices $\gamma \in \mathbb{N}^{K-1}$ with $|\gamma| = \lceil s \rceil - 1$,

$$\left| (g \circ \psi^{-1})^{(\gamma)}(\mathbf{x}_1) - (g \circ \psi^{-1})^{(\gamma)}(\mathbf{x}_2) \right| \leq L \|\mathbf{x}_1 - \mathbf{x}_2\|^{s - \lceil s \rceil + 1}. \quad (58)$$

In particular, $\mathcal{H}_K(1, L)$ denotes all L -Lipschitz functions.

8.2.2 Two-sample goodness-of-fit tests

Here we state and slightly extend the results of Arias-Castro et al. (2018); Kim et al. (2022). For $d \in \mathbb{N}_+$, let μ be a measure on $[0, 1]^d$ which is absolutely continuous with respect to Leb_d and satisfies

$$\nu_l \leq \frac{d\mu}{d\text{Leb}_d} \leq \nu_u \quad (59)$$

almost everywhere for some constants $\nu_l, \nu_u > 0$. For $n_1, n_2 \in \mathbb{N}_+$, suppose we have two samples $\{V_1, \dots, V_{n_1}\}$ and $\{W_1, \dots, W_{n_2}\}$ i.i.d. sampled from the distributions on $[0, 1]^d$ with densities f_1 and f_2 , respectively, with respect to μ . We also assume $f_1 - f_2$ is (s, L) -Hölder continuous for a Hölder smoothness parameter $s > 0$ and a Hölder constant $L > 0$.

For $m \in \mathbb{N}_+$ and $\mathbf{i} = (i_1, \dots, i_d)^\top \in [m]^d$, let $R_{m,\mathbf{i}} := \prod_{k=1}^d [\frac{i_k-1}{m}, \frac{i_k}{m})$.

$$v_{\mathbf{i},m} := |\{j \in [n_1] : V_j \in R_{m,\mathbf{i}}\}|,$$

$$w_{\mathbf{i},m} := |\{j \in [n_2] : W_j \in R_{m,\mathbf{i}}\}|.$$

The unnormalized chi-squared statistic is defined by

$$\Gamma_{m,n_1,n_2} := \sum_{\mathbf{i} \in [m]^d} (n_2 v_{\mathbf{i},m} - n_1 w_{\mathbf{i},m})^2.$$

Theorem 8.2 (Chi-squared test, Arias-Castro et al. (2018)). *Consider the two-sample goodness-of-fit testing problem described above. Assume the Hölder smoothness parameter s is known and let $m^* = \lfloor (n_1 \wedge n_2)^{2/(4s+d)} \rfloor$. For any $\alpha \in (0, 1)$ and $\beta \in (0, 1 - \alpha)$, there exist $c_{\text{crit}} > 0$ depending on (d, L) and $c_{\text{ts}} > 0$ depending on $(s, d, L, \nu_l, \nu_u, \alpha, \beta)$ such that*

$$\begin{aligned} P(\Gamma_{m^*,n_1,n_2} \geq n_1 n_2 (n_1 + n_2) + c n_1 n_2 (m^*)^{-d/2}) &\leq \alpha && \text{if } f_1 = f_2, \\ P(\Gamma_{m^*,n_1,n_2} \geq n_1 n_2 (n_1 + n_2) + c n_1 n_2 (m^*)^{-d/2}) &\geq 1 - \beta && \text{if } \|f_1 - f_2\|_{L^2(\mu)} \geq c_{\text{ts}} (n_1 \wedge n_2)^{-\frac{2s}{4s+d}}. \end{aligned}$$

For $m \in \mathbb{N}_+$, let $k_m : ([0, 1]^d)^4 \rightarrow \mathbb{R}$ be the kernel

$$\begin{aligned} k(v_1, v_2, w_1, w_2) &= \sum_{\mathbf{i} \in [m]^d} (\mathbb{1}_{R_{m,\mathbf{i}}}(v_1) \mathbb{1}_{R_{m,\mathbf{i}}}(v_2) + \mathbb{1}_{R_{m,\mathbf{i}}}(w_1) \mathbb{1}_{R_{m,\mathbf{i}}}(w_2) \\ &\quad - \mathbb{1}_{R_{m,\mathbf{i}}}(v_1) \mathbb{1}_{R_{m,\mathbf{i}}}(w_2) - \mathbb{1}_{R_{m,\mathbf{i}}}(w_1) \mathbb{1}_{R_{m,\mathbf{i}}}(v_2)). \end{aligned}$$

For the two samples $\{V_1, \dots, V_{n_1}\}, \{W_1, \dots, W_{n_2}\}$ described above, define

$$U_{m,n_1,n_2} := \frac{1}{n_1(n_1-1)n_2(n_2-1)} \sum_{i_1 \neq i_2 \in [n_1]} \sum_{j_1 \neq j_2 \in [n_2]} k_m(V_{i_1}, V_{i_2}, W_{j_1}, W_{j_2}).$$

For any $\alpha \in (0, 1)$, the $1 - \alpha$ quantile $c_{1-\alpha,m,n_1,n_2}$ of the U-statistic U_{m,n_1,n_2} can be found by the permutation procedure described in Section 2.1 of Kim et al. (2022).

Theorem 8.3 (Permutation test, Kim et al. (2022)). *Consider the two-sample goodness-of-fit testing described above. Assume the Hölder smoothness parameter s is known and let $m^* = \lfloor (n_1 \wedge n_2)^{2/(4s+d)} \rfloor$. For any $\alpha \in (0, 1)$ and $\beta \in (0, 1 - \alpha)$, there exists $c_{\text{ts}} > 0$ depending on $(s, d, L, \nu_l, \nu_u, \alpha, \beta)$ such that*

$$\begin{aligned} P(U_{m^*,n_1,n_2} \geq c_{1-\alpha,m^*,n_1,n_2}) &\leq \alpha && \text{if } f_1 = f_2, \\ P(U_{m^*,n_1,n_2} \geq c_{1-\alpha,m^*,n_1,n_2}) &\geq 1 - \beta && \text{if } \|f_1 - f_2\|_{L^2(\mu)} \geq c_{\text{ts}} (n_1 \wedge n_2)^{-\frac{2s}{4s+d}}. \end{aligned}$$

Corollary 8.4 (Multi-scale permutation test, Kim et al. (2022)). *Consider the two-sample goodness-of-fit testing problem described above. Let $B = \lceil \frac{2}{d} \log_2(\frac{n_1 \wedge n_2}{\log \log(n_1 \wedge n_2)}) \rceil$ and define*

$$\xi_{n_1,n_2}^{\text{perm}} := \max_{b \in \{1, \dots, B\}} I(U_{2^b,n_1,n_2} \geq c_{1-\alpha/B, 2^b, n_1, n_2}).$$

For any $\alpha \in (0, 1)$ and $\beta \in (0, 1 - \alpha)$, there exists $c_{\text{ad}} > 0$ depending on $(d, L, \nu_l, \nu_u, \alpha, \beta)$ such that

$$\begin{aligned} P(\xi_{n_1,n_2}^{\text{perm}} = 1) &\leq \alpha && \text{if } f_1 = f_2, \\ P(\xi_{n_1,n_2}^{\text{perm}} = 1) &\geq 1 - \beta && \text{if } \|f_1 - f_2\|_{L^2(\mu)} \geq c_{\text{ad}} \left(\frac{n_1 \wedge n_2}{\log \log(n_1 \wedge n_2)} \right)^{-\frac{2s}{4s+d}}. \end{aligned}$$

Remark 3 (Comment on the proofs). *Theorem 8.2, Theorem 8.3, and Corollary 8.4 are generalization of Theorem 4 of Arias-Castro et al. (2018), Proposition 4.6 of Kim et al. (2022), and Proposition 7.1 of Kim et al. (2022), respectively. The original statements are for $\mu = \text{Leb}_d$. The proofs in Arias-Castro et al. (2018); Kim et al. (2022) can be adapted with only minor differences. For example, equation (93) of Arias-Castro et al. (2018) is still true assuming (59) above. Also, we proved Lemma 8.1 in this paper, which is a generalization of Lemma 3 of Arias-Castro et al. (2018) to a general measure μ . Other parts of the proofs in Arias-Castro et al. (2018); Kim et al. (2022) can be repeated without any modification.*

8.2.3 Binning scheme for the simplex

Here we describe a binning scheme for $\Delta_{K-1} \subseteq \mathbb{R}^K$.

Hypersimplex. For $u \geq 2$ and $v \in [u-1]$, define the $(u-1)$ -dimensional polytope hypersimplex $\Delta_{u-1,v}$ as

$$\Delta_{u-1,v} := \{(x_1, \dots, x_u)^\top \in [0,1]^u : x_1 + \dots + x_u = v\}.$$

Let $A_{u-1,v-1}$ be the Eulerian number:

$$A_{u-1,v-1} := \sum_{i=0}^v (-1)^i \binom{u}{i} (v-i)^{u-1}.$$

It is known that the hypersimplex $\Delta_{u-1,v}$ can be partitioned into $A_{u-1,v-1}$ simplices (Stanley, 1977; Sturmfels, 1996) whose volumes are identical to that of the unit simplex Δ_{u-1} .

Construction. Let $m \in \mathbb{N}_+$ and $R_{m,\mathbf{i}} := \prod_{k=1}^K \left[\frac{i_k-1}{m}, \frac{i_k}{m}\right)$ for $\mathbf{i} = (i_1, \dots, i_K)^\top \in [m]^K$. The hypercube $R_{m,\mathbf{i}}$ has a positive-volume intersection with Δ_{K-1} when

$$m+1 \leq \sum_{k=1}^K i_k \leq m+K-1. \quad (60)$$

Suppose that (60) holds and we write $|\mathbf{i}| = \sum_{k=1}^K i_k$. Then, the intersection is

$$\begin{aligned} \Delta_{K-1} \cap R_{m,\mathbf{i}} &= \{(x_1, \dots, x_K)^\top \in R_{m,\mathbf{i}} : x_1 + \dots + x_K = 1\} \\ &= \frac{\mathbf{i} - \mathbf{1}_K}{m} + \frac{1}{m} \{(x_1, \dots, x_K)^\top \in [0,1]^K : x_1 + \dots + x_K = m+K-|\mathbf{i}|\}, \end{aligned}$$

which is a $\frac{1}{m}$ -scaled and translated version of the hypersimplex $\Delta_{K-1, m+K-|\mathbf{i}|}$. Recall that this hypersimplex can be further partitioned into $A_{K-1, m+K-|\mathbf{i}|-1}$ simplices with the volume $\text{vol}(\Delta_{K-1})/m^{K-1}$. Let $\mathcal{S}_{\mathbf{i}}$ be the set consists of such $A_{K-1, m+K-|\mathbf{i}|-1}$ simplices. Now, we define

$$\mathcal{B}_m := \bigcup_{\substack{\mathbf{i} \in [m]^K \\ m+1 \leq |\mathbf{i}| \leq m+K-1}} \left\{ \frac{\mathbf{i} - \mathbf{1}_K}{m} + \frac{1}{m} \Delta : \Delta \in \mathcal{S}_{\mathbf{i}} \right\},$$

which is the collection of all simplices obtained from decomposing $\Delta_{K-1} \cap R_{m,\mathbf{i}}$ for each $\mathbf{i} \in [m]^K$ satisfying (60). Since each simplex in \mathcal{B}_m has a volume $\text{vol}(\Delta_{K-1})/m^{K-1}$, it follows that $|\mathcal{B}_m| = m^{K-1}$. Noting that there are $\binom{j-1}{K-1}$ multi-indices $\mathbf{i} \in [m]^K$ with $|\mathbf{i}| = j$, it also directly follows from Worpitzky's identity (Equation 6.37 in Graham et al. (1994)) that

$$|\mathcal{B}_m| = \sum_{j=m+1}^{m+K-1} \binom{j-1}{K-1} A_{K-1, m+K-j-1} = \sum_{j=0}^{K-2} \binom{m+j}{K-1} A_{K-1, K-j-2} = \sum_{j=0}^{K-2} \binom{m+j}{K-1} A_{K-1, j} = m^{K-1}.$$

We finally index the partition as $\mathcal{B}_m = \{B_1, \dots, B_{m^{K-1}}\}$.

8.2.4 Calibration test for discrete predictions

Testing calibration of discrete probability predictions has been studied in Cox (1958); Miller (1962); Harrell (2015). Here we describe a test based on testing multiple binomial parameters. This test is related to the chi-squared test from Miller (1962), but does not use the asymptotic distribution of the test statistic when choosing critical values. Let $\{v_1, \dots, v_t\} \subseteq [0, 1]$ be the range of a discrete-valued probability predictor f . For each $i \in [t]$, we let $N_i = |\{j \in [n] : f(X_j) = v_i\}|$, $M_i = |\{j \in [n] : f(X_j) = v_i, Y_j = 1\}|$, and $p_i = P(Y = 1 \mid f(X) = v_i)$. In this setting, the random variable M_i , under the null hypothesis of perfect calibration, follows the binomial distribution $\text{Binom}(N_i, p_i)$ with N_i trials and success probability p_i , given N_i . We use an exact binomial test to test the null hypothesis $H_{0,i} : p_i = v_i$ for each $i \in [t]$ and apply the Bonferroni correction to control the false detection rate under the null hypothesis $H_0 = \cap_{i=1}^t H_{0,i}$.

8.3 More experiments

In this subsection, we provide additional experiments, to evaluate calibration methods whose outputs range over a finite set. When the predicted probabilities belong to a finite set, Kumar et al. (2019) propose a debiased version of the empirical ℓ_2 -ECE, whose sample complexity required is smaller than that of the plug-in estimator; see Section 3.3 for more discussion. We calculate Kumar et al. (2019)'s debiased estimator along with calibration testing results. We use models trained on CIFAR-10 (Table 4), CIFAR-100 (Table 5), and ImageNet (Table 6). The values of the debiased ℓ_2 -ECE estimator are typically very small, which is consistent with the experimental results in Kumar et al. (2019). As can be observed, there is no clear relation between the debiased empirical ℓ_2 -ECE values and test results.

	DenseNet 121		ResNet 50		VGG-19	
	$\widehat{\ell_2\text{-ECE}}^{\text{db}}$	Calibrated?	$\widehat{\ell_2\text{-ECE}}^{\text{db}}$	Calibrated?	$\widehat{\ell_2\text{-ECE}}^{\text{db}}$	Calibrated?
Hist. Binning	0.02%	reject	0.02%	reject	0.05%	reject
Scal. Binning	0.11%	reject	0.10%	reject	0.20%	reject

Table 4: The values of the debiased empirical ℓ_2 -ECE (Kumar et al., 2019) and the testing results, via multiple binomial testing, of models trained on CIFAR-10 with two discrete calibration methods.

	MobileNet-v2		ResNet 56		ShuffleNet-v2	
	$\widehat{\ell_2\text{-ECE}}^{\text{db}}$	Calibrated?	$\widehat{\ell_2\text{-ECE}}^{\text{db}}$	Calibrated?	$\widehat{\ell_2\text{-ECE}}^{\text{db}}$	Calibrated?
Hist. Binning	0.04%	reject	0.09%	reject	0.15%	reject
Scal. Binning	0.04%	reject	0.03%	reject	0.02%	accept

Table 5: The values of the debiased empirical ℓ_2 -ECE (Kumar et al., 2019) and the testing results, via multiple binomial testing, of models trained on CIFAR-100 with two discrete calibration methods.

	DenseNet 161		ResNet 152		EfficientNet-b7	
	$\widehat{\ell_2\text{-ECE}}^{\text{db}}$	Calibrated?	$\widehat{\ell_2\text{-ECE}}^{\text{db}}$	Calibrated?	$\widehat{\ell_2\text{-ECE}}^{\text{db}}$	Calibrated?
Hist. Binning	0.01%	reject	0.03%	reject	0.02%	reject
Scal. Binning	0.05%	reject	0.03%	reject	0.06%	reject

Table 6: The values of the debiased empirical ℓ_2 -ECE (Kumar et al., 2019) and the testing results, via multiple binomial testing, of models trained on ImageNet with two discrete calibration methods.

References

E. Arias-Castro, B. Pelletier, and V. Saligrama. Remember the curse of dimensionality: The case of goodness-of-fit testing in arbitrary dimension. *Journal of Nonparametric Statistics*, 30(2):448–471, 2018.

P. C. Austin and E. W. Steyerberg. Graphical assessment of internal and external calibration of logistic regression models by using loess smoothers. *Statistics in medicine*, 33(3):517–535, 2014.

R. Berk. An impact assessment of machine learning risk forecasts on parole board decisions and recidivism. *Journal of Experimental Criminology*, 13(2):193–216, 2017.

P. Berman, S. Raskhodnikova, and G. Yaroslavtsev. L_p -testing. In *Proceedings of the forty-sixth annual ACM symposium on Theory of computing*, pages 164–173, 2014.

J. E. Bickel. Some comparisons among quadratic, spherical, and logarithmic scoring rules. *Decision Analysis*, 4(2):49–65, 2007.

M. Bojarski, D. Del Testa, D. Dworakowski, B. Firner, B. Flepp, P. Goyal, L. D. Jackel, M. Monfort, U. Muller, J. Zhang, et al. End to end learning for self-driving cars. *arXiv preprint arXiv:1604.07316*, 2016.

G. W. Brier. Verification of forecasts expressed in terms of probability. *Monthly weather review*, 78(1):1–3, 1950.

J. Bröcker. Estimating reliability and resolution of probability forecasts through decomposition of the empirical score. *Climate dynamics*, 39(3):655–667, 2012.

J. Bröcker and L. A. Smith. Increasing the reliability of reliability diagrams. *Weather and forecasting*, 22(3):651–661, 2007.

A. Buja, W. Stuetzle, and Y. Shen. Loss functions for binary class probability estimation and classification: Structure and applications, 2005.

M. Burnashev. On the minimax detection of an inaccurately known signal in a white gaussian noise background. *Theory of Probability & Its Applications*, 24(1):107–119, 1979.

C. Butucea and K. Tribouley. Nonparametric homogeneity tests. *Journal of statistical planning and inference*, 136(3):597–639, 2006.

Y. Chen. Pytorch cifar models. online, 2021. URL <https://github.com/chenyaof0/pytorch-cifar-models>.

D. R. Cox. Two further applications of a model for binary regression. *Biometrika*, 45(3/4):562–565, 1958.

A. P. Dawid. The well-calibrated bayesian. *Journal of the American Statistical Association*, 77(379):605–610, 1982.

C. Dawkins, T. N. Srinivasan, and J. Whalley. Calibration. In *Handbook of econometrics*, volume 5, pages 3653–3703. Elsevier, 2001.

B. De Finetti. Does it make sense to speak of ‘good probability appraisers’. *The scientist speculates: An anthology of partly-baked ideas*, pages 257–364, 1962.

M. H. DeGroot and S. E. Fienberg. The comparison and evaluation of forecasters. *Journal of the Royal Statistical Society: Series D (The Statistician)*, 32(1-2):12–22, 1983.

A. Esteva, B. Kuprel, R. A. Novoa, J. M. Ko, S. M. Swetter, H. M. Blau, and S. Thrun. Dermatologist-level classification of skin cancer with deep neural networks. *Nature*, 542:115–118, 2017.

C. A. Ferro and T. E. Fricker. A bias-corrected decomposition of the brier score. *Quarterly Journal of the Royal Meteorological Society*, 138(668):1954–1960, 2012.

D. P. Foster and R. V. Vohra. Asymptotic calibration. *Biometrika*, 85(2):379–390, 1998.

A. Franklin. Calibration. In *Can that be Right?*, pages 237–272. Springer, 1999.

U. Garczarek. *Classification rules in standardized partition spaces*. PhD thesis, Universität Dortmund, 2002.

M. Gebel. *Multivariate calibration of classifier scores into the probability space*. PhD thesis, Citeseer, 2009.

T. Gneiting, F. Balabdaoui, and A. E. Raftery. Probabilistic forecasts, calibration and sharpness. *Journal of the Royal Statistical Society: Series B (Statistical Methodology)*, 69(2):243–268, 2007.

I. Good. Rational decisions. *Journal of the Royal Statistical Society. Series B (Methodological)*, pages 107–114, 1952.

R. L. Graham, D. E. Knuth, and O. Patashnik. *Concrete Mathematics: A Foundation for Computer Science*. Addison-Wesley Longman Publishing Co., Inc., USA, 2nd edition, 1994. ISBN 0201558025.

C. Guo, G. Pleiss, Y. Sun, and K. Q. Weinberger. On calibration of modern neural networks. In *International Conference on Machine Learning*, pages 1321–1330. PMLR, 2017.

C. Gupta and A. K. Ramdas. Top-label calibration and multiclass-to-binary reductions. *arXiv preprint arXiv:2107.08353*, 2021.

C. Gupta, A. Podkopaev, and A. Ramdas. Distribution-free binary classification: prediction sets, confidence intervals and calibration. *Advances in Neural Information Processing Systems*, 33, 2020a.

K. Gupta, A. Rahimi, T. Ajanthan, T. Mensink, C. Sminchisescu, and R. Hartley. Calibration of neural networks using splines. *arXiv preprint arXiv:2006.12800*, 2020b.

L. Györfi, M. Kohler, A. Krzyżak, and H. Walk. *A distribution-free theory of nonparametric regression*, volume 1. Springer, 2002.

D. J. Hand. *Construction and assessment of classification rules*. Wiley, 1997.

F. E. Harrell. *Regression modeling strategies: with applications to linear models, logistic and ordinal regression, and survival analysis*, volume 3. Springer, 2015.

T. Hastie and R. Tibshirani. Classification by pairwise coupling. *Advances in neural information processing systems*, 10, 1997.

J. Hilden, J. D. F. Habbema, and B. Bjerregaard. The measurement of performance in probabilistic diagnosis. *Methods of information in medicine*, 17(04):227–237, 1978.

D. W. Hosmer and S. Lemeshow. Goodness of fit tests for the multiple logistic regression model. *Communications in statistics-Theory and Methods*, 9(10):1043–1069, 1980.

Y. Huang, W. Li, F. Macheret, R. A. Gabriel, and L. Ohno-Machado. A tutorial on calibration measurements and calibration models for clinical prediction models. *Journal of the American Medical Informatics Association*, 27(4):621–633, 2020.

Y. I. Ingster. An asymptotic minimax testing of nonparametric hypotheses on the density of the distribution of an independent sample. *Journal of Soviet Mathematics*, 33(1):744–758, 1986.

Y. I. Ingster. Minimax testing of nonparametric hypotheses on a distribution density in the L_p metrics. *Theory of Probability & Its Applications*, 31(2):333–337, 1987.

Y. I. Ingster. Adaptive chi-square tests. *Journal of Mathematical Sciences*, 99(2):1110–1119, 2000.

Y. Ingster and I. A. Suslina. *Nonparametric goodness-of-fit testing under Gaussian models*, volume 169. Springer Science & Business Media, 2012.

J. Ivanov, J. V. Tu, and C. D. Naylor. Ready-made, recalibrated, or remodeled? issues in the use of risk indexes for assessing mortality after coronary artery bypass graft surgery. *Circulation*, 99(16):2098–2104, 1999.

I. T. Jolliffe and D. B. Stephenson. *Forecast verification: a practitioner’s guide in atmospheric science*. John Wiley & Sons, 2012.

J. B. Kadane and S. Lichtenstein. A subjectivist view of calibration. Technical report, DECISION RESEARCH EUGENE OR, 1982.

D. Kahneman and A. Tversky. Prospect theory: An analysis of decision under risk. In *Handbook of the fundamentals of financial decision making: Part I*, pages 99–127. World Scientific, 2013.

G. Keren. Calibration and probability judgements: Conceptual and methodological issues. *Acta Psychologica*, 77(3):217–273, 1991.

I. Kim, S. Balakrishnan, and L. Wasserman. Minimax optimality of permutation tests. *The Annals of Statistics*, 50(1):225–251, 2022.

J. Kodovský and J. Fridrich. Calibration revisited. In *Proceedings of the 11th ACM workshop on Multimedia and security*, pages 63–74, 2009.

M. Kull, T. M. Silva Filho, and P. Flach. Beyond sigmoids: How to obtain well-calibrated probabilities from binary classifiers with beta calibration. *Electronic Journal of Statistics*, 11(2):5052–5080, 2017.

M. Kull, M. Perello Nieto, M. Käängsepp, T. Silva Filho, H. Song, and P. Flach. Beyond temperature scaling: Obtaining well-calibrated multi-class probabilities with dirichlet calibration. *Advances in Neural Information Processing Systems*, 32:12316–12326, 2019.

A. Kumar, P. Liang, and T. Ma. Verified uncertainty calibration. In *Proceedings of the 33rd International Conference on Neural Information Processing Systems*, pages 3792–3803, 2019.

A. Kumar, S. Sarawagi, and U. Jain. Trainable calibration measures for neural networks from kernel mean embeddings. In *International Conference on Machine Learning*, pages 2805–2814. PMLR, 2018.

B. Lakshminarayanan, A. Pritzel, and C. Blundell. Simple and scalable predictive uncertainty estimation using deep ensembles. In *Proceedings of the Conference on Neural Information Processing Systems*, 2017.

E. L. Lehmann and J. P. Romano. *Testing statistical hypotheses*. Springer Science & Business Media, 2005.

S. Lichtenstein, B. Fischhoff, and L. D. Phillips. Calibration of probabilities: The state of the art. *Decision making and change in human affairs*, pages 275–324, 1977.

M. G. Low. On nonparametric confidence intervals. *The Annals of Statistics*, 25(6):2547–2554, 1997.

H. Mann and A. Wald. On the choice of the number of class intervals in the application of the chi square test. *The Annals of Mathematical Statistics*, 13(3):306–317, 1942.

D. Milioto, R. Camoriano, P. Michiardi, L. Rosasco, and M. Filippone. Dirichlet-based gaussian processes for large-scale calibrated classification. In *Proceedings of the 32nd International Conference on Neural Information Processing Systems*, pages 6008–6018, 2018.

M. E. Miller, S. L. Hui, and W. M. Tierney. Validation techniques for logistic regression models. *Statistics in medicine*, 10(8):1213–1226, 1991.

M. E. Miller, C. D. Langefeld, W. M. Tierney, S. L. Hui, and C. J. McDonald. Validation of probabilistic predictions. *Medical Decision Making*, 13(1):49–57, 1993.

R. G. Miller. Statistical prediction by discriminant analysis. In *Statistical Prediction by Discriminant Analysis*, pages 1–54. Springer, 1962.

J. Mukhoti, V. Kulharia, A. Sanyal, S. Golodetz, P. Torr, and P. Dokania. Calibrating deep neural networks using focal loss. *Advances in Neural Information Processing Systems*, 33, 2020.

M. P. Naeini, G. Cooper, and M. Hauskrecht. Obtaining well calibrated probabilities using bayesian binning. In *Twenty-Ninth AAAI Conference on Artificial Intelligence*, 2015.

A. Niculescu-Mizil and R. Caruana. Predicting good probabilities with supervised learning. In *Proceedings of the 22nd international conference on Machine learning*, pages 625–632, 2005.

J. Nixon, M. W. Dusenberry, L. Zhang, G. Jerfel, and D. Tran. Measuring calibration in deep learning. In *CVPR Workshops*, 2019.

C. Osborne. Statistical calibration: a review. *International Statistical Review/Revue Internationale de Statistique*, pages 309–336, 1991.

J. Platt. Probabilistic outputs for support vector machines and comparisons to regularized likelihood methods. In *Advances in Large Margin Classifiers*, pages 61–74, 1999.

C. R. Rao. Large sample tests of statistical hypotheses concerning several parameters with applications to problems of estimation. In *Mathematical Proceedings of the Cambridge Philosophical Society*, volume 44, pages 50–57. Cambridge University Press, 1948.

R. Roelofs, N. Cain, J. Shlens, and M. C. Mozer. Mitigating bias in calibration error estimation. *arXiv preprint arXiv:2012.08668*, 2020.

L. J. Savage. Elicitation of personal probabilities and expectations. *Journal of the American Statistical Association*, 66(336):783–801, 1971.

F. Seillier-Moisiewitsch and A. Dawid. On testing the validity of sequential probability forecasts. *Journal of the American Statistical Association*, 88(421):355–359, 1993.

N. Serrano. Calibration strategies to validate predictive models: is new always better?, 2012.

N. D. Shah, E. W. Steyerberg, and D. M. Kent. Big data and predictive analytics: recalibrating expectations. *Jama*, 320(1):27–28, 2018.

S. D. Silvey. The lagrangian multiplier test. *The Annals of Mathematical Statistics*, 30:389–407, 1959.

V. G. Spokoiny. Adaptive hypothesis testing using wavelets. *The Annals of Statistics*, 24(6):2477–2498, 1996.

R. Stanley. Eulerian partitions of a unit hypercube. *Higher Combinatorics*, 31:49, 1977.

E. W. Steyerberg, A. J. Vickers, N. R. Cook, T. Gerdts, M. Gonen, N. Obuchowski, M. J. Pencina, and M. W. Kattan. Assessing the performance of prediction models: a framework for some traditional and novel measures. *Epidemiology (Cambridge, Mass.)*, 21(1):128, 2010.

E. W. Steyerberg et al. *Clinical prediction models*. Springer, 2019.

B. Sturmfels. *Grobner bases and convex polytopes*, volume 8. American Mathematical Soc., 1996.

A. Tamás and B. C. Csáji. Exact distribution-free hypothesis tests for the regression function of binary classification via conditional kernel mean embeddings. *IEEE Control Systems Letters*, 2021.

P. E. Tetlock and D. Gardner. *Superforecasting: The art and science of prediction*. Random House, 2016.

S. Thulasidasan, G. Chennupati, J. A. Bilmes, T. Bhattacharya, and S. E. Michalak. On mixup training: Improved calibration and predictive uncertainty for deep neural networks. In *Proceedings of the Conference on Neural Information Processing Systems*, 2019.

D. Toll, K. Janssen, Y. Vergouwe, and K. Moons. Validation, updating and impact of clinical prediction rules: a review. *Journal of clinical epidemiology*, 61(11):1085–1094, 2008.

J. Vaicenavicius, D. Widmann, C. Andersson, F. Lindsten, J. Roll, and T. Schön. Evaluating model calibration in classification. In *The 22nd International Conference on Artificial Intelligence and Statistics*, pages 3459–3467. PMLR, 2019.

B. Van Calster and A. J. Vickers. Calibration of risk prediction models: impact on decision-analytic performance. *Medical decision making*, 35(2):162–169, 2015.

B. Van Calster, D. Nieboer, Y. Vergouwe, B. De Cock, M. J. Pencina, and E. W. Steyerberg. A calibration hierarchy for risk models was defined: from utopia to empirical data. *Journal of clinical epidemiology*, 74:167–176, 2016.

B. Van Calster, D. J. McLernon, M. Van Smeden, L. Wynants, and E. W. Steyerberg. Calibration: the achilles heel of predictive analytics. *BMC medicine*, 17(1):1–7, 2019.

R. Vershynin. *High-dimensional probability: An introduction with applications in data science*, volume 47. Cambridge University Press, 2018.

V. Vovk and G. Shafer. Good randomized sequential probability forecasting is always possible. *Journal of the Royal Statistical Society: Series B (Statistical Methodology)*, 67(5):747–763, 2005.

D. Widmann, F. Lindsten, and D. Zachariah. Calibration tests in multi-class classification: A unifying framework. *Advances in Neural Information Processing Systems*, 32:12257–12267, 2019.

R. L. Winkler, J. Munoz, J. L. Cervera, J. M. Bernardo, G. Blattenberger, J. B. Kadane, D. V. Lindley, A. H. Murphy, R. M. Oliver, and D. Ríos-Insua. Scoring rules and the evaluation of probabilities. *Test*, 5(1):1–60, 1996.

B. Zadrozny and C. P. Elkan. Obtaining calibrated probability estimates from decision trees and naive bayesian classifiers. In *Proceedings of the International Conference of Machine Learning*, 2001.

B. Zadrozny and C. P. Elkan. Transforming classifier scores into accurate multiclass probability estimates. In *Proceedings of the ACM International Conference on Knowledge Discovery and Data Mining*, 2002.

J. Zhang, B. Kailkhura, and T. Y.-J. Han. Mix-n-match: Ensemble and compositional methods for uncertainty calibration in deep learning. In *International Conference on Machine Learning*, pages 11117–11128. PMLR, 2020.

S. Zhao, T. Ma, and S. Ermon. Individual calibration with randomized forecasting. In H. D. III and A. Singh, editors, *Proceedings of the 37th International Conference on Machine Learning*, volume 119 of *Proceedings of Machine Learning Research*, pages 11387–11397. PMLR, 13–18 Jul 2020.